Chemical Transformation of Chitosan Oligosaccharides via Solvent-Free Mechanochemistry; Biomass Valorization from Ocean-Sourced Renewable Feedstock to Biobased Platform Chemicals

Say Yenh (Eric) Hong, Department of Mechanical Engineering, McGill University, Montreal

August, 2018

A thesis submitted to McGill University in partial fulfillment of the requirement of the degree of Doctor of Philosophy

© Say Yenh (Eric) Hong 2018

TABLE OF CONTENTS

ABSTRACT

Valorization of biomass waste has been postulated as the 'new frontier in green chemistry', moving the field beyond waste remediation and minimization. It has been boldly proposed that biomass waste could serve as complementary and alternative feedstocks to conventional fossil-based raw materials, leading to the emergence of a new paradigm: the biorefinery concept, i.e., envisaged as sustainable conversions of biomass into a broad spectrum of biobased products.

In this work, we will explore a novel encapsulation design concept of employing a carbohydrate shell to encapsulate a biosensor envisaged for in vivo deployment. We will present a novel concept of producing modified oligosaccharide molecules with tailor-made properties intended for specialty/niche biomedicine biosensor application. To this end, the deliberate utilization of mechanical forces and energy by means of high speed ball milling (HSBM) to effect purposeful chemical transformations of recalcitrant oligosaccharides, as a non-thermal and solvent-free method for the preparation of useful new materials and platform molecules will be demonstrated, in this case, a tailor-made chitosan oligosaccharide. Chitosan oligosaccharides were reported in the literature to exhibit augmented antibacterial, antifungal, antitumour, immunoenhancing, lower haemolytic or hepatotropic profile, lower toxicity and other biological activities at the cellular or molecular level whilst forming thinner, more transparent, and smaller sized films than high molecular weight chitosan or polymeric chitin commonly used in many applications; the above properties would undeniably be desirable for biosensing applications. This work aims to demonstrate a proof-of-concept for producing high-value oligosaccharide biomaterials from abundant and renewable biomass carbohydrate residues (shellfish waste) which are inherently biodegradable, as a sustainable carbon based feedstock, hence fully embracing the concept of a waste-based biorefinery. The biomass conversion in this work is guided by the design philosophy of using milder processing/treatment conditions (enabled by mechanochemistry) in order to preserve Nature's highly functionalized biomacromolecules (valorized as precious resources), retaining a high proportion of the original chemical structure, functionality, and complexity, as a value creation strategy, thus departing from the normative tradition of synthesizing complex molecules from simpler starting precursors.

RÉSUMÉ

La valorisation des déchets de la biomasse a été postulée comme la «nouvelle frontière de la chimie verte», faisant passer le champ au-delà de l'assainissement et de la réduction des déchets. Il a été audacieusement proposé que les déchets de biomasse puissent servir de matières premières complémentaires et alternatives aux matières premières fossiles conventionnelles, conduisant à l'émergence d'un nouveau paradigme: le concept de bioraffinerie, envisagé comme une conversion durable de la biomasse en un large éventail de produits d'origine biologique.

Dans ce travail, nous allons explorer un nouveau concept de conception d'encapsulation en utilisant une enveloppe de glucides pour encapsuler un biocapteur prévu pour le déploiement in vivo. Nous présenterons un nouveau concept de production de molécules d'oligosaccharides modifiées avec des propriétés sur mesure destinées à l'application de biocapteurs spécialisé en biomédecine. À cette fin, l'utilisation délibérée de forces mécaniques et d'énergie au moyen d'un broyeur à boulets de forte énergie pour effectuer des transformations délibérées et utiles chimiques d'oligosaccharides récalcitrants, en tant qu'une méthode non-thermique et sans solvant pour la préparation de nouveaux matériaux utiles et des molécules de plate-forme sera démontrée, dans ce cas, un oligosaccharide de chitosan sur mesure. Plusieurs études ont démontrées que les oligosaccharides de chitosan montrent de nombreuses activités biologiques rehaussées antibactériennes, antitumorales, immunostimulatrices, de moindre toxicité, et d'autres tout en formant des films plus minces, plus transparents et de taille inférieure à ceux formés à partir de la chitine polymérique ou du chitosan à haut poids moléculaire couramment utilisé dans de nombreuses applications. Ce travail vise à démontrer comme preuve de concept la production de biomatériaux oligosaccharidiques de grande valeur à partir de résidus de glucides provenant d'origine de biomasses abondantes et renouvelables (déchets de coquillages) qui sont de nature intrinsèquement biodégradables, en tant que matière première de carbone durable, ainsi, entièrement épouser l'idée et le concept de bioraffinerie à base de déchets.

La conversion de la biomasse dans ce travail est guidée par la philosophie de conception privilégiant des conditions de processus/traitement plus modérées ou douces (mécanochimie) afin de préserver les biomacromolécules hautement fonctionnalisées de la nature (valorisées comme ressources précieuses), conservant une proportion élevée de la structure, fonction, et complexité chimique originale, en tant que stratégie de création de valeur, s'écartant ainsi de la tradition normative de la synthèse de molécules complexes à partir de précurseurs de départ plus simples.

ACKNOWLEDGEMENTS

Prof./Dr. Rosaire Mongrain (supervisor, Department of Mechanical Engineering) for the kind guidance, support, advice, constructive suggestions and encouragements (including the exploration of new ideas) provided throughout the Ph.D. program, all of which helped me overcome numerous difficult moments and setbacks in the course of the work. It is a privilege and honor to have had the opportunity to work to with a supervisor of extraordinary human qualities, benefiting from his research experience, knowledge, wisdom, positive outlook and confidence, which inspired and motivated me to bring this work to completion.

Prof./Dr. Vamsy Chodavarapu (co-supervisor, Department of Electrical and Computer Engineering) for offering the opportunity to work on a challenging sensor encapsulation related project, and for introduction to the sensor field through various venues, including invaluable access to professional networks such as the McGill Institute for Advanced Materials and NSERC-CREATE Integrated Sensor Systems (ISS) Ph.D. Training Program, and for teaching the ECSE 574 Sensor CMOS Microsystems graduate level course which covered important microsensor, microsystems, and microfabrications related topics.

Prof./Dr. Chao-Jun Li (co-supervisor, Department of Chemistry) for providing access to his Green Chemistry laboratory where the work related to the generation of substrates, work-ups, and purifications was performed, as well as for access to the expertise and knowledge from his staff of visiting scholars, namely Dr. Ning Chen (陳寧), Dr. Xiaobo Yang (楊曉博), Dr. Jiangsheng Li (李江勝), and Dr. Zhongzhen Zhou (周中振) for training on common organic chemistry laboratory techniques and for some fruitful discussions.

Prof./Dr. Tomislav Friščić (Department of Chemistry) for providing access to his solvent-free research (mechanochemistry) laboratory where mechanochemistry related work was performed, as well as to his graduate student Mr. Igor Huskic for introduction to the mechanochemistry field and for training related to usage of the shaker/mixer/vibratory/grinding mills (Retsch MM200 and MM400).

Dr. Robin Stein (McGill Chemistry NMR/EPR Facility, Department of Chemistry) for 1D and 2D NMR spectroscopy training (individual and group) on the instruments/spectrometers and software (TopSpin, MestReNova) for the acquisition, processing, and interpretation of spectra, including advanced experimental techniques such as variable temperature experiments, manual probe switching of the Varian/Agilent 500 MHz VNMRS instrument/spectrometer, as well as macros of TopSpin commands to automate 2D spectra processing.

The McGill Institute for Advanced Materials and NSERC-CREATE Integrated Sensor Systems (ISS) Ph.D. Training Program (ISS Director Prof./Dr. Andrew Kirk and ISS Administrator Ms. Aube Mamias) for planning and hosting several training related activities, e.g., hands-on workshops, professional skills short-courses, and other activities, symposia, and workshops, as well as for the opportunity to take part in the Graduate Student Planning Committee (GSPC) acting as the VP IT.

Last but not least, the author gratefully acknowledges financial support from the following sources: McGill Institute for Advanced Materials, NSERC-CREATE Integrated Sensor Systems (ISS) Ph.D. Fellowship Award, and NSERC-CIHR grant number MUHC 5817.

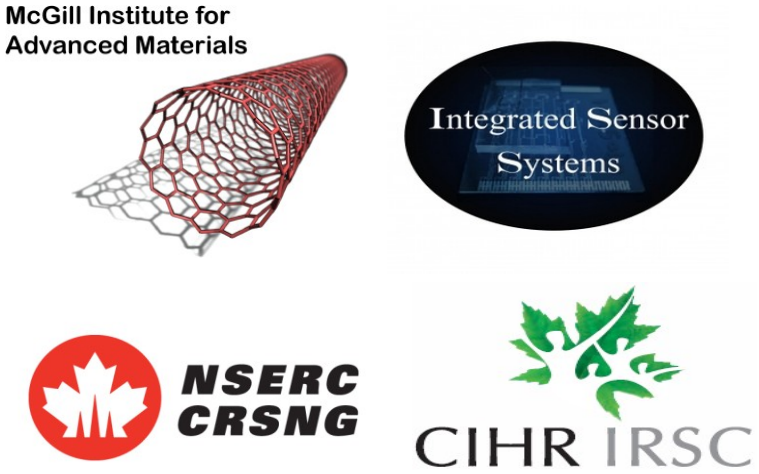

LIST OF FIGURES

LIST OF TABLES

ORGANIZATION OF THE THESIS: LOGICAL DEPENDENCY AMONGST SUBCHAPTERS AND CHAPTERS

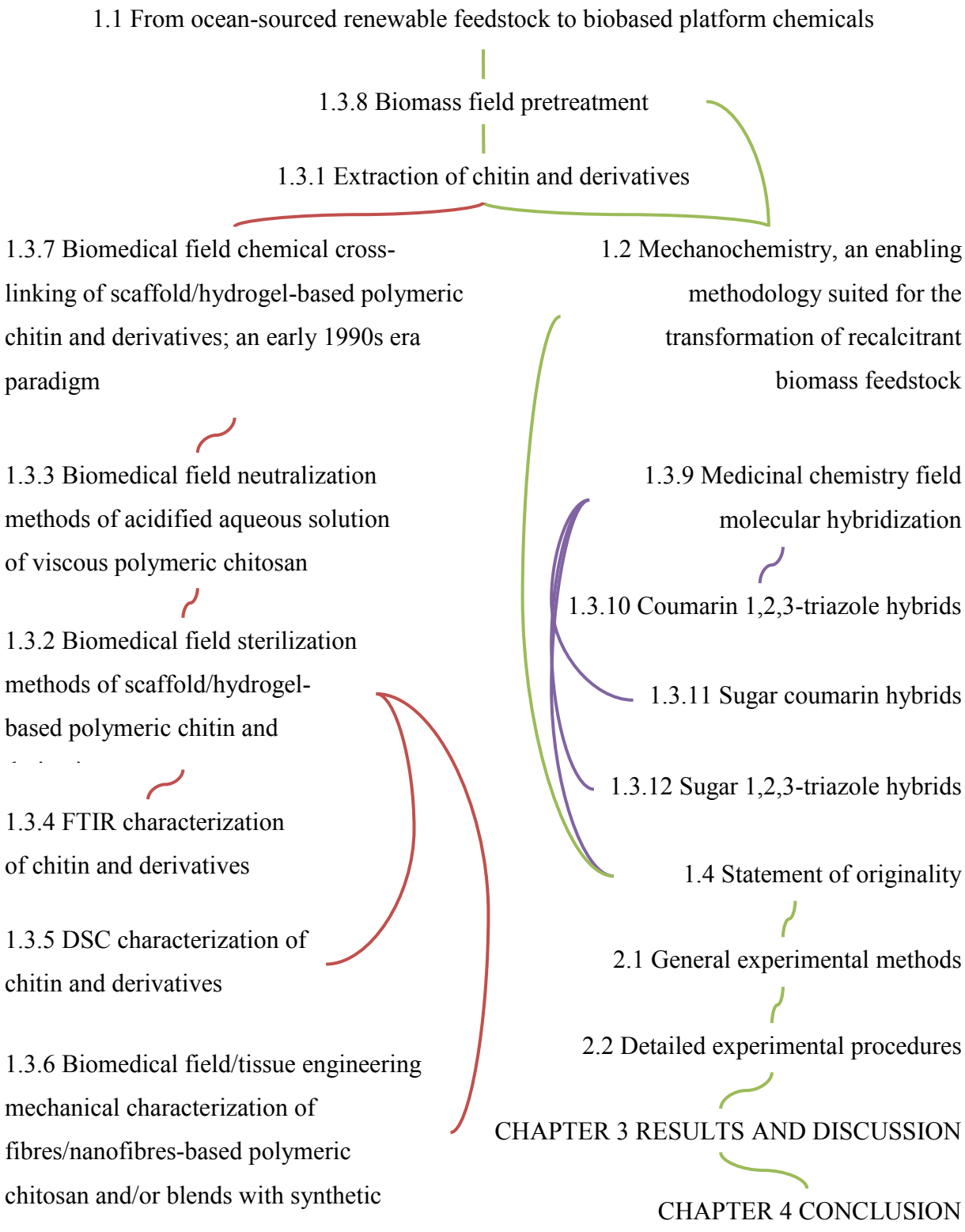

This thesis is divided into four parts. Chapter 1 presents the research background and motivation, and culminates with the introduction of the Statement of originality in section 1.4. In Chapter 2, the general experimental methods in section 2.1 are presented, followed with the detailed experimental procedures in section 2.2. In Chapter 3, experimental results are presented and discussed. Chapter 4 summarizes this thesis with an emphasis on its original contribution to the body of knowledge, and closes the thesis with a discussion on possible future work, along with offering perspective on the long-term implications of the HSBM solvent-free methodology developed in this thesis on several fields such as green chemistry, medicinal chemistry, pharmaceutical and biomedical fields. As illustrated above, an outline of the logical dependency amongst subchapters and chapters is shown to reveal the overall structure of the thesis. Attempts were made to make each chapter self-contained and cross-references were introduced throughout the thesis to highlight the intricate interdependencies between subchapters and chapters, to re-emphasize important points, concepts, ideas, groups of supporting and/or pertinent references that were previously introduced, offer a slightly different perspective on a topic but looked at from a different viewpoint (i.e., from a different section or chapter), as well as to aid the reader in navigating between the subchapters and chapters with clickable cross-reference links (electronic version of thesis only, idem for references).

LIST OF ABBREVIATIONS

AcOH	acetic acid
ACS	acute compartment syndrome
COS	chitooligosaccharides
COSY	correlation spectroscopy
D-GlcN	D-glucosamine
DMF	*N,N*-dimethylformamide
DMSO	dimethyl sulfoxide
DP	degree of polymerization
EtOH	ethanol
FCC	flash column chromatography
Fmoc	9-fluorenylmethoxycarbonyl
FSCW	food supply chain waste
HCl	hydrochloric acid
HMBC	heteronuclear multiple-bond correlation
HMWC	high molecular weight chitosan
HSBM	high speed ball milling
HSQC	heteronuclear single quantum coherence
KI	Knoop index
LAG	liquid-assisted grinding
LMWC	low molecular weight chitosan
MALDI-MS	matrix-assisted laser desorption/ionization mass spectroscopy
MEMS	microelectromechanical system
MeOH	methanol
Mn	number-average molecular weight
Mw	weight-average molecular weight
NMR	nuclear magnetic resonance
PDI	polydispersity index
PhMe	toluene
PTFE	polytetrafluoroethylene

TEG	tetraethylene glycol
THF	tetrahydrofuran
TLC	thin layer chromatography

CHAPTER 1
INTRODUCTION

1.1 From ocean-sourced renewable feedstock to biobased platform chemicals

Valorization of biomass waste has been postulated as the 'new frontier in green chemistry', moving the field beyond waste remediation and minimization, e.g., avoiding the use of toxic and/or hazardous reagents and/or solvents[1]. It has been boldly proposed that biomass waste could serve as complementary and alternative feedstocks to conventional fossil-based raw materials, leading to the emergence of a new paradigm: the biorefinery concept[1-9]. A biorefinery would be a facility producing multiple products, including fuel, power, bulk or fine chemicals, and materials from biomass feedstocks, in direct analogy to the more familiar petroleum refinery, which produces fuels and chemicals from crude oil[3,5]; the vision is of a future biobased economy in which integrated biorefineries would produce biofuels, commodity chemicals, and novel materials[1]. More succinctly, the biorefinery concept is envisaged as 'sustainable conversions of biomass into a broad spectrum of biobased products'[4].

The ultimate aim would be a gradual and eventual substitution of non-renewable based feedstocks such as fossil resources (crude oil, coal, or natural gas, which currently supply 90% of all our energy needs[9], e.g., untenable dependence on petroleum as a single energy source for transportation fuel[10]) with renewable biomass as a sustainable carbon based feedstock for the manufacture of commodity chemicals[1,3-6,9,11-14]. In fact, several governments have passed legislation mandating a fractional increase in gross domestic chemical production from renewable resources, especially of biomass-origin, e.g., the U.S. Department of Agriculture set an ambitious goal to derive 25% of U.S. chemical commodities from biomass by 2030[5]. In this context, food supply chain waste (FSCW), defined as 'any organic material produced for human consumption that is discarded, lost or degraded primarily at the manufacturing and retail stages, including waste arising from pest degradation or food spoilage'[2], is posited as a new and promising feedstock for this novel biorefinery concept[1,2,12]. The strategy of food waste

valorization through re-use as sustainable raw material for the production of higher value marketable products is highly alluring when compared with current waste processing practices[2], especially considering that the bulk of food waste either ends up in landfills[1,15] or gets dumped at sea[15,16]. Besides environmental impact (e.g., water supply contamination through inorganic matter leaching), and decreasing availability of landfill sites, landfill waste disposal can be costly[2]. For instance, the stricter regulations and standards of the EU landfill directive has caused the landfill gate fees to surge from £40–74 (2009) to £68–111 (2011)[2]. Similarly, landfill disposal costs in Australia has been reported to reach as high as $150 USD per tonne[15]. Given that such food waste is currently attributed an economic value less than the cost of collection, or is not being recovered nor recycled with intention of reuse for other purposes, the incentive is to discard such raw materials as waste[2]. For example, the monetary value of dried shrimp shell powders is about $100-$120 USD per ton[15], clearly valued below collection costs. Although specific regulations have been introduced in the 1970s prohibiting the dumping of untreated shellfish waste into the ocean[8], and similar legislation is being introduced in Canada[16], the questionable practice of uncontrolled biomass waste dumping at sea seems to continue unabated[17].

The fundamental issue is the sheer scale and rate at which the food supply chain industry in its present form produces biomass waste[2] for which supply greatly exceeds demand[18]. To illustrate the enormous amount of biomass waste generated by the seafood processing industry, consider the global annual harvest of crustaceans (shrimps, crabs, and lobsters) estimated to be over 13 million tonnes[19], of which at least 50% by weight consists of inedible seashells[17,19], materials traditionally considered as waste[4]. Worldwide annual production of shellfish waste has been estimated to be up to 1.44 tonnes (dry weight)[17], or between 6 and 8 million tons[8]. For the Canadian province of Newfoundland and Labrador, an estimated 39,000 tonnes per year of shellfish waste is generated; an amount which would make up about 35% by weight of the commercial harvest of northern shrimp and snow crab[16]. The large volume of generated biomass waste that (1) has slow environmental biodegradation rate[17], (2) is of putrescible nature[2], and (3) eventually accumulates in coastal areas after being dumped into the sea[17], which altogether create a major environmental problem that undoubtedly needs to be addressed.

A proposed path forward to meet several objectives such as environmental protection, e.g., minimizing the environmental impact of waste streams in terms of reduced volume and/or contamination loading[16], and more efficient resource and waste management is the development of new valorization routes, namely via the concept of a waste-based biorefinery[2]. Chiefly, FSCW feedstocks rich in organic residues would be fed back into a closed-loop supply chain biorefinery[2]. FSCW feedstocks offer several benefits such as being abundant, readily available, presently underutilized[2], renewable on a human time scale[19], and suited for decentralized production[19]. Most importantly, FSCW feedstocks have rich contents of valuable functionalized molecules such as carbohydrates, dietary fibres, proteins, lipids (triglycerides, fatty acids), and phytochemicals (phenolics, carotenoids, and tocopherols)[2,20]. Notably, dry crustacean shellfish biomass is a renewable source of chitin, which accounts for about 20-30 wt% of the former[19]. As nitrogen-containing functional groups are already present in chitin, it has been advanced that such biopolymer could serve as feedstock material for the sustainable production of nitrogen-containing bio-based commodity chemicals in a more economically viable, less energy-intensive, and with lighter environmental footprint than existing industrial processes (complex, multi-steps, redox-intensive, costly) which rely on petroleum-derived feedstock[15,18]. Indeed, the prospect of direct and redox-neutral conversion[18] from biomass carbohydrate residues (bio-waste or food waste) to value-added chemicals would be quite enticing, especially if a reasonable proportion of the inherent chemical complexity of the former is preserved in the latter[2,18,20]. Thus, biomass valorization and conversion from functionalized feedstocks of relative chemical complexity would represent a significant departure from the prevalent yet unsustainable tradition of synthesizing complex molecules from simpler starting materials and/or precursors[18]. Ultimately, renewable biomass (cellulose, chitin[9]) could be the only sustainable source of organic carbon for the long-term production of fuels and chemicals[9,21]. Additional drivers underpinning biomass valorization include dwindling worldwide supply of petroleum feedstock[2,5,6,9-11,14,18,22], its rising commodity price[2,10,18,23], its higher price volatility[2,22], along with public concern over its security[15,24,25], consequently, petroleum-based feedstock is becoming comparatively less appealing as a carbon source[10]. However, to harness the full potential of biomass as a renewable carbon feedstock for the production of valuable platform chemicals, a key prerequisite would be its deconstruction/separation into components[26]. This challenging problem is often referred to as 'biomass recalcitrance'[6,27], i.e., the innate recalcitrance of insoluble polysaccharides such as

chitin[27] to microbial[6] or enzymatic[6,27] or chemical (known over 100 years using mineral acids)[18,28] depolymerization into more useful constituent oligosaccharide building blocks (i.e., molecules containing multiple functional groups with recognized derivatization potential into new families of useful structures)[20], whereby efficient hydrolysis is hindered by such substrate's inherent chemical stability, insolubility, and crystalline nature[27]. As such, a recalcitrant substrate is generally subjected to a pretreatment processing step which aims to disrupt its crystalline structure[7,8,19,21,25-33], and/or to reduce its degree of polymerization or/and particle size (comminution), thereby promoting accessibility of the polymeric backbone to reagents in subsequent transformations[8,26,27,29,31], including enzymatic hydrolysis[27-29,31,33]. To this end, various pretreatment technologies are available, which can be classified into four categories[5]: physical or mechanical (e.g., ball milling[5,8], steam explosion[8,26]), solvent fractionation (e.g., organosolv process[5], phosphoric acid fractionation[5,8], dissolution/re-precipitation in non-derivatizing solvents such as ionic liquids[5,8,26]), chemical (e.g., pre-hydrolysis with acidic or alkaline solutions[5,8,26], oxidative[5]), and biological (e.g., fungi)[5]. Relating to pretreatment process design and selection, due consideration should be given to several factors like economic viability, environmental footprint, simplicity and efficiency[21]. From an industrial perspective, multi-step processing and/or separation decreases the overall atom economy, increases energy consumption and generates more waste[13]. From an environmental viewpoint, the large quantity of wastewater emission from biomass processing[3,6,8,13,20,21,25,33], engenders environmental toxicity[7,8,11,13,32], reactor/equipment corrosion[6-8,11,13,20,21,25,32,33], and catalyst recycling/recovery type of complications[6,11,13,20,21], which imposes additional treatment costs[6-8,20,21]. Moreover, established wastewater treatment processes are deemed energy intensive[34] and environmentally unfriendly[7,34]. Owing to the elevated capital costs associated with wastewater treatment[7,8,28] and/or solvent recycling[28] (e.g., effluent wastewater containing chemicals)[17], the general consensus is that efforts in designing and developing biorefinery schemes should lean towards solvent-free processes[3,28], in other words, limiting the production of aqueous effluents is *sine qua non* in biorefinery processes[13]. To this aim, ball-milling in neat grinding (solvent-free) mode emerges as an important mechanochemistry methodology for the pretreatment[27,31] and/or ensuing transformation of recalcitrant biomass[27,31] for several reasons: (1) comminution and/or amorphization of the crystalline domains of the biomass, rendering it more susceptible for following chemical or biochemical depolymerization[31], and (2) potential of the process to enable

access to solid-state chemical reactivity[7] for reagents with known inherent insolubilities in common solvents[35], which otherwise would be challenging (not readily accessible) or impossible using traditional solution-based methodologies[36-38]. The following section will further elaborate on the application of ball-milling as an invaluable means to conduct solvent-free mechanochemical reactions initiated or sustained through mechanical force[39,40]. From either an ecological or economic perspective, the possibility of avoiding 'tonnes of solvents' is a significant advantage[41]; all things considered, effective use of mechanical forces not merely provides an environmentally friendly entry-point (or as a key step) into biorefinery schemes[13,26,28,29,31], the economic viability of said biorefinery schemes may well depend on such key process[10,31,42].

1.2 Mechanochemistry, an enabling methodology suited for the transformation of recalcitrant biomass feedstock

Of fundamental interest in understanding chemical processes is finding the most effective way to 'activate covalent bonds' or the most appropriate method (least dissipative) to distribute, transfer, and supply energy into the reaction system to initiate and/or sustain chemical reactions[43,44], including the heating of reaction mixtures[43]. Late 19th century saw the formalization of the chemical disciplines into the branches of thermochemistry, electrochemistry, and photochemistry, using a classification system based on the type of energy input used for chemical activation[37,44]. Collectively, they embody the current paradigm of solution-based protocols whereby the solvent is considered an essential medium for mass and energy transport, without which, the latter are deemed impeded[44]. Surprisingly, the persistent belief that neither reactions[44] nor transformations[38] can proceed in the absence of solvent(s) was held for a long time, as attested by an early translation into Latin of ancient Greek philosopher Aristotle's (384 - 322 B.C.) quotation *'corpora non agunt nisi fluida (or liquida) seu soluta'* which was later translated into English as *'compounds do not react unless fluid (or if dissolved)'*[37,38,43]. The statement reputedly originates from Aristotle's work *De Generatione et Corruptione*, where it was suggested that the original text in native Greek would translate into a less problematic (read softer) version as *'it is chiefly the liquid substances which react...for instance liquids are the type of bodies liable to mixing'*[37,45]. Around the same period circa 315 B.C., Aristotle's student, Theophrastus of Eresus, wrote a booklet containing a reference to the application mortar and pestle to reduce cinnabar to

elemental mercury by grinding it in the presence of vinegar (acetic acid) in a copper vessel[37,40,46]. This surviving record would suggest that the possibility of initiating chemical reactions by grinding inorganic materials was known early (Classical Greece, 4th century B.C.), without necessarily implying that ancient Greeks knowingly practiced mechanochemistry[46], hence the statement that chemical and structural transformations by mechanical milling or grinding have been central to the processing and synthesis of materials 'since antiquity'[20,47,48] is indeed supported by early historical documents. In spite of its long history[37,46,49], one has to fast forward for about 2000 years[46] (including the Middle Ages[37] where the mortar and pestle was the standard laboratory instrument of the alchemist and early chemist, and observations on chemical effects were seldom recorded[46]) for a modern perspective on the topic of mechanochemistry. The present view is often ascribed to Wilhelm Ostwald (1853-1932) who in 1919 recognized mechanochemistry in its broader sense as one of the four sub-disciplines part of the framework of physical chemistry at the same level or equivalency as thermochemistry, electrochemistry and photochemistry[37,44-46,48,49], i.e., as a fourth way of chemical activation, albeit one which is still presently poorly understood comparatively to the other three fields[41,44,50]. Whilst still in its infancy, he commented that *'we shall call it mechanochemistry for lack of a better name, as it involves dispersion or defloculation by mechanical means, thereby bringing about so-called colloidal dispersions'*[49]. At present, the most commonly cited definition[37,38,41,43-45,49] of a *mechano-chemical reaction* is the one described by the IUPAC's Compendium of Chemical Terminology (the Gold Book) as a *'chemical reaction that is induced by the direct absorption of mechanical energy'* with additional note for usage regarding polymers[37] *'shearing, stretching, and grinding are typical methods for the mechano-chemical generation of reactive sites, usually macroradicals, in polymer chains that undergo mechano-chemical reactions'*. This basic definition is considered appropriate for general usage, i.e., sufficiently broad without restrictions at the atomic scale mechanism[37], although it leaves numerous specifics undefined according to some of the *cognoscenti*[43,45]. The definition's generality highlights the interdisciplinary nature of a field which draws interest from researchers across different disciplines such as chemistry (physical, inorganic, organic, colloid), engineering (chemical, mechanical), materials science, metallurgical science, mineralogy, geology, and physics, whose diverse objectives, methods, and terminologies stimulate mechanochemical questions originating from very different contexts[46]. Pertaining to mechanochemistry of organic soft matter, a prudent advice is offered to analyze the

literature critically because 'with rare exceptions, the research of organic systems is done by groups which have not been previously involved in mechanochemistry, but are experts in organic chemistry, catalysis, crystallography, coordination chemistry'[41]. Since interest in the field is no longer restricted to inorganic and materials scientists[38,44], it should be emphasized that the most widely referred microscopic level[47] mechanistic models, i.e., hot spot (circa early 1950s)[37,38,46-51] and magma-plasma (1967)[37,38,41,46,47,49,51], were both developed in relation to inorganic systems[47] and materials (e.g., metals and metal oxides)[37]. In both models, mechanical initiation of chemical reactions is hypothesized to be mediated by the generation of short-lived local microscopic surface areas (ca. 1 μm^2) of high temperatures, e.g., greater than 1,000 °C for hot-spot theory (lateral frictional/sliding processes) and over 10,000 °C for the magma-plasma model (colliding/direct impacts processes inducing highly excited transient (ca. 10 ns) plasma-like state with ejection/emission of energetic species such as free electrons, photons, and fragments of solid substance)[37,38,46,48,49]. The premise that such high-energy surfaces (i.e., hot spots or magma-plasma sites) are the primary reactive sites for solid reactivity[37] whilst plausible when grinding hard and abrasive inorganic materials[50], has been the target of much criticisms for the transformation of soft molecular substances at typical ball milling operating frequencies (i.e., between 20 Hz and 50 Hz)[50], in other words, the reactive site's size and the duration in which the intense thermal effect can exist are mostly dependent on the material type[48]. Firstly, the required temperatures and pressures which can induce reactions in organic compounds are lower than those needed for inorganic substance[41], especially for grinding organic or coordination chemistry type of reactions where the reactions rates are very sensitive to small changes in temperature[38]. Furthermore, it would be sensible to expect extensive decomposition of organic substance at such localized surfaces (extremely high temperatures) but since decomposition is not experimentally observed (*vide infra*), this would be suggestive that these phenomena may be too brief and/or too localized as primary reactive sites of organic reactions[37]. To separate the influence of mechanical from thermal effects on the transformation of biomass substrates, a study utilized the most thermolabile moiety as an internal probe relative to other more thermostable linkages[52]. The observation that there was no appreciable extent of cleavage of the former in proportion to the latter was taken as an indication that ball milling transformations on biopolymers are initiated by the action of mechanical forces rather than by the existence of hot spots[52] (in situ and real-time monitoring of mechanochemical reactions using synchrotron X-ray

powder diffraction (PXRD) revealed very negligible temperature increase from room temperature, ca. 7-12 °C)[53]. The assumption that localized heating initiates some chemical[46,49] or physical[49] processes is based on the knowledge that mechanical energy is mostly converted into thermal energy during impact or sliding[46,49]. For this reason, the idea that 'some chemical reactions occur indirectly due to temperature increase'[46] is intuitive yet evidence suggests that heat is not the major driving force of mechanochemical transformation, despite its involvement amongst several active processes[45]. Therefore, the presumption of merely using one mechanism type to describe mechanochemical processes would be disingenuous[50]; instead, it would be more fruitful to recognize such processes as complex[46,50], i.e., implicating several length[46,49] (macroscopic, grain, dislocation, and atomic level)[46] and time scales[37,46], being system specific[46] (reactant's type/nature)[37,41], and taking place under diverse reaction conditions[37,46] and types[37,41]. Additionally, when assessing the scope or range of applicability of existing mechanistic models mostly focused on inorganic materials, one is faced with the hurdle that relatively few studies relate to the highly diverse class of metal-organic reactions[37], let alone organic reactions[41]. The labilities of reactant types (inherent different nature) span a wide range, where molecular crystals are regarded as softer and more mobile/labile at the molecular scale[37], in addition to emphasizing hydrogen bonding's contribution for molecular crystals[37,41], ergo, such reactions may share mechanistic similarities with cocrystallization models[37]. A general three-step mechanism or conceptual framework describing the reactions of molecular substances and/or solids under mechanochemical milling was put forth by means of three basic processes: (1) reactants' diffusion (molecular transport across surfaces)[37] through a mobile phase (gas, eutectic, or amorphous solid)[47] and reaction via an amorphous intermediate phase[37,54], (2) nucleation and growth of the product phase[47], and (3) product separation exposing fresh reactant surface[37,41,47]. The formation of an intermediate bulk phase (vapour, liquid, or amorphous solid) exhibiting enhanced mobility and/or higher energy of reactant molecules than corresponding starting crystalline form is a common thread to many mechanisms presented thus far[54], i.e., increased reactivity under mechanochemical conditions via formation of amorphous phases for molecules held relatively strongly in their lattice positions through substantial hydrogen bonding[37]. Clearly, the circumstances under which mass transport occur for mechanochemical processes differ significantly from solution-based ones, viz., the inherent mixing efficiency[35,37,41,43,49,55-57] and fast movement of milling balls can be used to overcome solid-state diffusion and mass transport

limitations[37,41,43,49,55,56] (bulk of molecules remain within the interior of solid reactants' crystals, hence, relatively immobile)[54] for the former, whereas for the latter, reactant molecules are intimately mixed and possess free mobility for reacting[54]. Solid-state mass transport can introduce peculiar effects such as reduced steric hindrance to reactivity along with other unpredictable patterns of reactivity[45], which can astonishingly reveal alternative[36,38,41,44,51] or novel reactivity routes[36,38] or enable access to elusive structures previously believed unreachable by solution-based procedures due to perceived stability or steric issues[36,38,43-45,51,58].

The fundamental insight on mechanochemistry's non-thermal *sui generis* nature has been known since time immemorial, dating back since circa 1880s[46,59], i.e., mechanical activation[49] or action[46] induces differing mass transport processes from the ones under thermal activation conditions[49], consequentially altering the physical and chemical behaviour of solids at different scales[49], including effecting chemical changes in distinct manners from thermochemical reactions[45,46]. Mechanically and thermally activated processes differ from one another in the following important ways: first, the former take place under non-equilibrium conditions[41,49,54] where several active processes[45] such as unbalanced mechanical forces[39,40,45,48,49], diffusion and mass transfer[41,43,45,56], generation of solid-state defects (high-energy structures)[59], interphases[37,41,45,48,49], and structural relaxation phenomena[45,49] promote chemical reactivity; second, mechanical deformations occur on a local basis being mediated by relaxation phenomena such as crystalline lattice disruption, dislocations, and other defects[45,49] (considerable amount of energy can be added to the reaction system with negligible increase in macroscopic temperature)[45] in contrast to temperature which is an intensive thermodynamic state variable[49]; third, mechanical activation using ball milling as a quintessential discontinuous[41,49] (pulse mode operation; pulses of pressure and temperature)[41] or discrete[49] method can give rise to different milling/working regimes[38,49,50] (ratio of shear/impact/compression)[41,49], which can have material bearing on energy transfer[38] (inhomogeneous distribution of local mechanical stresses)[49] or reactivity[38,50] (in some cases, alternate reaction kinetics or product formation)[38] or process outcome[41], particularly, a shearing regime is found prominently in the main body (central part) of the milling jar whilst an impact and/or compression regime resides predominantly at the jar's ends[38,50] and within its vicinity; fourth, the former cannot be understood on the basis of thermodynamic principles alone[46]. Rather, a holistic viewpoint from three main aspects

(structural disordering, structure relaxation, and structural mobility) can elucidate the concurrent influence of these three factors on the reactivity of solids and their behaviour upon exposure to mechanical energy[49]; fifth, the former's various relaxation processes can manifest themselves in the form of heating, new surface formation, aggregation, defect generation, and enhanced chemical reactivity[49], i.e., mechanical stress relaxation can proceed via several pathways and is highly influential for any ensuing chemical transformations[41]; last, for reasons discussed above, it is hardly unexpected that mechanochemical reactions' outcome need not be the same as in solution or when externally heated[45]. In the end, the lack of predictive models[46] and/or understanding for mechanochemistry's mechanistic aspects[37,46,49,54] could well be responsible for the trial-and-error method/approach[37,38,41,54] or serendipitous results[41] in this practically-oriented field[41], whether it concerns small-scale laboratory transformations[38] or process conversion/scale-up[38].

The application of ball milling as a non-thermal technology with demonstrated capability in efficiently converting polysaccharides (cellulose, chitin, chitosan) to their soluble glucan constituents in mild processing conditions has been pointed out as a 'pivotal' processing/treatment attribute in terms of maintaining carbohydrate stability and purity[60]. Mild processing conditions is undoubtedly preferable over the harsh conditions typically associated with traditional carbohydrate synthesis and modification[4]. Specifically, reactions involving D-glucopyranose type of units carried out under harsh conditions (elevated temperature[30,61] (thermal heating)[62], long reaction times[30,62], (excess) strong acid[4,8,17,22,33,61], (excess) corrosive alkali[17,22]) readily undergo problematic side reactions such as isomerization[4,14], condensation[14], rehydration[14], dehydration[4,14,22], reversion[14], fragmentation[14], and methylation[22], thus forming myriad complex compounds[15,61]. Carbohydrate procedures also frequently involve multi-step protection/deprotection and the employment of copious amount of harmful/hazardous chemicals and solvents which in due course will detrimentally impact human health and the environment[4]. Another notable advantage that ball milling can provide is the ability to effect chemical modification of biological molecules (nucleosides, nucleobases, carbohydrates, etc) in the absence of solvent, circumventing the need for toxic or carcinogenic high boiling polar aprotic solvents such as pyridine or DMF or DMSO[37,63], which were traditionally required because of the characteristic poor solubility of said molecules in conventional solvents[4,30,37]. The

advantageous solvent-free and mild processing characteristics of ball milling offer a simple, efficient, and eco-friendly promising route for the production of high value carbohydrate-based products, but one which hitherto has remained largely unexplored.

Carbohydrates serve important biological functions in cell physiology and metabolism; as fundamental structural building blocks or components of cell surface, they are intricately involved in vital intercellular recognition pathways/events, including bacterial and viral infection, cancer metastasis, apoptosis, and neuronal proliferation to name a few[4]. Carbohydrates being functionalized substrates[2] and readily available in large amount from biomass sources, are promising raw materials for large-scale applications, as such they are of great interest to the chemical, pharmaceutical, cosmetic, detergent and food industries[4]. As previously discussed in section 1.1, chitin biomass produced as waste material from the seafood and fishery industries can be a considerable source of renewable carbohydrates, but at the present time, only a negligible amount of chitin biomass waste is being utilized, mostly in pharmaceutical formulations such as skin moisturizers[20,64], joint-pain analgesic/relievers[20,64], antitumoural[64], anticancer[20], and antimicrobial agents[20,64]. Hence, the potential for sustainable and large scale transformation of chitin biomass waste to high value chemical products offers plentiful economic and environmental opportunities[20]. Chitin and its derivatives (chitosan as the most notable[4,7,20] with a global market valued at 1.5 billion USD in 2015[7]) have a long history in material synthesis, modification, and utilization as functional biopolymers, one which still continues to captivate the attention of researchers in academia and industry[7,65-67], notwithstanding the known difficulties caused by their native solid state morphology, i.e., challenging methods of identification, characterization, modification, processing, and utilization as a biomaterial[4]. Early independent discoveries of chitin have been attributed to several researchers: English scientist A. Hachett in 1799 who described it as a *'material particularly resistant to usual chemicals'*; French botanist Henri Braconnot who isolated chitin in 1811 from the cell wall of fungi by cooking its residue in an alkaline solution after treatment in sulfuric acid, and named it *"fungine"*; French naturalist Odier who used a similar chemical process to isolate chitin from insects in 1823, and named it *"chitine"*; and finally in 1929, chitin's structure was elucidated by Albert Hofmann after its isolation via enzymatic hydrolysis using chitinase[8]. Nowadays, chitosan and its derivatives are used extensively as versatile biomaterials in pharmaceutical[66],

cosmetic[4,8,66], agricultural[4,8] (insecticides)[8] and food[4,8,66] (dietary supplements, food preservatives, antioxidants)[8] industries where different properties such as biocompatibility[8,65-68], biodegradability[4,8,65-68], hydrophilicity[66], non-allergenicity[4,65], non-toxicity[4,65,66], hemostat[65], mucoadhesivity[68], and biological activities[4,65] (antimicrobial[65], antibacterial[8,67], antitumour[8], also *vide infra*) are tailored to meet specific application requirements in drug[8,65,66,68] and gene delivery[8], tissue engineering[8,65], wound dressing[8,65], bone regeneration[8], wastewater treatment/water purification[4,8,65,66], catalysis[65,67], material sciences[66], pharmaceutical[7,65], biomedicine/biomedical[4,7,65], and biosensors[66]. For electrochemical biosensors applications, chitosan's biocompatibility, film-forming capability, and ease in processing it into films, hydrogels, or microspheres makes it an ideal immobilization material[8].

This work will focus on chitooligosaccharides (COS) which due to their low degree of polymerization[28] or shorter chain lengths (less than 20 and an average molecular weight less than 3.9 kDa)[69] and unsubstituted amino groups[4], exhibit enhanced solubility in water at neutral pH values[4,7,28,68,70-72] and reduced viscosity[4,71], thus facilitating their usage under physiological conditions which is of particular significance for biomedical or pharmaceutical applications[7,70]. Also of great pertinence to such fields is that low molecular weight chitosan (LMWC) display heightened antibacterial[7] (against Gram-negative bacterium[73] with proposed mechanism of COS absorbing into cells and penetrating to the bacteria's DNA, resulting in the blockade of RNA transcription)[72], antifungal[74], antitumour[7,72], immunoenhancing[7,72], lower haemolytic[75-79] or hepatotropic[70,75,76,78,79] profile, lower toxicity[68,75-79] (cytotoxicity decreased with decreasing molecular weight)[71,76], and other valuable biological activities at the cellular or molecular level[72] (oligosaccharide fragments eliciting enhanced cellular attachment[80], proliferation[80], increased production of lymphokines[72], mediating cell-cell recognition[81], including cellular infection by bacteria and viruses[81], moderating the behaviour of enzymes and other proteins[81], fulfilling various immune response functions[81], possessing greater information-carrying potential than that of proteins or nucleic acids of equivalent molecular weight[81], and their presence on cell surfaces and many proteins suggests their biological importance in cellular regulation, metabolism and transportation across cell membranes[81], etc) than chitin or high molecular weight chitosan (HMWC), e.g., LMWC with average molecular weight between 5 and 10 kDa show augmented biological activities[7,68] than chitin or HMWC, as such the former are especially fitting as carriers

for DNA delivery[7,70,75,78] or drug delivery (paclitaxel) via oral administration[68]. Additionally, LMWC reveal improved reactivity in grafting, crosslinking, and other types of modification compared to chitin or HMWC, a quality which is favourable in material synthesis[7]. In fact, exploiting the increased chemical reactivity of oligosaccharide residues[4,82] to 'engineer' chemical reactivity on cell surfaces[83] or to introduce a 'specific binding site' on sterically hindered synthetic polymers (but suitably functionalized), proteins, or glycoproteins is a very common polymer field strategy for grafting or modification or bioconjugation that dates back to the mid 1990s[84,85]. Furthermore, LMWC (2 to 6 kDa) utilized as a pH-sensitive coating agent for tumour-specific drug delivery formed smaller size nanoparticles than those originated from HMWC, whilst chitosan-alginate films formed using LMWC resulted in reduced thickness and enhanced transparency compared to those derived from HMWC[7]. LMWC's ability to form films which are thinner, more transparent, and smaller in size than those emanated from HMWC is of prime relevance to biosensors applications, given that such characteristics from the encapsulant material have a direct bearing on the encapsulated biosensor's functionality (sensitivity, selectivity) and intrinsic attribute (impedance). The original motivation for this work was to design a custom encapsulation membrane for the type of specialty biosensors designed, developed, and tested by Dr. Chodavarapu's group, i.e., MEMS capacitive pressure for the timely monitoring of pressure levels in acute compartment syndrome (ACS), a condition in which increased pressure within a closed compartment compromises the circulation and function of tissues within that space[86]. Most common cause of ACS is trauma, usually after a fraction, and its diagnosis is challenging yet requires prompt diagnosis and follow-up[86]. Any delays in treatment could result in significant disability, e.g., neurological deficit, muscle necrosis, amputation, or possibly death[86]. This represents significant challenges including the sparsely available literature, if not non-existent regarding the encapsulation of biosensors, to say the least of this particular niche biomedicine biosensing application. Moreover, it is not obvious that large-scale commodity packaging solutions can be readily adapted for use with this specialty biosensor to meet stringent biomedical requirements, nor is there a clear path from niche/specialty to commodity production scale, thus there exists important hurdles in the way of developing overarching schemes/templates.

1.3 Comparative review

1.3.1 Extraction of chitin and derivatives

Exoskeletons from crustacean shell wastes such as shrimp, crab, lobster, and krill contain significant amounts of the polysaccharide chitin[69], which may be extracted via various steps such as drying[69,87], washing[69,87], precipitation[87], sterilization[87], grinding into powders[69,87], demineralization[17,69,87-89], deproteinization[17,69,87-89], and bleaching/decoloration[17,69] by chemical[17,69,87-90] (including ionic liquids (ILs))[90-92] and/or biological[17,69,87-89] (enzymatic[87-89] or microbiological[17,87-89]) methods. Deacetylation of polysaccharide chitin leads to polysaccharide chitosan, which can proceed via chemical[17,69,89,93] and/or biological (enzymatic)[17,69,89,93] routes. Hydrolysis of biopolymers chitin or chitosan produces chitooligosaccharides by means of physical (hydrothermal[89], microwave[89], or ultrasound[89,94]) and/or chemical[69,89] (including oxidative-reductive depolymerization)[69] and/or biological (enzymatic)[69,89] methods.

1.3.2 Biomedical field sterilization methods of scaffold/hydrogel-based polymeric chitin and derivatives

Sterilization concerns arise when polymers or polymer blends based materials are intended to be in contact with serous fluids, e.g., wounded tissues, as such, additional post-processing/post-modification sterilization protocol steps are required[95]. The biomedical literature is replete with experimental details regarding sterilization methods of scaffold/hydrogel-based polymeric chitin and derivatives, including exposure to dry heat[95,96], saturated steam[95-101], ethylene oxide[95,102], followed with a de-gassing period of 7 days[102], γ-irradiation[95,103], immersion in ethanol solution[104-110], followed with rinsing/washing/solvent exchange with copious amounts of double-distilled[104] or deionized water[109] and/or sterile phosphate-buffered saline (PBS) solution[105-108] and/or further equilibrated for a period of 24 hours[107], whilst acidified aqueous solution of viscous polymeric chitosan are filter-sterilized[99,100].

1.3.3 Biomedical field neutralization methods of acidified aqueous solution of viscous polymeric chitosan

Experimental details concerning neutralization methods of acidified aqueous solution of viscous polymeric chitosan are readily available in large amounts in the biomedical literature, the interested reader is referred to the following references[108-112].

1.3.4 FTIR characterization of chitin and derivatives

FTIR characterization of chitin and derivatives has been extensively reported, the interested reader is referred to the results and discussion of spectra in the following references for the biomedical field[113,114] or biomass pretreatment/valorization/conversion/refining field[19,30,61,87,115-117].

1.3.5 DSC characterization of chitin and derivatives

DSC characterization of chitin and derivatives has been extensively reported in the biomedical literature, the interested reader is referred to the results and discussion of DSC thermograms/curves in the following references[113-116].

1.3.6 Biomedical field/tissue engineering mechanical characterization of fibres/nanofibres-based polymeric chitosan and/or blends with synthetic polymers

It should be recognized that high mechanical strength or performance is neither critical nor essential for implant functionality[118] in many pharmaceutical, e.g., controlled release drug delivery[118] or biomedical applications such as: (1) tissue engineering/temporary scaffolds/hydrogels where providing temporary mechanical function is merely one of the scaffold's roles, albeit a limited one[118,119] which is superseded by the more preeminent role of delivering biofactors, molecules, and biological cells for tissue regeneration[119] or therapeutic payloads[120,121], and (2) wound dressing where a low strength of 0.1 MPa is adequate to meet the strength standard for a wound dressing material, which is satisfied by almost any hydrogel whether non-porous or porous, air-dried or with water content[65]. Recent biomedical literature has been forthcoming about acknowledging the relatively weak/poor mechanical strength of chitosan hydrogels[96,121] which does not preclude such scaffolds (including chitin-based)[122] from being

widely used in nonload bearing areas of tissue engineering[65,102,122], drug delivery[65], wound dressing[65], water purification[65], catalysis[65], and many other areas[65]. Therefore the ensuing brief discussion will exclude the broader tissue engineering field (bladder[65], blood vessel[65,123], bone[65,123], cartilage[65,123], fat[65], ligament[65], liver[65,123], muscle[65], neuron[65], nerve[123], skin[65,123], tendon[65]) and focus on limited load bearing applications which emphasize some mechanical strength, namely bone tissue engineering[121]. Mechanical characterization of randomly oriented and aligned fibres/nanofibres-based polymeric chitosan and/or blends with synthetic polymers has been extensively reported in the tissue engineering field, the interested reader is referred to the results and discussion section of the following references (including chitin fibres)[92,109,110,121,124]. It is important to note that for scaffolds possessing sufficient mechanical strength (26 MPa)[121] for bone tissue engineering load bearing applications, chitosan's content of the fibre scaffold/specimen was reported to be as low as 15% when blended with other synthetic polymers and 65% inorganic crystalline particles of calcium phosphate cement[121,124]. It must also be stressed that temporary mechanical function is but one role expected from the fibre scaffold, other more important ones include: (1) covalent immobilization of biofactors such as BMP-2 (bone morphogenetic protein)[125] and IGF-1 (insulin-like growth factor)[125] into the chitosan nanofibres which impacts higher bioactivity and greater cell proliferation when compared to plain absorption as demonstrated by histological results (good proliferation of osteoblasts and fibroblasts, along with vascularization and reticular networks)[125], (2) delivery of hUCMSCs human umbilical cord stem cells (stem cell seeding)[121,124] which are more potent than bone marrow MSCs (mesenchymal or stromal stem cells)[124], and (3) generally provide a favourable microenvironment for live cell seeding, retention, viability, density, and proliferation[121].

1.3.7 Biomedical field chemical cross-linking of scaffold/hydrogel-based polymeric chitin and derivatives; an early 1990s era paradigm

The tissue engineering concept of a porous, degradable, and bioactive scaffold material of temporary mechanical function able to accommodate and deliver biofactors such as cells, genes, and/or proteins using stem-cell and/or gene-therapy approaches to stimulate tissue repair is one that arose in the early 1990s[119] as an alternative to autografts[126-128] which presents several limitations such as tissue availability[126-128], donor-site pain[128], donor-site morbidity[126-128], secondary deformities[126], potential differences in tissue structure and size[126], infections[128], extra

blood loss[128], and higher patient cost due to longer surgical/operating times[128]. Chemical cross-linking was then considered a novel technique to: (1) enhance mechanical properties but one which unfortunately also reduced biocompatibility[129], and (2) confer a hydrogel surface which is lacking in many bulk synthetic polymers[129]; scaffold design strategy and thinking in the 1990s was rather simple, i.e., strike a balance or find a tradeoff between cross-linking density[129], mechanical strength[119,129], biocompatibility[129], and provide better biofactor delivery[119]. Mid 2010s tissue engineering hydrogel scaffolds are expected to meet an expanded number of design criteria to properly function and promote new tissue formation, which include polymer processability[65], hydrolytic or enzymatic biodegradability[65], biocompatibility, i.e., cell viability/proliferation without triggering inflammatory responses[65], bioactivity[65], e.g., loading antibacterial agent/antibiotic/drug such as minocycline to inhibit both Gram-positive and Gram-negative bacteria by inhibiting bacterial protein synthesis through binding to their ribosomal subunits[130], promote cellular adhesion[65,130], acting as a carrier for controlled drug delivery and release[130], and more advanced design concepts such as hybridization with a second polymer to improve one or several properties[65].

Polymer modifications using physical association networks strategies (ionic complexes[120,121], polyelectrolyte complexes (PECs)[120,121], polymer blends with water-soluble non-ionic polymers[65,106,120,121,131,132], thermoreversible hydrophobic association hydrogels[65,120,121,132]) which exploit physical ionic, electrostatic, hydrophobic, and/or hydrogen bonding interactions (purely physical) between polymer chains create physical hydrogels (gel formation) which are reversible[120,121]. As such, physical hydrogels suffer from severe drawbacks such as weak mechanical strength[120,121], lack of chemical functionalization[120,121], and difficulty in controlling cross-linking degree, physical gel pore size[120,121], and especially, uncontrolled dissolution[106,120,121,131], i.e., lack of stability in aqueous media and/or control over degradation/dissolution rates leading to inconsistent in vivo performance[120,121] which do not match those obtained from in vitro experiments (possibly due to the composition difference between PBS solution in vitro and body fluid in vivo)[130]. Thus, the combination of the above factors are restricting the number of possible applications of such physical hydrogel polymers, including chitosan hydrogels[120,121]. Specific to water-soluble charged ionic polymers such as ionic complexes or PECs with complex set of heterogeneous charged, polar, and apolar groups

capable of interacting with ions via various mechanisms[133], additional concerns related to aqueous stability under saline conditions (salt effects[133], salt concentrations regime[133], Hofmeister salt solutions[133], different salt cations[134], response to subsequent salt additions[134]) need to be addressed; the ionic complex or PECs literature is replete with studies of salt effects on polymer and/or protein solubility and stability at high salt concentration regimes (physiologically irrelevant in vitro conditions)[133] to which the interested reader is referred to[134-136]. In addition to salt concentration effects, other factors which influence PECs complex macromolecular architecture formation and dissociation include: degree of ionization of the polyanions and polycations[68], charge distribution over the polymer chain[68], polymer chain flexibility[68], amount and length of the neutral polymer block[135], electrostatic interaction screening of polymer blocks by small ions[136], pH[68], temperature[68], interaction time[68], ionic strength[68], and concentration of the polymeric solutions[68].

In view of the aforementioned complications associated with polymers based on physical association networks approaches, chemical cross-linking is a proposed solution in the polymer modification field to: (1) improve mechanical strength[129,131,137-139] relative to physical hydrogels[120], and (2) confer stability in aqueous media[140], e.g., chemical cross-linking of water-soluble non-ionic synthetic polymer poly(vinyl alcohol) (PVA) and water insoluble biopolymer derivative carboxymethyl chitin (CMC) using glutaraldehyde to render a polymer blend water insoluble[106] or cross-linking polyblends of collagen-chitosan, collagen-collagen of various source/type or collagen-elastin, and chitin-silk fibroin to prevent aqueous dissolution[138] or chitosan-poly(ethylene oxide) (PEO) (high and low molecular weight) cross-linked with genipin to reduce the weight % loss of LPEO and HPEO (neutral water insoluble chitosan is not included in the in vitro studies of solubility and stability in neutral water)[131]. The polymer modification field relies on small molecule chemical cross-linkers such as glutaraldehyde[108,120,138,140,141], formaldehyde[120,140], D,L-glycealdehyde[140,141], diacrylate[120], diglycidyl ether[108,120], diethyl squarate[120], diisocyanate[108,120], *N*-hydroxysuccinimide[138], carbodiimide[138,140], or genipin (bulky heterocyclic compound)[108,120,131,139-141], and more. However, several shortcomings associated with the use of toxic small molecule chemical cross-linkers[120,138] for polymer modifications have been well documented in the biomedical literature, namely: (1) demonstrated in vitro cytotoxicity[120,138], i.e., negative influence on cell viability, proliferation[141], and activities, which

critically impairs the biocompatibility of cross-linked polymers for use as biomaterials[108], (2) excess amount or concentration of cross-linkers required to push cross-linking reactions of bulky polymers towards completion[139,142], (3) long cross-linking time needed to push cross-linking reactions of bulky polymers towards completion[139], (4) presence of unreacted cross-linkers reagents which are cytotoxic when uncoupled[76,140], thus concern for potential in vivo leaching which could lead to consequent toxic products formation during in vivo biodegradation[140] or confounding results[76], (5) unknown clinical effects (mechanisms of action, reactivity, safety issues), i.e., fate of small molecule cross-linkers in the body has not been established[120], thus currently clinically unviable, (6) possibility of cross-linkers binding covalently to cells[130] or biological tissues[120], (7) increased risk of in vivo calcification[138], (8) in the presence of a therapeutic (e.g., drug, active agent), liable for unfavourable interaction with payloads (e.g., induced chemical reactions with an active agent[121], deactivating[120] or limiting therapeutic release[120]), (9) the need for cross-linked polymers to undergo stringent purifications prior to administration to thoroughly remove trace amounts of unreacted cross-linker agents[76,120], and lastly (10) complete removal of unreacted cross-linking agents could prove challenging or elusive[121]. Therefore, the choice for clinically safe and biocompatible covalent cross-linkers is presently still lacking for biomedical applications[120]. It is important to recall that biocompatibility is of paramount importance in the biomaterials field, if not a central paradigm, and that if techniques such as chemical cross-linking generate biomaterials that have non-specific or inappropriately directed activities or are of dubious clinical safety, then the existence of such biomaterials will always be questionable as there is little point using such materials that do harm (i.e., eliciting any undesirable local or systemic effect in that host), thus violating the first principle of Hippocrates that '*the doctor should do no harm*'[143]. Last but not least, it bears noting that chemically cross-linking chitosan hydrogels is known to: (1) reduce their hydrophilicity[144] and results in hydrogels that are not highly hydrophilic[142], (2) increase their resistance to enzymatic degradation[144], (3) only achieve a low degree of cross-linking (9.9%) for high surface area microspheres in spite of excess amount of cross-linkers used and long cross-linking time[139], and lastly (4) generate uneven cross-linking for high surface area microspheres where cross-linking mostly occurred in the outer layers[139], prompting concerns about possible polymeric leaching of unreacted cross-linkers emanating from the inner layers. Thus, there is a growing body of evidence which suggests that chemical cross-linking, a technique rooted in the early

1990s era and developed for bulk synthetic polymers to confer some mechanical strength, reduce/limit but not entirely prevent dissolution of highly water-soluble non-ionic synthetic polymer or copolymer(s) in aqueous media, and bestow otherwise innately lacking hydrophilicity to hydrophobic surfaces of some copolymer(s), does not adapt/translate well into the processing and/or modification of crystalline, recalcitrant, renewable feedstock cellulosic, chitinous, or lignocellulosic biomass type of substrates; it is imperative in late 2010s to find, pursue, and develop alternative, novel, efficient, and above all sustainable approaches including solvent-free protocols for the chemical conversion and biomass valorization of renewable feedstocks.

1.3.8 Biomass field pretreatment methods

Biomass pretreatment methods have been extensively reported elsewhere and are usually classified into physical, physiocochemical, chemical, and biological classes of pretreatment methods; the interested reader is referred to the following references for the biomass field[145-148] from which tables containing a brief description and/or process conditions, advantages, and disadvantages for different classes of pretreatment methods and biomass pretreatment methods were compiled (see Tables 1.1-1.3).

Table 1.1
Comparison of different physical biomass pretreatment methods

Pretreatment methods	Brief description and/or process conditions	Advantages	Disadvantages
Mechanical comminution	• Biomass comminution using milling or grinding machines such as ball, vibro, hammer, knife, two-roll, colloid, and attrition mills, as well as extruders	• Reduction in particle size • Reduction in crystallinity • Increase in surface area • Depolymerization possible under right conditions • Ease of sample handling • Not restricted to laboratory scale • Thermal energy not required	• Relatively energy intensive process
Microwave irradiation	• Microwave heating of biomass	• Simple operation • Energy-efficient • Possibility of accelerating reaction rates • Possibility of short reaction time	• Relatively high cost • Restricted to laboratory scale
Hydrothermal pretreatment/liquid hot water pretreatment	• Pressure (1-3.5 MPa) is applied to maintain water in the liquid state at elevated temperature (160-240 °C) • pH range is 4-7 and reaction time from 15 min to several hours	• Does not require any catalysts or chemicals • Uses low costs reactors • No hydrolysis to monosaccharides	• High water demands • High energy requirements • Relatively low biomass loading • Less efficient compared to methods using chemical agents

Table 1.1 Comparison of different physical biomass pretreatment methods

Table 1.2
Comparison of different physicochemical biomass pretreatment methods

Pretreatment methods	Brief description and/or process conditions	Advantages	Disadvantages
Acid catalyzed stream explosion	• Biomass treatment with steam at high temperature (160-220 °C) and pressure (0.7-4.8 MPa) • Steam explosion is catalyzed by addition of H_2SO_4 or SO_2	• Lesser energy requirements than mechanical processes • Lesser corrosion • Limited chemical use	• Byproducts (furfural, HMF, acetic acid) formation which inhibit enzymatic hydrolysis and fermentation • Need to wash the solids • Risk of condensation and/or precipitation of soluble fractions
Ammonia fibre explosion (AFEX)	• Biomass treatment with anhydrous liquid ammonia at 60-120 °C and above 3 MPa for 30-60 min, followed by rapid decompression	• Reduction in crystallinity • Increase in surface area • Moderate temperature and lesser residence time used	• Cost and environmental concerns • Less efficient for softwood based biomass
$scCO_2$ explosion	• $scCO_2$ is delivered at high pressure to a vessel or into a high pressure vessel containing biomass • Vessel is heated up to 200 °C and held for set duration allowing CO_2 penetration into biomass • Pressure release causes explosion of biomass structure increasing surface area • Carbonic acid formation catalyzes hydrolysis of hemicellulose type of biomass	• Low cost of CO_2 • High solids capacity	• High capital costs (high pressure vessels are required) • Proven effectiveness restricted to small scale • Effect on carbohydrate biomass yet to be established

Table 1.2 Comparison of different physicochemical biomass pretreatment methods

Table 1.3
Comparison of different chemical biomass pretreatment methods

Pretreatment methods	Brief description and/or process conditions	Advantages	Disadvantages
Concentrated acid pretreatment	• Operated under low temperature (40 °C) with concentrated acid (30-70%) • Inorganic acids (H_2SO_4, H_3PO_4) commonly used	• H_2SO_4 conc. is highly effective for cellulose hydrolysis and affords high glucose recovery yields • High hemicellulose solubility • Thermal energy not required	• Large amount of acidic waste • Large amount of salt formation • Highly toxic and corrosive process • Costly and specialized non-metallic reactors • High operational and maintenance costs
Dilute acid pretreatment	• Acid concentration range 0.1-4 % • Operated under high temperature (180-230 °C) for a short period of time or at milder temperature (120 °C) for longer retention time (30-90 min) • Inorganic acids (H_2SO_4, HCl, H_3PO_4, HNO_3) or organic acids (fumaric, maleic) can be used	• Effective • Inexpensive • High enzymatic digestibility • Relatively lesser corrosion • Relatively limited chemical use	• Large amount of acidic waste • Large amount of salt formation • Highly toxic and corrosive process • Costly and specialized non-metallic reactors • High operational and maintenance costs • Catalyst recovery issue • Extended high temperature treatment results in sugar degradation loss
Alkaline pretreatment	• Operated under low temperature for a long time with concentrated bases such as NaOH, KOH, $Ca(OH)_2$, NH_4OH, hydrazine, anhydrous ammonia, etc	• Thermal energy not required • Relatively lesser corrosion than acid pretreatment • Lower operating temperature and pressure results in lower concentration of degradation products	• Alkaline pretreatment processes not very suited for softwood recalcitrant biomass • Need for pH adjustments for subsequent processes • Conversion of alkali to irrecoverable salts or incorporation as salts into the biomass • High cost of organic bases

(*continued on next page*)

Table 1.3 (*continued*)

Pretreatment methods	Brief description and/or process conditions	Advantages	Disadvantages
Ozonolysis	• Treatment of lignocellulosic biomass with ozone gas, usually at mild ambient temperature and pressure • Reaction time is several hours	• Selective lignin degradation with minimal effects on on hemicellulose or cellulose • Lesser generation of furfural and HMF • Mild operational conditions are employed • On-site ozone generation and direct utilization • Ozonolysis byproducts like formic acid and acetic acid can be metabolized by microorganisms and animals	• Large amount of ozone required and high ozone generation cost (large energy demands) can make process economically unviable • Limited studies on lignin structure modification during ozone pretreatment • Full-scale biomass pretreatment with ozone has not yet been developed • Highly reactive, flammable, corrosive, and toxic properties of ozone makes the process dangerous • Exothermic characteristics of process may require cooling systems
Organosolv pretreatment	• Treatment with mixtures of organic solvents (methanol, ethanol, acetone, ethylene glycol) with acid catalyzed (HCl, H_2SO_4, oxalic, salicyclic) aqueous solutions to hydrolyze hemicellulose or lignin • Carried out at high temperatures (100-250 °C)	• High purity lignin can be obtained • Minimum cellulose loss (< 2%) • Low sugar degradation • High pretreatment material yield	• Need to remove solvents from the reactor by evaporation, condensation, and recycling • High cost and safety concerns with some of the solvents used
Ionic liquid pretreatment	• ILs can solubilize cellulose • ILs possibly compete and disrupt lignocellulosic material's hydrogen bonding network	• IL pretreatment decreases biomass recalcitrance and improves subsequent enzymatic hydrolysis • Reduces cellulose's crystallinity and increases its accessibility to chemical reagents	• High costs of ILs • Need for efficient IL recovery and recyclability • Toxicity of some ILs • Purity of ILs is crucial for biomass pretreatment • Recovery of solubilized cellulose/hemicellulose is a challenge • IL pretreatment of lignocellulosic biomass at a commercial scale is still a challenge

Table 1.3 Comparison of different chemical biomass pretreatment methods

1.3.9 Medicinal chemistry field molecular hybridization

The molecular hybridization design strategy of covalently combining two or more (similar or dissimilar) drugs or pharmacophores or active fragments or moieties into a single molecule or molecular platform or structural frame[149-159] is one which has been pursued with increasing prevalence in recent years the realm of medicinal chemistry[150,152,155-159]. It is a proven and effective approach for designing novel compounds or entities which exhibit increased[156,157] or additive[150,157] or synergistic[149,150,157] biological activities including the exploration (a worthy scientific endeavour)[153], discovery (urgent need to discover new drugs against some widespread and lethal diseases such as tuberculosis (1.4 million deaths and 10.4 million clinical cases), for which no new chemical entity has emerged in the last 50 years after the discovery of rifampicin (RIF))[160], investigation, and development of structurally new classes of agents with novel mechanism of action[151,152,157] or for the structural modification of existing scaffolds or agents or lead candidates[151-153,157,160] for further optimization/improvement of pharmacokinetic (PK) profiles[157,159], binding affinity[149,151-154,157-159], bioavailability[151,152,157], drug-like properties[149,153,154,156,157,160], enhanced solubility[149], stability to metabolic degradation[151,153,157-159], absorption, distribution, metabolism, and elimination (ADME) safety profiles[151,152,157,159,160], increased potency[151,153,154,156-158,160], lowered effective concentrations[156], increased selectivity[151,153,154,157], lowered cytotoxicity against normal cell lines[151,154,155,157] but increased cytotoxicity against cancer cell lines[153-155,158,159] or bacteria[151,156,157,160] or fungi[156] or parasites[156], and/or a spectrum of interesting biological activities[152,153,155,158,159] to fine-tune the interaction with targeted binding site(s), e.g., the employment of such design strategy offers the possibility of dual-action or hybrid drugs[152,161], where each drug moiety is designed to bind independently to two different biological targets and synchronously accumulate at both target sites which is an attractive approach to overcome bacterial strain resistance to clinically available drugs[152,153,160] (including the major public health concerns of emerging, reemerging, and alarmingly increasing microbial threats manifested worldwide[152] in the form of drug-resistant bacteria[160], multi-drug resistant (MDR) Gram-positive bacteria[152,153,160] such as methicillin-resistant *Staphylococcus aureus* (MRSA)[152,153] or vancomycin-resistant *Enterococcus faecium* (VRE)[153], extensively drug-resistant bacteria (XDR)[160], and totally drug resistant bacteria (TDR)[160]) and reduce the appearance of new resistant strains[151,152].

In this context, the application of copper(I)-catalyzed azide alkyne Huisgen [3 + 2] cycloaddition (CuAAC) click chemistry to connect other pharmacophores, including natural product-based scaffolds[153,154,156-159], employing the 1,2,3-triazole moiety product of this reaction not merely as a linker but also as an invaluable pharmacophore element that is widely used in medicinal chemistry[152-154,156-159,162], has acquired great significance in recent years[153,156,158,159]. The synthetic utility of the CuAAC reaction for regioselective 1,2,3-triazole formation can be better appreciated when one considers that the classical multi-step solution-based synthesis approach of preparing biologically active materials meeting pharmaceutical requirements for highly functionalized, combinatorially decorated, and sophisticated scaffolds that are more drug-like molecules from small, commercially available building blocks or monomers often requires at least ten transformations (long linear syntheses) for conversion into most modern drugs, and that for more complex molecules, it is not uncommon to use in excess of twenty steps[163]. Having presented the CuAAC reaction as a convenient, useful, proven, and reliable means to rapidly access complex drug-like molecules/scaffolds and practical solution for the preparation of large chemical libraries, i.e., a diverse compound library, it must be stressed that the recognition for cycloaddition type of reactions such as Diels-Alder or Pauson-Khand having undeniable combinatorial potential for the construction of carbocyclic compounds[164] actually pre-dates the development of the CuAAC reaction. In fact, the participation of the azide as a 1,3-dipole in a [3 + 2] cycloaddition with alkenes and alkynes was first reported as early as the end of nineteenth century, and later on when Rolf Huisgen introduced the concept of 1,3-dipolar cycloadditions in the 1950s, the reaction was proposed to proceed by a concerted cycloaddition[165]. Whilst it must be acknowledged that the palette of chemical reactions developed within the last 100 years is exceedingly broad, however, many of these established reactions reveal major limitations within a contemporary twenty-first century setting[166]. In the case of the Huisgen [3 + 2] cycloaddition reaction, high temperatures or pressures are required to promote the cycloaddition of azides and most dipolarophiles[165,167] (i.e., it has the limitations associated with any thermal process that requires heat)[168], but more severely, it usually produces two regioisomers, 1,4- and 1,5-[167,168]. Moreover, Huisgen's [3 + 2] cycloaddition is usually slow in the absence of an appropriate catalyst as alkynes are poor 1,3-dipole acceptors[166]. Thus, Huisgen's 1,3-dipolar cycloaddition was a long-neglected reaction[166] and his findings was largely confined to the sphere of academic teaching tools with no other perceived utility to fulfil application-based goals[169]. Although it is

very rare in contemporary science to uncover a very simple modification of a classical "named reaction" that dramatically improves its value, but in the case of the Huisgen [3 + 2] cycloaddition, this happened when the groups of Meldal, then Sharpless independently found that copper(I) catalysts dramatically accelerate the reaction and more remarkably, render it totally regioselective for the 1,4-regioisomer[165,168]. As such, Huisgen's [3 + 2] cycloaddition experienced a renaissance[166,169] and is now termed the CuAAC reaction. By leveraging the formation of a copper acetylide to activate terminal alkynes toward reacting with azides, the catalyzed cycloaddition proceeds roughly seven orders of magnitude faster than the original Huisgen [3 + 2] cycloaddition, and can be further accelerated by the use of specific ligands for copper(I)[165]. Indeed, the CuAAC reaction has become the quintessential or archetypical example of a click reaction[165,166] which measures up to the set of stringent criteria described by the click chemistry concept introduced by Sharpless in 2001, i.e., highly thermodynamically-driven, rapidly proceeding to completion, wide scope, high yielding, modular, stereospecific but not necessarily enantioselective reactions that generate inoffensive byproducts, and ideally, reactions that are insensitive to oxygen and water, make use of readily available starting materials and reagents, can proceed solventless, or by using easily removed solvent(s) or benign solvent(s) such as water, and lastly, forming product that are stable under physiological conditions[170]. Unfortunately, too few reactions are able to fit these criteria in organic chemistry[168]!

1.3.10 Coumarin 1,2,3-triazole hybrids

As alluded to in the previous section, the exploration of new heterocycles that can exhibit potency to multiple biological target is a worthy scientific endeavour. Amongst the oxygen heterocycles, coumarins: (1) constitute an important class of benzopyrones (privileged structural motif as α-benzopyrones) that are widely found in nature in numerous plant-derived compounds, (2) act as a structural subunit of more complex natural products, (3) generally display a broad spectrum of biological activities such as antibacterial[151,153,157,171] (e.g., aminocoumarin analogues such as novobiocin[153,172], chlorobiocin[172], coumermycin[172], and simocyclione[172]), antiproliferation[157], anticancer[151,153,157,173,174] (novobiocin analogues)[159], anticonvulsant[157], anticoagulant[153] (e.g., 4-hydroxycoumarin analogues such as warfarin)[157,172], anti-inflammatory[151,157], anti-HCV[151,157], anti-HIV[157] (e.g., 4-hydroxycoumarin analogues such as phenprocoumon)[172], anti-Alzheimer[157], antifungal[151,157], antimalarial[157], antioxidant[157],

rodenticide (e.g., warfarin)[157,172], antitubercular[151,157,174], antithrombotic[153], DNA gyrase inhibitor (e.g., novobiocin)[174] and antiviral (e.g., phenprocoumon)[172] profiles, and (4) of high relevance for medicinal chemistry, coumarins possess an innate ability to exert a multitude of noncovalent interactions (π-π, hydrophobic, electrostatic, hydrogen bonding, metal coordination, van der Waals force, etc) with various active sites in organisms[157]. In addition to the abovementioned ones, other coumarin based drugs approved for therapeutic purposes include acenocoumarol, dicoumarolum, hymecromone, and carbochromen; their successful clinical usage thereby serves as an inspiration for more research towards the exploration and creation of a library of structurally diverse derivatives based on the coumarin skeleton[157]. A sound rationale for its inclusion in molecular hybridization designs is underpinned by observations that hybridizing the coumarin nucleus with other moieties such as 1,2,3-triazole has afforded new molecules with improved antibacterial and anticancer activity profiles[153]. Coumarin hybridized derivatives were reported to target a multitude of cancer related pathways such as kinase inhibition, angiogenesis inhibition, heat shock protein (Hsp90) inhibition (e.g., known DNA gyrase inhibitor novobiocin binds to a nucleotide-binding site located on the Hsp90 C-terminus and induces degradation of Hsp90-dependent client proteins in breast cancer cells)[174], telomerase inhibition, cell cycle arrest, antimitotic activity, carbonic anhydrase inhibition, mono-carboxylate transporters inhibition, aromatase inhibition, and sulfatase inhibition[153].

On the other hand, azoles such as 1,2,3-triazole, 1,2,4-triazole, thiazole, benzothiazole, benzotriazole, triazolopyrimidine, imidazole, pyrazole, and 1,3,4-oxadiazole, are amongst the most important classes of nitrogen-containing heterocycles[151,157]. 1,2,3-triazole derivatives have especially drawn considerable attention in medicinal chemistry and drug discovery for: (1) being one of the key structural subunit found in a large collection of bioactive molecules with wide range pharmaceutical uses as antibacterial[152,153,158], antineoplastic[175], analgesic[175], anti-allergic[158], anticancer[152,153], anticonvulsant[175,176], anti-inflammatory[158,175,176], local anesthetic[175], anti-HIV[152,158,175], antifungal[152,158], dopamine D2 receptor ligands (related to Schizophrenia)[176], DNA cleaving[175], β-lactamase inhibitors[176], antimalarial[175], antimicrobial[175,176], antiplatelet[176], antitubercular[152,158,175] agents, (2) possessing excellent PK characteristics[159], favourable safety profile[159], latent ability for hydrogen bonds formation which could facilitate binding to biomolecular targets[151-153,157,159,160], moderate dipole character[151,157,159,160], stability under in vivo

conditions (metabolic degradation) to acidic or basic hydrolysis or oxidation or reduction[151-153,157,159,160], and (3) showing potential as promising candidates for the treatment of tuberculosis, i.e., emerging as an important novel class of antituberculosis agents[151] (1,2,3-triazole based mycobacterium tuberculosis (Mtb) inhibitors)[154]. Triazoles, akin to isoniazid (INH), inhibit the growth of mycobacteria by blocking lipid biosynthesis and/or additional mechanisms[151], which is one of the most appealing strategies for developing effective antitubercular agents[151]. Given that: (1) INH has been used over 60 years and remains one of the most effective first-line antituberculosis drug for the treatment of tuberculosis infection, and (2) both INH and 1,2,3-triazole act by similar mechanism(s), thus hybridizing both pharmacophores into a single molecule is a promising strategy which could result in candidates with reinforced antitubercular activity[151]. A few 1,2,3-triazole based drugs approved for therapeutic purposes include antibacterial agents tazobactam[156,158,160], antibiotic agent cefatrizine[151,156,158,160], anti-HIV agent TSAO[151,160], and anticancer agent carboxyamidotriazole (CAI)[151,158,160,162].

A library of coumarin 1,2,3-triazole hybrids were synthesized and screened for different bioactivity with the coumarin nuclei conjugated in the 3th, 4th, or 7th position; the novobiocin analogues exhibited potent cytotoxic activity against breast cancer cell lines by inducing apoptosis or displayed antitumour activity through arresting G_2/M cell-cycle and inducing apoptosis[153,159].

1.3.11 Sugar coumarin hybrids

A sugar coumarin hybrid (7-amino-4-methylcoumarin-β-D-glucopyranoside) derivative was prepared as an antitumour agent and was evaluated for anticancer activity in various cancer cell lines (human prostate (PC-3), human gastric (SGC-7901), human lung (A549), and human breast (MDA-MB-435) cancer cells) using 5-fluorouracil (5-FU) as standard[173]; 5-FU, a well-known antimetabolite drug[177], has been widely employed as first-line treatment against cancer for many years[178]. The sugar coumarin hybrid derivative was tested in normal human liver (L-02) cells and was found to inhibit all four cancer cell lines (IC_{50} 48.7, 25.4, 6.1, and 68.4 μM respectively)[173].

A US patent describes the use of coumarin-3-carboxamide novobiocin analogues either possessing or lacking a noviose sugar substituent in the treatment of polycystic kidney disease (PKD), which is a genetic kidney disorder characterized by cyst formation and progressive enlargement of both kidneys, leading to end-stage renal disease[179]. The autosomal dominant (ADPKD) is the most common type and is a severe disorder affecting approximately 1 in every 400-1000 live births[179]. Note that PDK manifestations are not limited to the kidneys, cyst development can also occur in the liver, pancreas, membranes surrounding the brain and central nervous system, as well as in seminal vesicles. Thus, the development of therapeutically effective analogues that can interfere with the molecular pathways of cystogenesis to reduce cyst formation and/or growth in ADPKD would be highly desirable[179].

1.3.12 Sugar 1,2,3-triazole hybrids

A set of pentose sugar (D-xylose, D-ribose, and D-arabinose) 1,2,3-triazole hybrids were synthesized and evaluated for in vitro antitubercular potential, and all hybrids displayed moderate antitubercular activity against Mtb $H_{37}Rv$ with MIC $\geq$ 12.5 μg/mL[151].

A series of sugar 1,2,3-triazole hybrids were synthesized as potential inhibitors of mycobacterial cell wall biosynthesis in order to systematically investigate the effect of varying the hydrophobic substituent[151]. A study revealed the strong dependence on the identity of the hydrophobic side chain on the sugar 1,2,3-triazole hybrids' anti-mycobacterial activities against *M. bovis* BCG[151]. Furthermore, the preliminary results showed that the most active derivatives were potent against Mtb $H_{37}Rv$ with MIC of 6.25 μg/mL, though they were less active than the references ethambutol (EMB) (MIC: 1.56 μg/mL), RIF (MIC: 0.10 μg/mL), and INH (MIC: 0.05 μg/mL). Thus, further modifications of sugar 1,2,3-triazole hydrids-based lead candidates may result in more potent antitubercular hybrids, which are emerging as an important class of novel antitubercular candidates[151].

1.4 Statement of originality

In this work, we hypothesize that a novel encapsulation design concept of employing a carbohydrate (oligosaccharide) shell may be used to encapsulate a biosensor envisaged for in vivo deployment. We will present a novel concept of producing modified oligosaccharide molecules with tailor-made properties intended for specialty/niche biomedicine biosensor application. To this end, the deliberate utilization of mechanical forces and energy by means of high speed ball milling (HSBM) to effect purposeful and constructive chemical transformations of recalcitrant oligosaccharides, as a non-thermal and solvent-free method for the preparation of useful new materials and platform molecules will be demonstrated, in this case, a tailor-made chitosan oligosaccharide (COS) with late-stage incorporation of a side chain with potential anticancer, antitumour, and/or antitubercular profiles (see discussions in sections 1.3.10, p. 29, 1.3.11, p. 29, 1.3.12, p. 30, and Chapter 3, p. 79). COS and LMWC have been extensively reported in the literature (see discussion in section 1.2, p. 12) to exhibit augmented antibacterial, antifungal, antitumour, immunoenhancing, lower haemolytic or hepatotropic profile, lower toxicity (cytotoxicity decreased with decreasing molecular weight), and other biological activities at the cellular or molecular level (oligosaccharide fragments eliciting enhanced cellular attachment, proliferation, increased production of lymphokines, mediating cell-cell recognition, including cellular infection by bacteria and viruses, moderating the behaviour of enzymes and other proteins, fulfilling various immune response functions, possessing greater information-carrying potential than that of proteins or nucleic acids of equivalent molecular weight, and their presence on cell surfaces and many proteins suggests their biological importance in cellular regulation, metabolism and transportation across cell membranes, etc) whilst forming thinner, more transparent, and smaller sized films than the polymeric chitin or HMWC commonly used in many applications; the above properties would undeniably be desirable for biosensing applications (see discussion in section 1.2, p. 13). This work aims to demonstrate a proof-of-concept for producing high-value oligosaccharide biomaterials from abundant and renewable biomass carbohydrate residues (shellfish waste) which are inherently biodegradable, as a sustainable carbon based feedstock, hence fully embracing the concept of a waste-based biorefinery. The biomass conversion in this work is guided by the design philosophy of using milder processing/treatment conditions (enabled by mechanochemistry) in order to preserve

Nature's highly functionalized biomacromolecules (valorized as precious resources), retaining a high proportion of the original chemical structure, functionality, and complexity, as a value creation strategy[3,18], thus departing from the normative tradition of synthesizing complex molecules from simpler starting precursors[18].

The following chapter will describe the general experimental methods and the detailed procedures/protocols that have been employed in this work for the versatile and efficient construction of said high-value oligosaccharide biomaterial envisaged for biosensor encapsulation by means of non-thermal and solvent-free HSBM methodology.

CHAPTER 2
MATERIALS AND METHODS

2.1 General experimental methods

Unless otherwise stated, solution-based reactions were carried out with magnetic stirring. Moisture or air sensitive solution-based reactions are performed under argon (Ar) atmosphere with freshly dried solvents using standard Schlenk techniques (syringe, cannula, septum) in oven-dried glassware (120 °C vacuum oven temperature, overnight storage). Molecular sieves (4 Å 4-8 mesh, ACP Chemicals) were activated overnight in the said vacuum oven. If dried solvents were required, tetrahydrofuran, dichloromethane, and other solvents were purified using a Pure Solv (Innovative Technology) solvent purification system. Furthermore, glassware, syringes, and needles were dried with a heatgun at 260-399 °C or flamed-dried using a Bunsen burner immediately prior to use. External bath thermometers were used to record all reaction temperatures. Low temperature reactions were carried out in a Dewar vessel filled with acetone/dry ice (temperature between -78 °C and 0 °C) or deionized water/ice (0 °C). High temperature reactions were conducted using a heated silicon oil bath in reaction vessels equipped with a reflux condenser or in pressure tubes. Organic solutions were concentrated *in vacuo* under reduced pressure (diaphragm pump) on a Büchi rotary evaporator using a water bath, and if required, further concentrated under a high vacuum line reduced pressure (oil pump) at room temperature. Except for acetone purchased from ACP Chemicals as 'Lab-grade' reagents, all other solvents (ethyl acetate, hexane, methylene chloride, methanol, ethanol, tetrahydrofuran, diethyl ether, triethylamine) were purchased from commercial sources including Fisher Scientific and Sigma-Aldrich as 'certified ACS' reagents. Unless otherwise stated, chemicals and reagents with purity > 95% (purum) were used as received. 3-(Bromoacetyl)coumarin (97%), copper(II) sulfate pentahydrate ACS reagent (≥98%), 9-fluorenylmethyl chloroformate (97%), sodium azide, reagent plus® (≥99.5%), propargyl bromide solution purum, ~80% in toluene (PhMe), (+)-sodium L-ascorbate BioXtra (≥99.0%), phosphorous tribromide (97%), and low molecular

weight chitosan (Poly(D-glucosamine)*Deacetylated chitin) were purchased from Sigma-Aldrich Canada Co.

Retsch MM200 and MM400 shaker/mixer/vibratory/grinding mills

Typical neat/solvent-free ball milling procedures/mechanochemical experiments (see Figure 2.1) were performed by placing a mixture of solid reactants into a 15 mL PTFE Teflon milling/grinding jar, along with four hardened stainless steel ball bearings (grinding balls) of 5 mm diameter or one zirconia grinding ball of 10 mm diameter. The jar were sealed with Parafilm M® laboratory film (however not hermetically) and the samples were then ground in a Retsch MM200 grinding mill operating at a frequency of 25 Hz (30 Hz for the Retsch MM400 grinding mill) in increments/segments of 60 or 90 min. Post-reaction, the crude mixtures were meticulously scraped from the jar using clean laboratory spatulas, readily available for the ensuing work-up.

Reactions involving either a Retsch MM200 or MM400 grinding mill will be denoted as 'MM' for mixer mill (see any Scheme in references)[44,57], and in this work, see Eqs in Figures 2.10 and 2.20. Note that the use of 'Scheme' is more often encountered in the chemical literature as a label to refer to reaction equations, see references[44,57,180], whether it appears in conjunction with co-label 'Figure' or not, regardless of their order of co-appearance (very common in the body of the text), including their usage as caption in the form of 'Figure x. Scheme', see references[40,181-185].

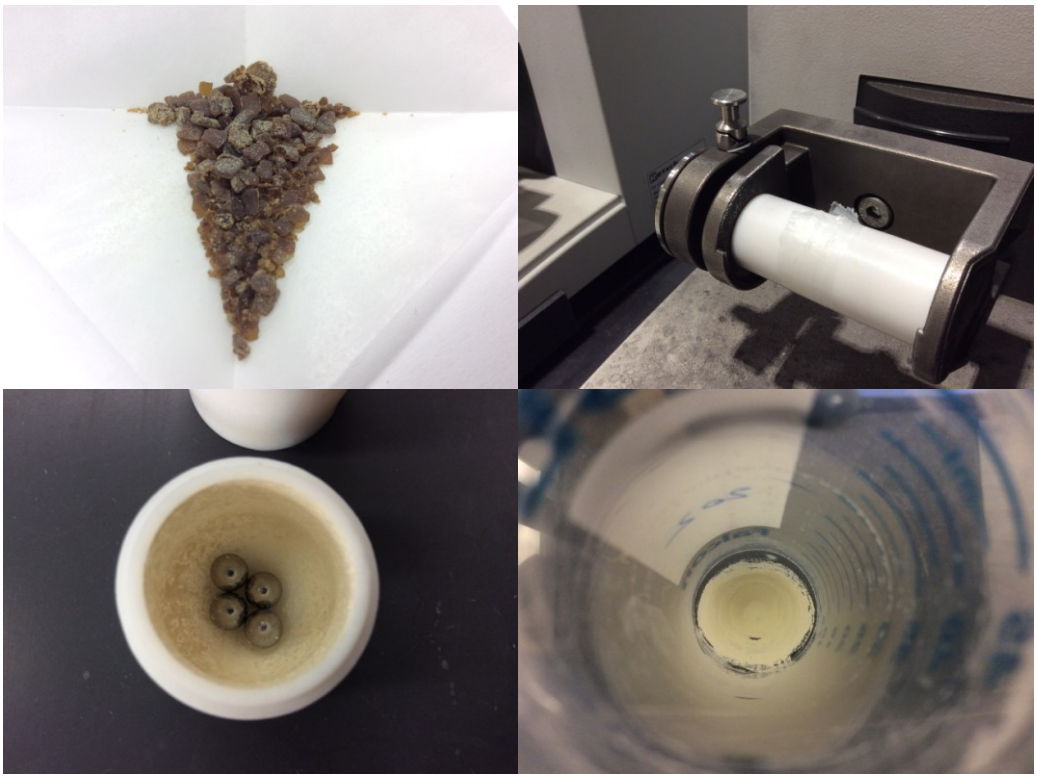

Figure 2.1 Illustration of the procedure for a typical neat/solvent-free ball milling/mechanochemical experiment

Flash column chromatography (FCC)

FCC was performed using silica gel (SiliaFlash® P60, particle size 40-63 μm, 230-400 mesh) purchased from Silicycle. All reactions were monitored by analytical thin layer chromatography (TLC) using EMD/Merck silica gel 60 F254 pre-coated/glass-backed plates (purchased from Sigma-Aldrich Canada Co.) which were visualized under UV light at 254 nm and/or further developed/dipped/heated using H_2SO_4 (conc.), I_2, or basic $KMnO_4$ stains.

NMR spectroscopy

Unless otherwise stated, 1D experiments (^{1}H, ^{13}C) and 2D experiments (COSY, HSQC, HMBC) NMR spectra were recorded at room/ambient temperature on Bruker 500 MHz AVIIIHD 500, Bruker 400 MHz AVIIIHD 400, and Varian/Agilent 500 MHz VNMRS solution NMR instruments/spectrometers, using as received deuterated solvents purchased from Cambridge Isotope Laboratories: deuterium oxide (D_2O), deuterochloroform ($CDCl_3$), and hexadeuterodimethyl sulfoxide (DMSO-d_6). ^{1}H and ^{13}C NMR spectra were referenced to the appropriate residual solvent peaks used as internal reference, e.g., $CDCl_3$ (δH = 7.26 ppm, δC = 77.2 ppm), DMSO-d_6 (δH = 2.50 ppm, δC = 39.5 ppm). NMR spectra are reported using the following abbreviations: chemical shift δ in ppm (multiplicity, coupling constant *J* in Hz, number of protons) for ^{1}H NMR spectra and chemical shift δ in ppm for ^{13}C NMR spectra. Multiplicities are abbreviated as follows: s = singlet, d = doublet, t = triplet, q = quartet, p = quintet, m = multiplet, br = broad, or combinations thereof. Assignments of ^{1}H and ^{13}C NMR signals were made, where possible, using information ascertained from COSY, HSQC, and HMBC experiments.

All reactions were carried out at least in triplicate, except for the Cu(I)-catalyzed Huisgen [3 + 2] cycloaddition which was run in duplicate, and the highest yield is given. Unless otherwise specified, all yields are isolated, and for unfamiliar readers, the yield was calculated based on the molar amount of each starting material.

The author would prefer to describe the complete synthesis and modification routes using the concise narrative style in the chemical literature (good scientific writing should be as terse and concise as possible) as in 'The synthesis began with the preparation of ... to yield/to furnish ... (Scheme...)', see reference[180]. Here instead, an engineering style objective-driven description of the work will be employed:

The work was broken down into the following sub-objectives:

Preparation of highly deacetylated chitosan oligosaccharides (COS) (key intermediate):

- Purification of polymeric chitosan (starting material, see Figure A.22)
- One-step simultaneous depolymerization and deacetylation (see Figure 2.8)
- Neat/solvent-free ball milling installation for Fmoc-N-protection of oligosaccharides (see Figure 2.10)

Preparation of a side chain with potential medicinal/therapeutic relevance (key intermediate)

- Mono-propargylation of tetraethylene glycol (see Figure 2.12)
- Bromination of mono-propargylated tetraethylene glycol (see Figure 2.14)
- Cu(I)-free Sandmeyer azidation of 7-amino-4-methylcoumarin (see Figure 2.16)
- Cu(I)-catalyzed Huisgen 1,3-dipolar cycloaddition (see Figure 2.18)

AND

Neat/solvent-free ball milling installation of medicinally/therapeutically relevant side chain on the highly deacetylated chitosan oligosaccharides (COS) main substrate (see Figure 2.20)

Thus, for the complete synthesis route of a side chain with potential medicinal/therapeutic relevance, see Figures 2.2-2.4. For the completion of the modification of highly deacetylated chitosan oligosaccharides (COS), see Figures 2.5 and 2.6.

Scheme 1. Synthesis of propargylated and brominated heterobifunctional tetraethylene glycol-based spacer/linker 1-bromo-3,6,9,12-tetraoxapentadec-14-yne 7

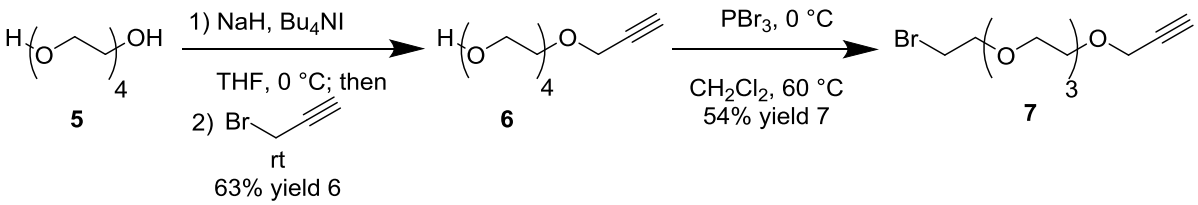

Figure 2.2 Synthesis of propargylated and brominated heterobifunctional tetraethylene glycol-based spacer/linker 1-bromo-3,6,9,12-tetraoxapentadec-14-yne **7**

Scheme 2. Synthesis of 7-azido-4-methyl-2*H*-chromen-2-one 9

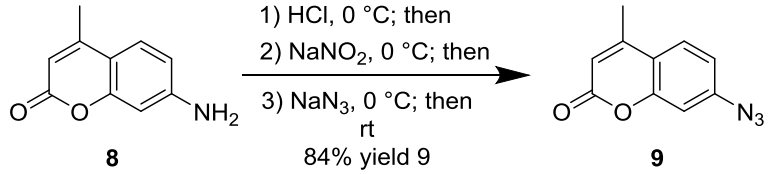

Figure 2.3 Synthesis of 7-azido-4-methyl-2*H*-chromen-2-one **9**

Scheme 3. Convergent synthesis of a medicinally/therapeutically relevant precursor side chain 10

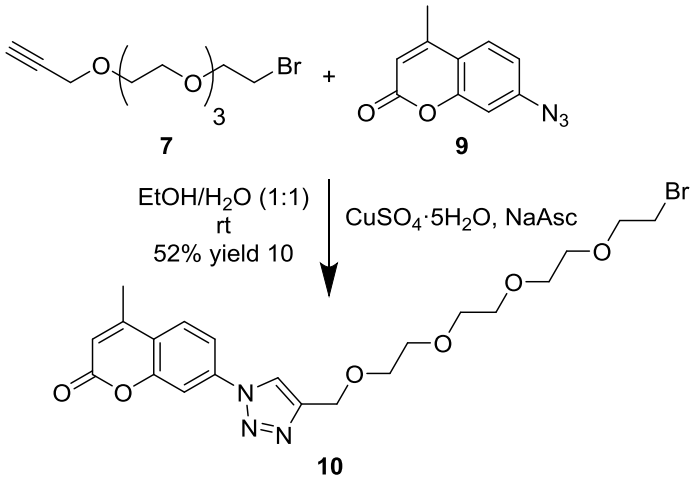

Figure 2.4 Convergent synthesis of a medicinally/therapeutically relevant precursor side chain **10**

Scheme 4. Modification of a highly deacetylated chitosan oligosaccharides (COS) precursor 4

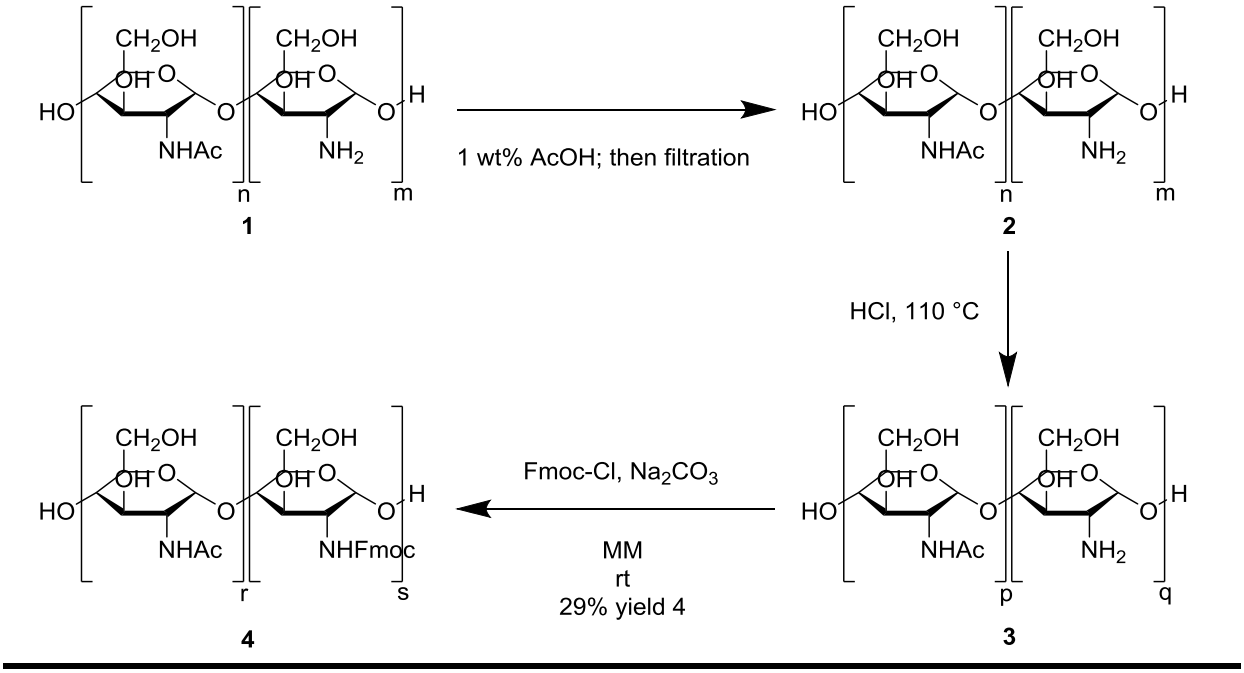

Figure 2.5 Modification of a highly deacetylated chitosan oligosaccharides (COS) precursor **4**

Scheme 5. Completion of the modification of a (COS) functionalized/hybridized with 1,2,3-triazole heterocycle/coumarin scaffolds as a desired final product 11

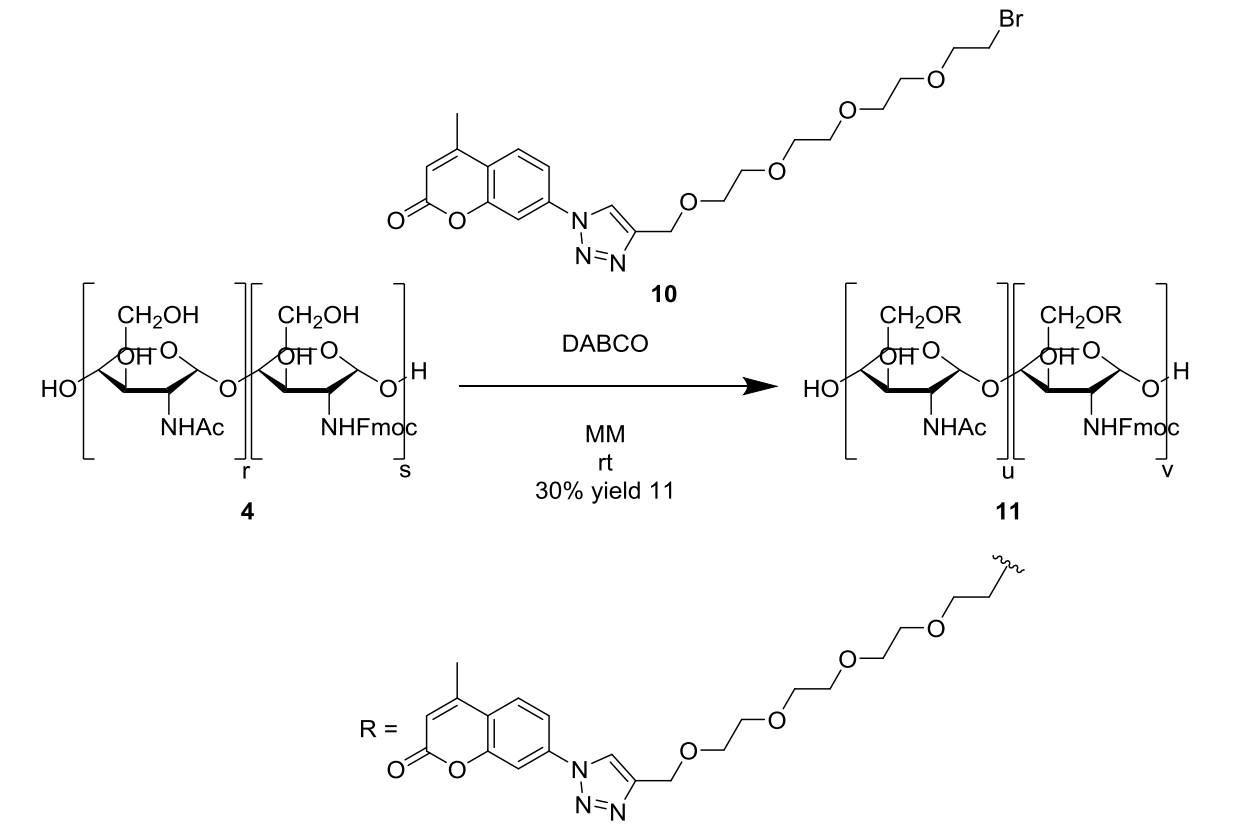

Figure 2.6 Completion of the modification of a (COS) functionalized/hybridized with 1,2,3-triazole heterocycle/coumarin scaffolds as a desired final product **11**

2.2 Detailed experimental procedures

2.2.1 Purification of polymeric chitosan (starting material) **1**

The polymeric chitosan starting material (molecular weight range 50-190 KDa, 75-85% deacetylated, α-form) **1** was purified before use with the following procedure (see Figures A.22 and 2.7), 2,655.0 mg of the chitosan sample was dissolved in deionized water (1 wt% AcOH), with the help of sonication and stirring until complete solubilization was attained. The resulting viscous solution was filtered using Whatman filter papers and a conical funnel to remove insoluble substances. The filtrate **2** was subsequently transferred to a three-necked round-bottom flask for the next procedure.

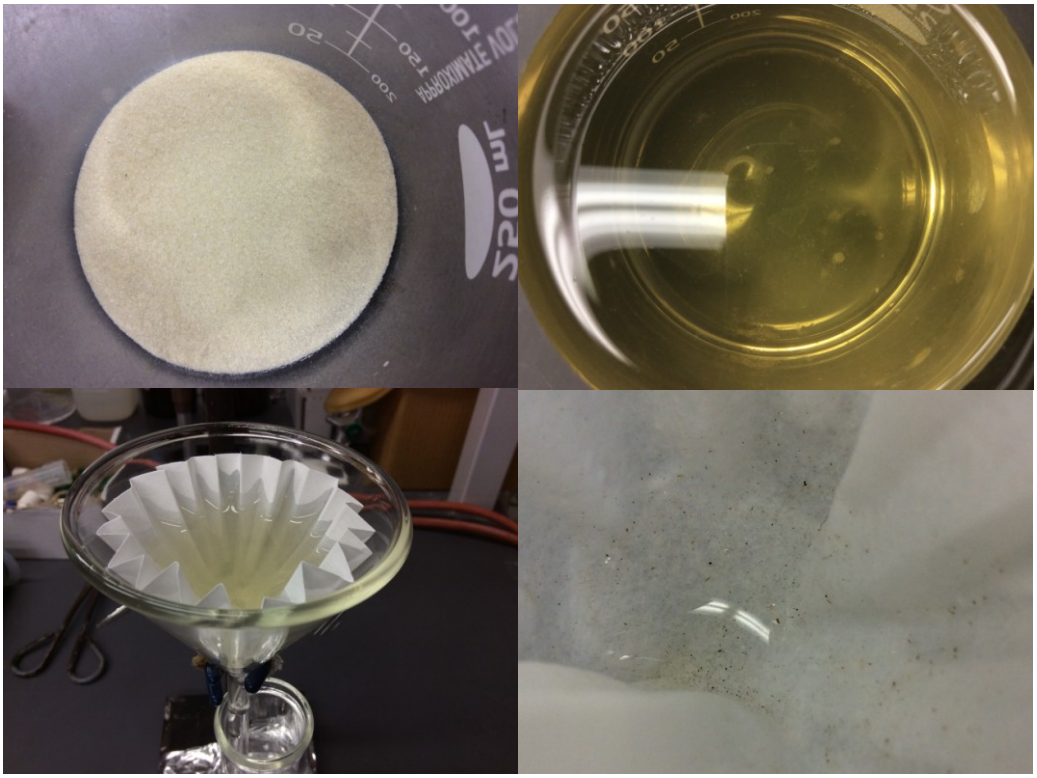

Figure 2.7 Illustration of the procedure for the purification of polymeric chitosan (starting material)

2.2.2 Preparation of highly deacetylated chitosan oligosaccharides (COS) **3**

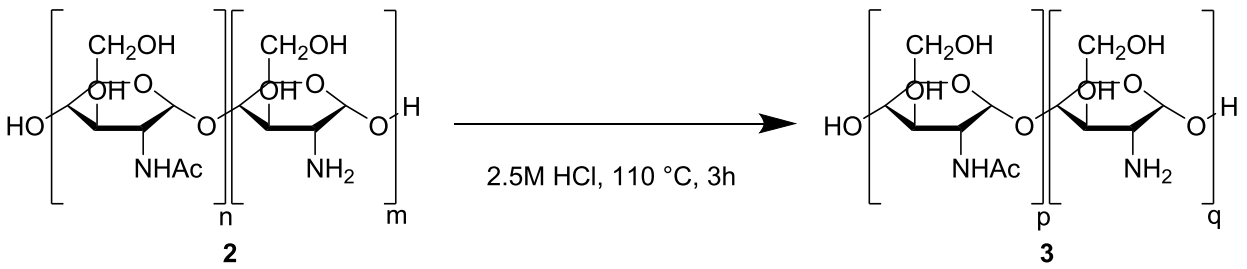

Figure 2.8 One-step simultaneous depolymerization and deacetylation; heating and acidic hydrolysis under reflux

The following one-step procedure for simultaneous depolymerization and deacetylation of purified polymeric chitosan filtrate **2** was derived from a previous literature procedure[186] (see Figures 2.8 and 2.9). A three-necked round-bottom flask equipped with a magnetic stir bar, reflux condenser, and two glass stoppers was charged with filtrate **2**, followed with deionized water, and then acidified to a 2.5M HCl aqueous solution. The flask was immersed into an oil bath preheated to 110 °C and the reaction mixture was refluxed under stirring for 3 h. After cooling to room temperature, the reaction mixture was transferred to a separate round-bottom flask and basified dropwise via an addition funnel with a freshly prepared 2.5M NaOH aqueous solution, until the pH of the aqueous portion was adjusted to 8-9. The supernatant solution was decanted, the white precipitate was washed with deionized water and sonicated. This process was repeated until a neutralized and clear aqueous layer formed. After final decantation, the white precipitate was concentrated *in vacuo* under the reduced pressure, affording brown crystalline solids of highly deacetylated chitosan oligosaccharides (COS) **3**.

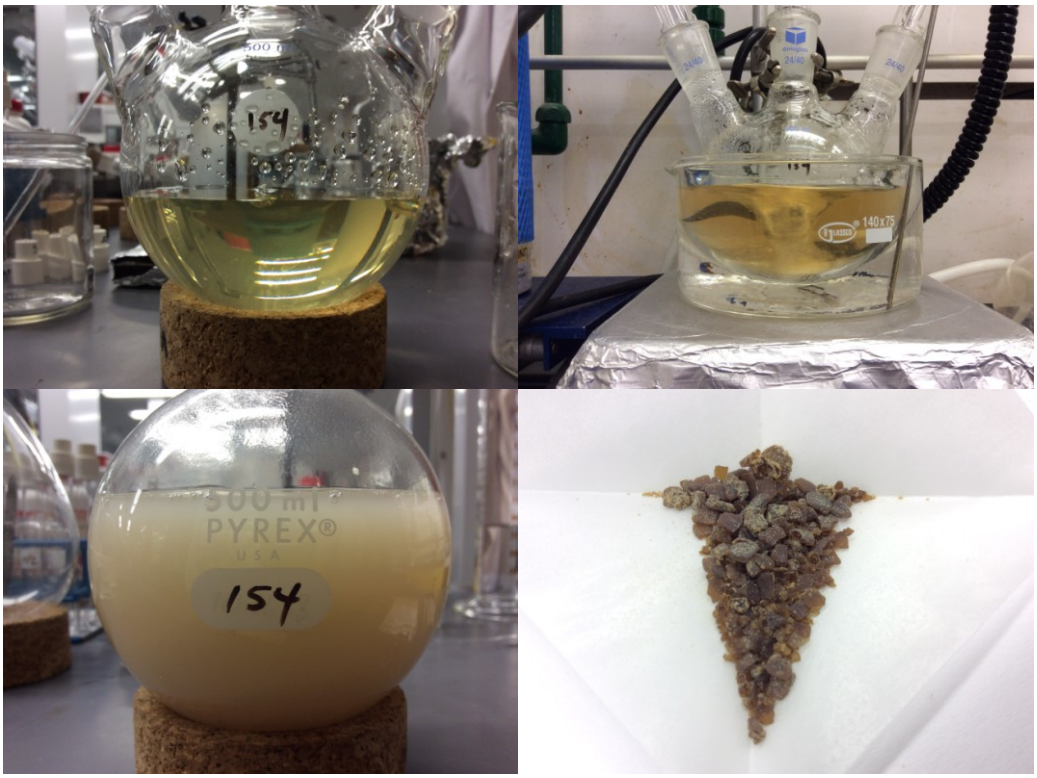

Figure 2.9 Illustration of the procedure for a one-step simultaneous depolymerization and deacetylation; heating and acidic hydrolysis under reflux

2.2.3 Preparation of Fmoc-N-protected highly deacetylated chitosan oligosaccharides (COS) **4**

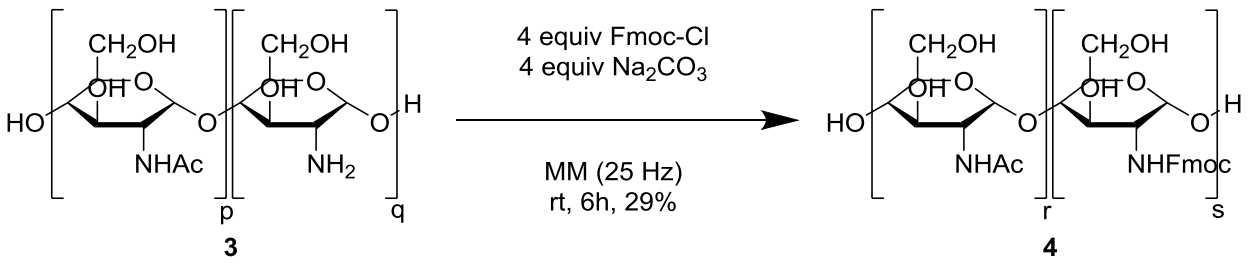

Figure 2.10 Neat/solvent-free ball milling installation of a carbamate moiety for Fmoc-N-protection of oligosaccharides (COS)

Compound **3**, 9-fluorenylmethyl chloroformate (4 equiv), and Na_2CO_3 (4 equiv) were charged into a 15 mL PTFE Teflon milling/grinding jar, along with four stainless steel ball bearings of 5 mm diameter and milled in a Retsch MM200 grinding mill (mixer mill denoted as MM) operating at a frequency of 25 Hz in four increments/segments of 90 min according to the general procedure described in section 2.1, p. 34, also see Eq in Figure 2.10 (structures, Eqs, named reactions, mechanisms, and most importantly, experimentally-derived evidence and knowledge (empiricism) make-up the language of the chemical disciplines) and Figure 2.11. Post-reaction, the crude mixture was meticulously scraped from the jar, and transferred to a 50 mL sterile Polypropylene (PP) conical tube where it was washed and sonicated with the following sequence of solvents: CH_2Cl_2, Me_2CO. After decantation, residual supernatant was TLC monitored, and this process was repeated until a clear supernatant layer formed and TLC indicated the disappearance of starting materials and other compounds. The sample (loosely covered with foil) was then placed in a ventilated fume hood overnight to allow evaporation of residual solvent, furnishing Fmoc-N-protected highly deacetylated chitosan oligosaccharides (COS) (oligo(9-fluorenylmethyloxycarbonyl-glucosamine (Fmoc-GlcN))) **4** as pale beige powders.

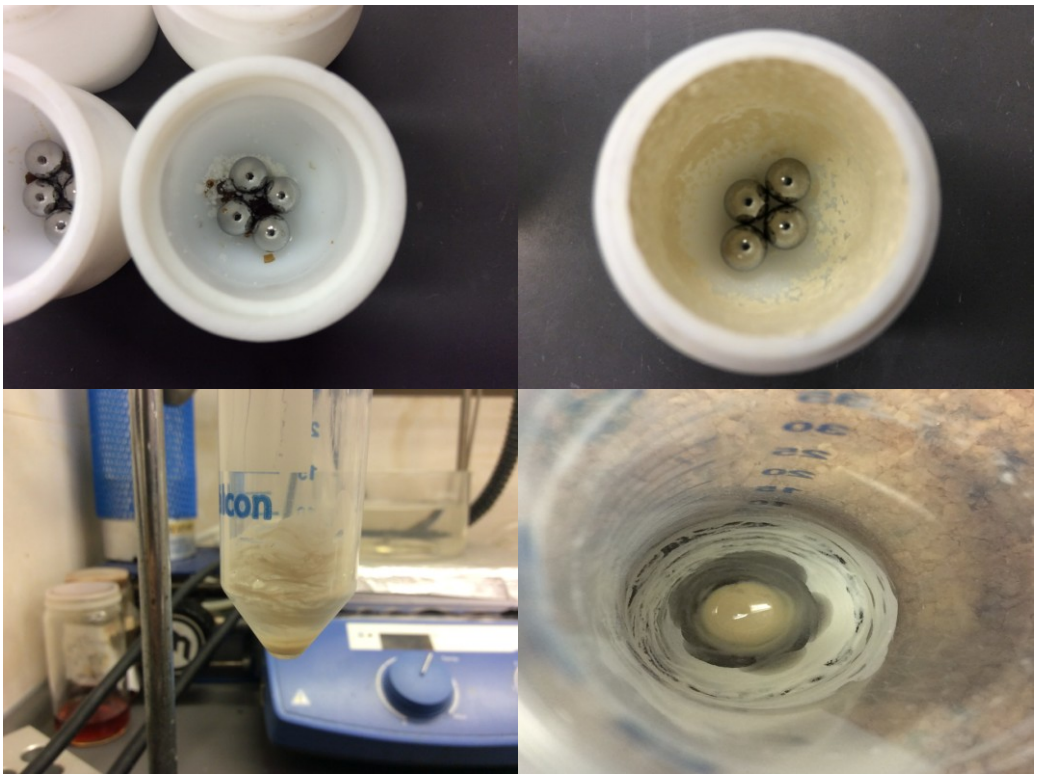

Figure 2.11 Illustration of the procedure for a neat/solvent-free ball milling installation of a carbamate moiety for Fmoc-N-protection of oligosaccharides (COS)

2.2.4 Preparation of *O*-propargyltetra(ethylene glycol) **6**

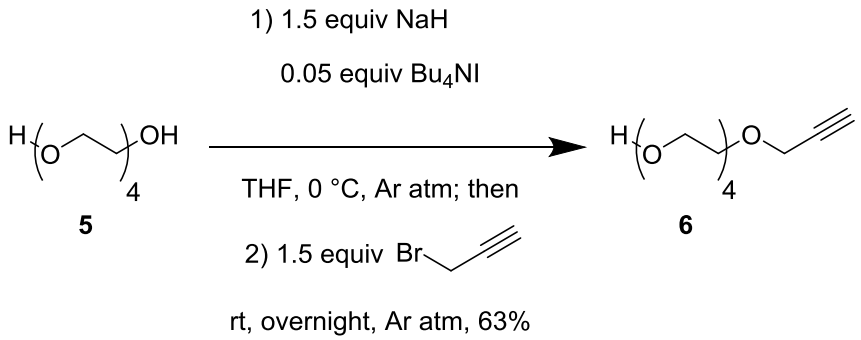

Figure 2.12 Mono-propargylation of tetraethylene glycol

Compound **6** was synthesized as described earlier[187] (see Figures 2.12 and 2.13). NaH (60% w/w in mineral oil, 1.5 equiv) and a catalytic amount of Bu_4NI (0.05 equiv) were added to an oven-dried and flame-dried round-bottom flask which was backfilled with argon. Anhydrous THF and tetraethylene glycol **5** were added via syringe through the rubber septum at 0 °C under an argon atmosphere, and the reaction mixture was stirred for an additional 0.5 h. Propargyl bromide (1.5 equiv) was dropwise added to the reaction mixture, which was allowed to warm to rt to be stirred overnight, upon which it was concentrated *in vacuo* under reduced pressure, and purified by flash column chromatography to afford *O*-propargyltetra(ethylene glycol) or 3,6,9,12-tetraoxapentadec-14-yn-1-ol **6** as pale yellow oils.

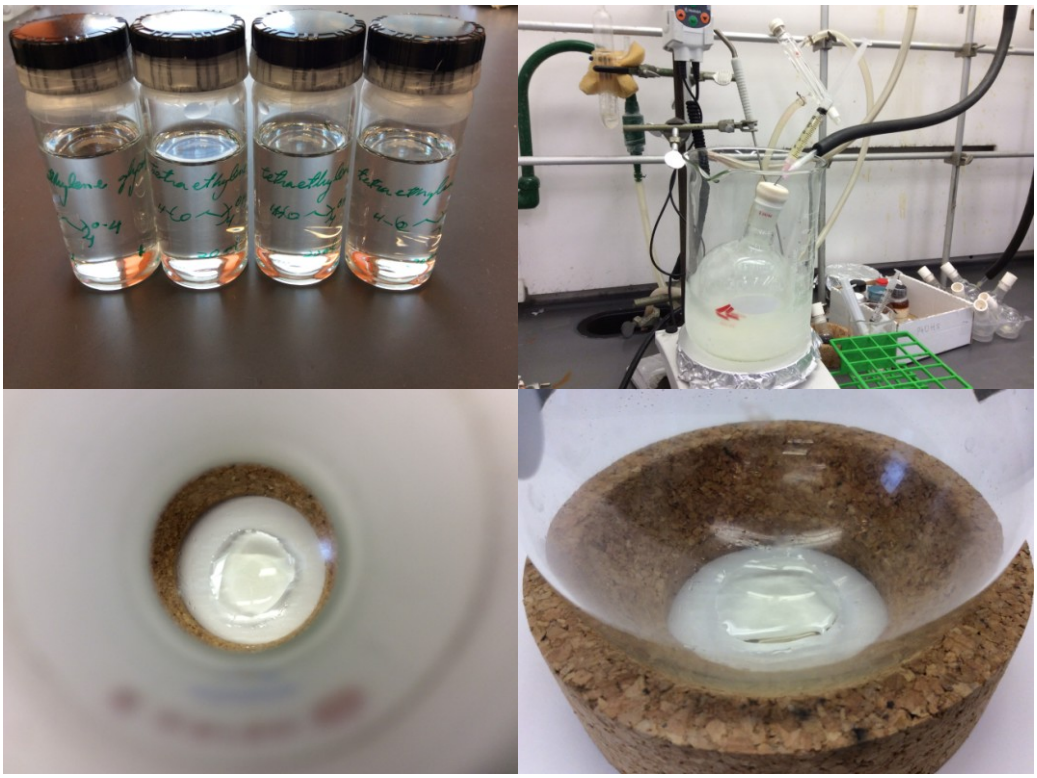

Figure 2.13 Illustration of the procedure for the mono-propargylation of tetraethylene glycol

2.2.5 Preparation of propargylated and brominated heterobifunctional tetraethylene glycol-based spacer/linker 1-bromo-3,6,9,12-tetraoxapentadec-14-yne **7**

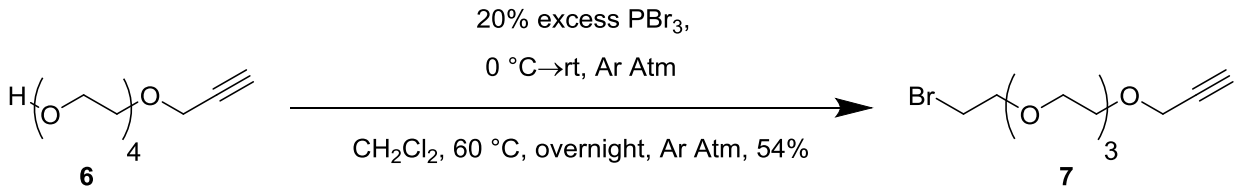

Figure 2.14 Bromination of mono-propargylated tetraethylene glycol

Compound **7** was synthesized by the adaptation of a previously reported procedure[188] (see Figures 2.14 and 2.15). Anhydrous CH_2Cl_2 and compound **6** were syringed through the rubber septum of an oven-dried and flame-dried round-bottom microwave vial previously purged with argon. The reaction mixture was cooled to 0 °C and PBr_3 (20% excess) was dropwise added under argon atmosphere. After warming to ambient temperature, the reaction mixture was lowered into an oil bath preheated to 60 °C and left overnight under stirring, at which time it was quenched with MeOH, concentrated *in vacuo* under reduced pressure, and purified by flash column chromatography which gave the propargylated and brominated heterobifunctional tetraethylene glycol-based spacer/linker 1-bromo-3,6,9,12-tetraoxapentadec-14-yne **7** as yellow oils.

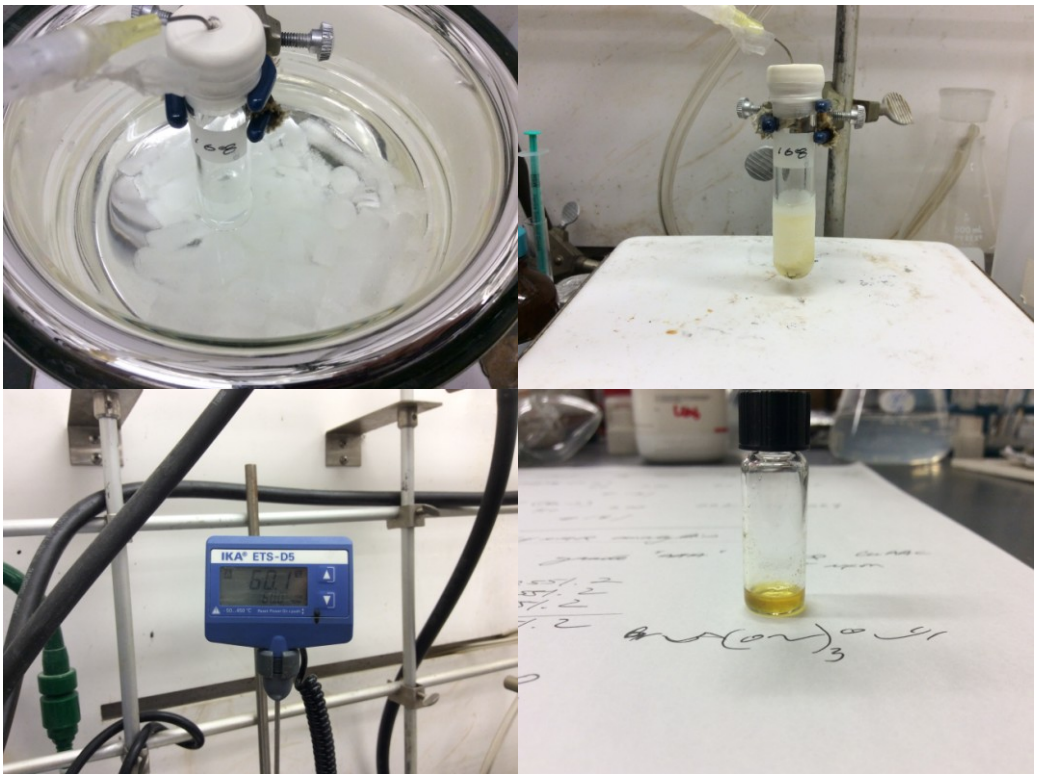

Figure 2.15 Illustration of the procedure for the bromination of mono-propargylated tetraethylene glycol

2.2.6 Preparation of 7-azido-4-methyl-2*H*-chromen-2-one **9**

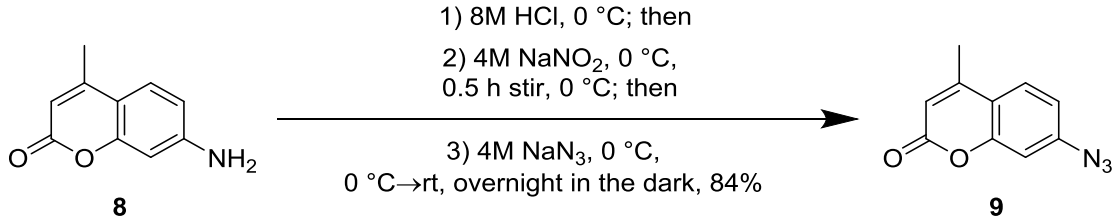

8 **9**

Figure 2.16 Cu(I)-free Sandmeyer azidation of 7-Amino-4-methylcoumarin

Compound **9** was synthesized using a procedure modified from the literature[189,190] (see Figures 2.16 and 2.17). 7-Amino-4-methylcoumarin **8** and deionized water were loaded in a round-bottom flask. Under ice bath temperature, concentrated HCl was dropwise added to the stirred suspension to an 8M aqueous solution. A freshly prepared 4M $NaNO_2$ aqueous solution was cooled to 0 °C and dropwise added to the reaction mixture, which was stirred for 0.5 h at 0 °C, during which a 4M NaN_3 aqueous solution was prepared and cooled to 0 °C. After 0.5 h, the NaN_3 solution was added to the reaction mixture in a dropwise fashion at 0 °C, at which point it was slowly warmed to ambient temperature and allowed to stir overnight in the dark. The crude mixture was extracted into $CHCl_3$, dried over anhydrous $MgSO_4$, concentrated *in vacuo* under reduced pressure, and purified by flash column chromatography which furnished 7-azido-4-methyl-2*H*-chromen-2-one **9** as yellow crystals.

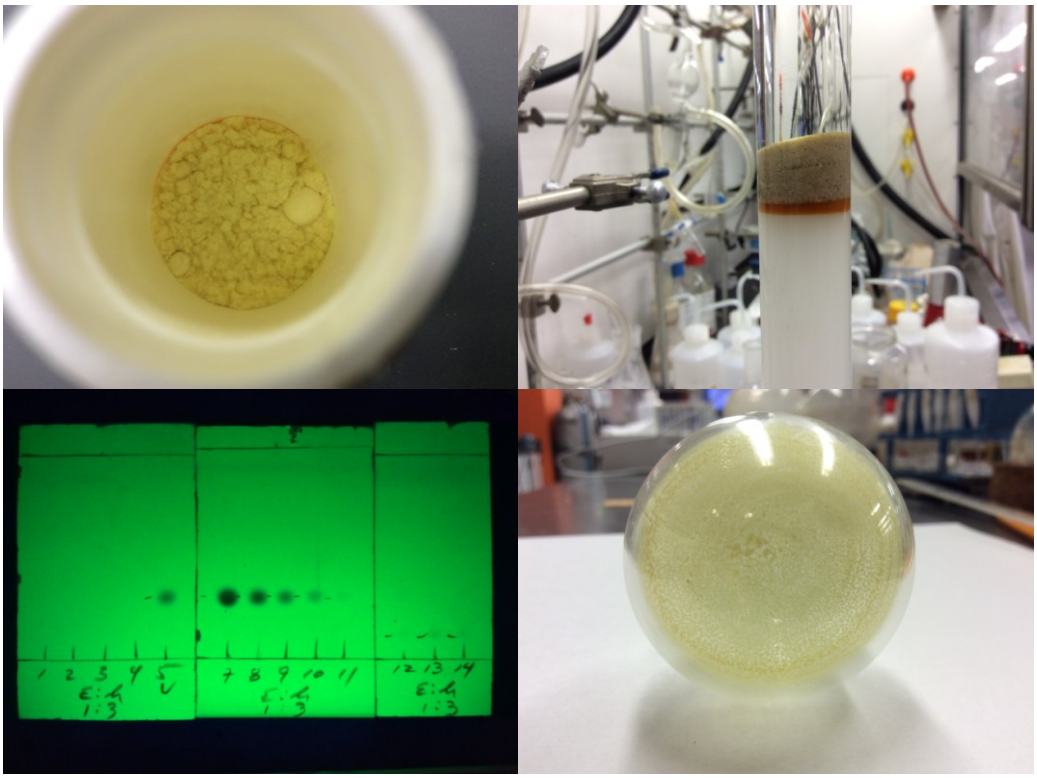

Figure 2.17 Illustration of the procedure for Cu(I)-free Sandmeyer azidation of 7-Amino-4-methylcoumarin

2.2.7 Preparation of 1,4-disubstituted 1,2,3-triazole heterocycle **10**

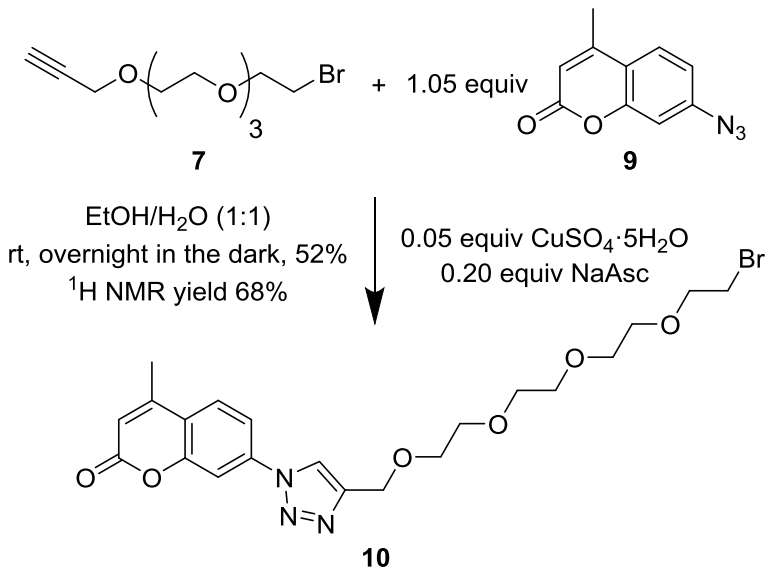

Figure 2.18 Cu(I)-catalyzed Huisgen 1,3-dipolar cycloaddition

Compound **10** was synthesized via an adapted published procedure[191] (see Figures 2.18 and 2.19). 1-Bromo-3,6,9,12-tetraoxapentadec-14-yne **7**, 7-azido-4-methyl-2*H*-chromen-2-one **9** (1.05 equiv), sodium ascorbate (0.20 equiv), and copper(II) sulfate pentahydrate (0.05 equiv) were added to a round-bottom microwave vial, followed by EtOH, and lastly deionized water (EtOH/DI H_2O 1:1). The reaction mixture was left to stir overnight in the dark. The crude mixture was extracted into CH_2Cl_2, dried over anhydrous $MgSO_4$, concentrated *in vacuo* under reduced pressure, and purified by flash column chromatography to yield the desired 1,4-disubstituted 1,2,3-triazole heterocyclic compound **10** as yellow solids.

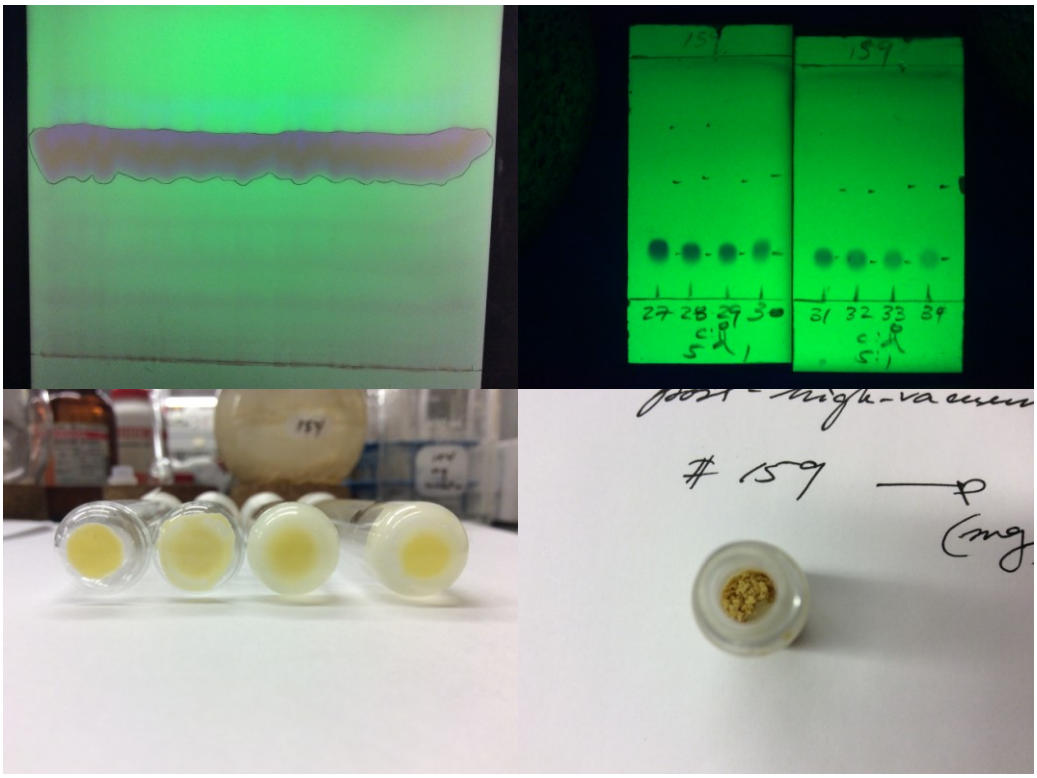

Figure 2.19 Illustration of the procedure for Cu(I)-catalyzed Huisgen 1,3-dipolar cycloaddition

2.2.8 Preparation of Fmoc-N-protected O-TEGylated spacer/linker 1,4-disubstituted 1,2,3-triazole heterocycle/coumarin functionalized highly deacetylated chitosan oligosaccharides (COS) **11**

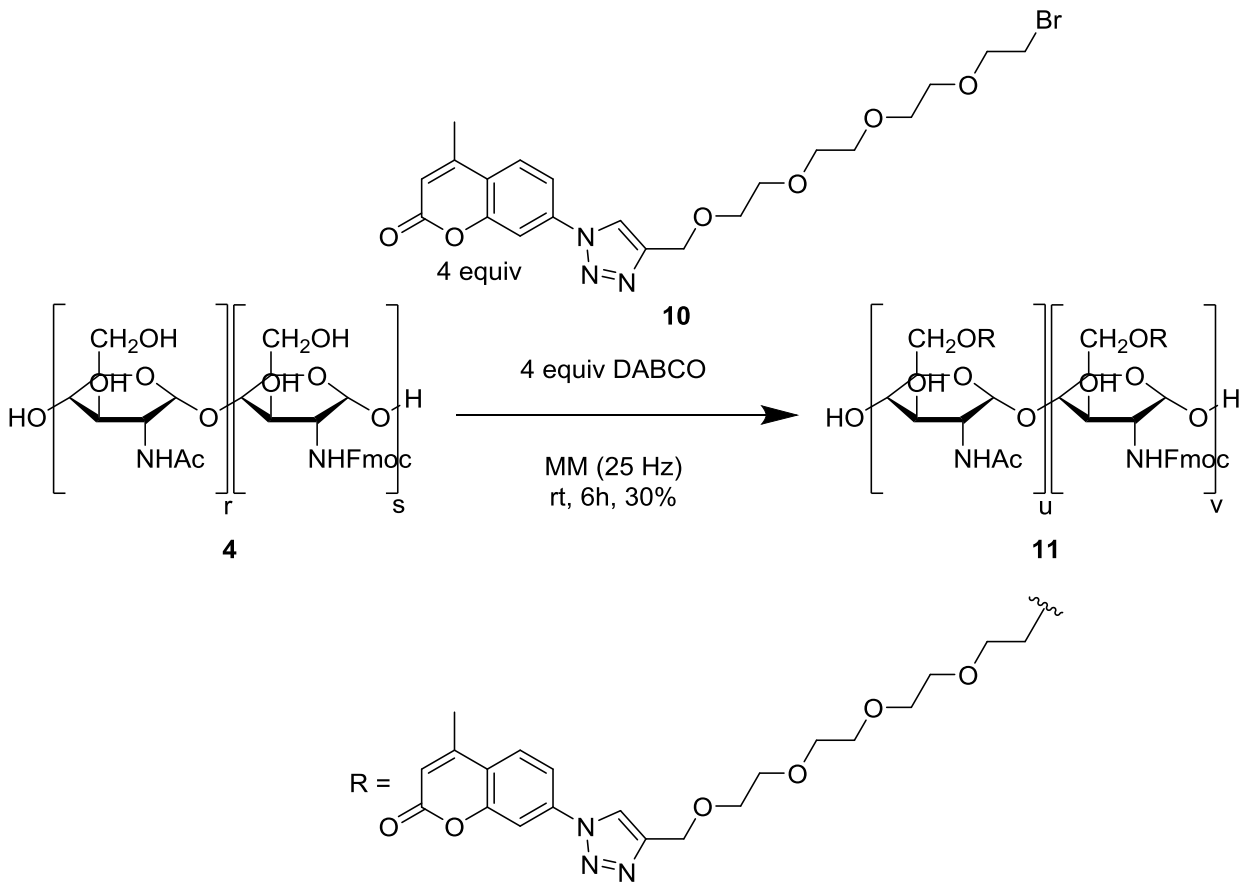

Figure 2.20 Neat/solvent-free ball milling installation of a medicinally/therapeutically relevant side chain

Fmoc-N-protected highly deacetylated chitosan oligosaccharides (COS) (oligo(9-fluorenylmethyloxycarbonyl-glucosamine (Fmoc-GlcN))) **4**, 1,4-disubstituted 1,2,3-triazole heterocyclic compound **10** (4 equiv), and 1,4-diazabicyclo[2.2.2]octane (4 equiv) were charged into a 15 mL PTFE Teflon milling/grinding jar, along with four stainless steel ball bearings of 5 mm diameter and milled in a Retsch MM200 grinding mill (mixer mill denoted as MM) operating at a frequency of 25 Hz in four increments/segments of 90 min according to the general procedure described in section 2.1, p. 34, also see Figures 2.20 and 2.21. Post-reaction, the crude mixture was meticulously scraped from the jar, and transferred to a 50 mL sterile Polypropylene (PP) conical tube where it was washed and sonicated with the following sequence

of solvents: CH_2Cl_2, Me_2CO. After decantation, residual supernatant was TLC monitored, and this process was repeated until a clear supernatant layer formed and TLC indicated the disappearance of starting materials and other compounds. The sample (loosely covered with foil) was then placed in a ventilated fume hood overnight to allow evaporation of residual solvent, to furnish the desired Fmoc-N-protected O-TEGylated spacer/linker 1,4-disubstituted 1,2,3-triazole heterocycle/coumarin functionalized highly deacetylated chitosan oligosaccharides (COS) **11** as pale beige powders.

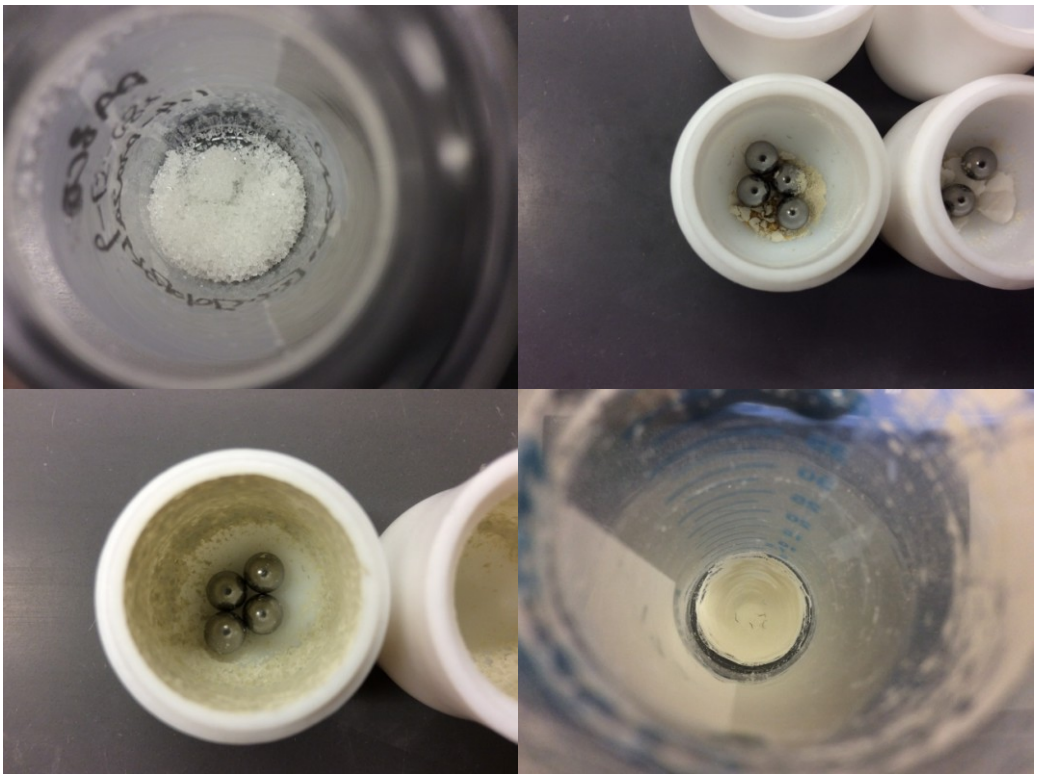

Figure 2.21 Illustration of the procedure for a neat/solvent-free ball milling installation of a medicinally/therapeutically relevant side chain

Relevant experimental results regarding the preparation of the abovementioned compounds using the methodologies described herein will be presented and discussed in detail in the subsequent chapter.

CHAPTER 3
RESULTS AND DISCUSSION

The oligosaccharide modification commenced with the purification of polymeric chitosan **1** (molecular weight range 50-190 KDa, 75-85% deacetylated, α-form, see Figure A.22) which serves as a readily available, inexpensive, and non-toxic starting material. After complete polymer dissolution in dilute aqueous acid and solution filtration to remove insoluble substances, the filtrate **2** was subjected to heating and acidic hydrolysis under reflux which effected in a one-step process simultaneous depolymerization and deacetylation (see Figure 2.8), i.e., cleavage of the α-(1→4) glycosidic linkage and the acetamido group (side chain). Avoiding one extra step, the brevity of this route is preferred over a sequential deacetylation (base-catalyzed) followed by depolymerization (one of the processing sequence investigated in reported study)[186], and afforded the desired highly deacetylated chitosan oligosaccharides (COS) **3** in a 56% combined yield over two-steps. The analytical data for ^{1}H and ^{13}C NMR matched those reported for the natural compound (NMR spectra for compound **1** are shown in Figures A.3-A.7). Furthermore, ^{1}H NMR analysis confirmed the high degree of deacetylation of 95-98% whilst MALDI-MS analytical data (see Figure A.2) reveals the following distribution of oligosaccharides: number average molecular weight (Mn = 3105 Da), weight average molecular weight (Mw = 3344 Da), polydispersity index (PDI = Mw/Mn = 1.08), and degree of polymerization (DP = 19 repeating units of D-GlcN).

^{1}H NMR (500 MHz, 1 wt% HCOOH/D_2O): δ = 4.80-4.75 (m, 1H), 3.88-3.58 (m, 5H), 3.11-3.04 (m, 1H) ppm.

^{13}C NMR (125 MHz, 1 wt% HCOOH/D_2O): δ = 97.6, 76.3, 74.7, 70.1, 59.9, 55.8 ppm.

NMR spectra for compound **3** are shown in Figures 3.1 and 3.2.

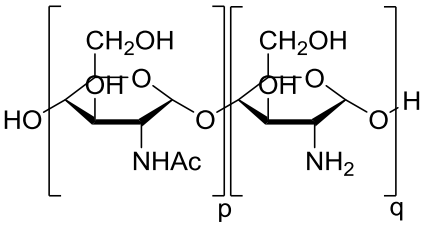

Compound 3

^{1}H NMR (500 MHz, 1 wt% HCOOH/D_2O)

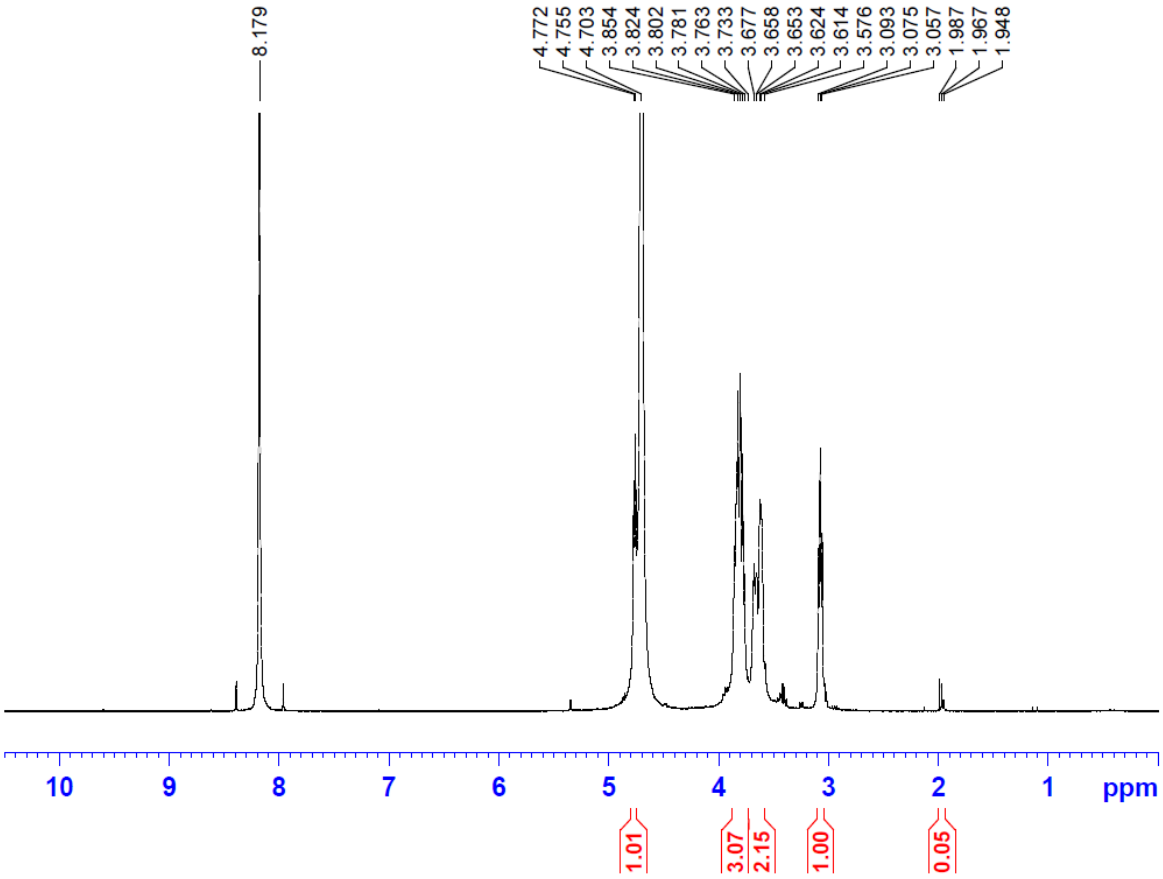

Figure 3.1 ^{1}H NMR spectra of compound **3**

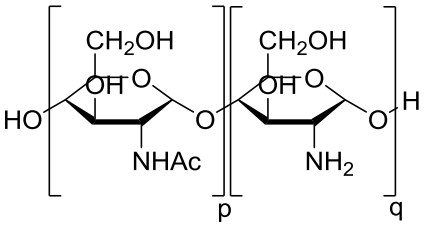

Compound 3

^{13}C NMR (125 MHz, 1 wt% HCOOH/D_2O)

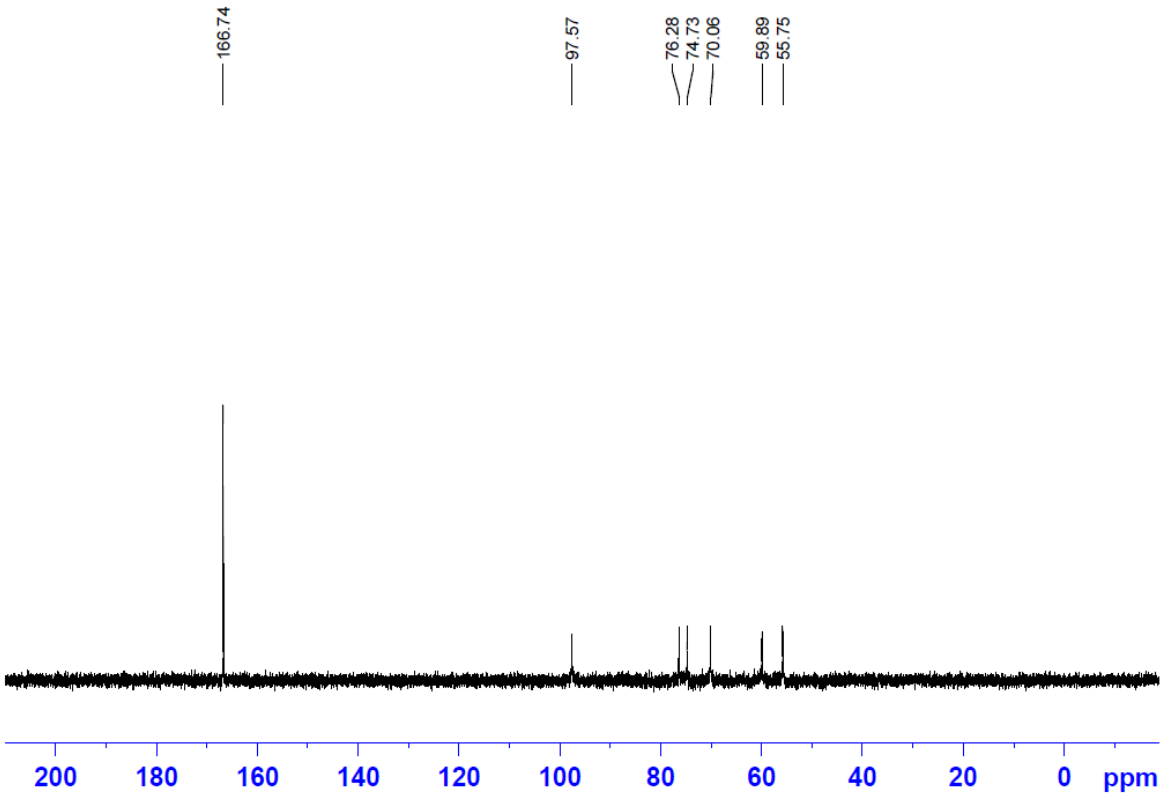

Figure 3.2 ^{13}C NMR spectra of compound **3**

Depolymerization is an important starting point for many recalcitrant biomass valorization strategies[21,117,192-198] in order to extract valuable chemicals from renewable sources of carbon[192,197] and/or to provide a source of low molecular mass feedstock more suited for downstream processing[117,192,196], including chemical and/or biological transformations[195,197,198]. Commonly referred to in the biomass literature is the need to overcome the crystallinity of natural biopolymers derived from recalcitrant biomass, as such depolymerization is often the first step to effective utilization of chitin[117,193], cellulose[21,194,195], hemicellulose, and/or lignin[192,196-198] (see section 1.3.8, Tables 1.1-1.3, biomass field pretreatment methods); depolymerization is also presented as the first step that is required for the large-scale use of recalcitrant biomass[194,196], their effective extraction (see discussion in section 1.3.1, p. 14, focused on chitinous type of biomass) and/or subsequent chemical/biological conversion efforts into higher value chemicals[117,192,196,197], both (market size and upgrading) are deemed crucial for the economic viability of contemporary integrated biorefineries[192,196]. From a practical point of view, depolymerization affords low molecular weight feedstocks that are more suited for downstream processing; the high viscosity[4,69,99,199,200], high molecular weight[8,69,89,99,199] and/or native solid-state[4,117] of starting biopolymers are often unattractive for downstream processing[4,8,69,89,99,117,199,200] (see experimental details of references in sections 1.3.2, p. 14 and 1.3.3, p. 15) and such properties could be undesirable for several applications. For example, in the pharmaceutical field: (1) body clearance of biopolymer alginate is hampered by its high molecular weight[199], and (2) high polymer fractions increase the viscosity of gelation liquid for the formation of thermal gelling polymer-based hydrogels (protection and release of drugs with poor aqueous solubility) and off-target effects, which can limit the application of such materials[132]. Whereas in the biomedical field, the high viscosity of biopolymer chitosan hampers the stirring efficiency and homogeneity of the medium in polymer blends[200] (see discussion in section 1.3.7, p. 17, polymer modifications using physical association networks strategies).

Additionally, there are distinct advantages (of therapeutic relevance) for utilizing chitosan oligosaccharides (COS) over their polymeric precursors for pharmaceutical or biomedical applications besides material processability considerations, namely: (1) enhanced susceptibility to degradation of COS over their polymeric counterparts as revealed by in vitro studies where degradation was predominantly caused by extracellular enzymes[76], (2) lower hepatotropic biodistribution profile as shown by in vivo studies after intravenous administration in male Wistar rats[76] (see discussion in section 1.2, p. 12), (3) in vitro toxicity studies demonstrating increasing cytotoxicity with higher molecular weight chitosan, e.g., in vitro cytotoxicity assessment against L929 cells for trimethyl chitosan of molecular weight: 400, 100, 50, 25, and 5 kDa (IC_{50}: 30, 70, 90, 270 mg/ml, and > 1000 μg/ml, respectively)[76] (see discussion in section 1.2, p. 12), and lastly (4) in vivo studies also revealed a dependency between cytotoxicity and increasing molecular weight for chitosan against CaCo-2 and HT29-H cell lines and in situ rat jejunum[76].

With highly deacetylated chitosan oligosaccharides (COS) **3** in hand, we then concentrated our efforts to install a carbamate moiety for Fmoc-N-protection of oligosaccharides. Initial attempts were carried out using solution-based (peptide synthesis protocols) and alternative energy methodologies such as microwave-assisted and ultrasonic (sonochemistry) irradiation, but were met with little success. Upon observation that the biomass substrate **3** proved remarkably unreactive (recalcitrant) under these conditions, we decided to try ball milling, an alternative

Table 3.1 Initial neat/solvent-free ball milling reaction condition screening[a]

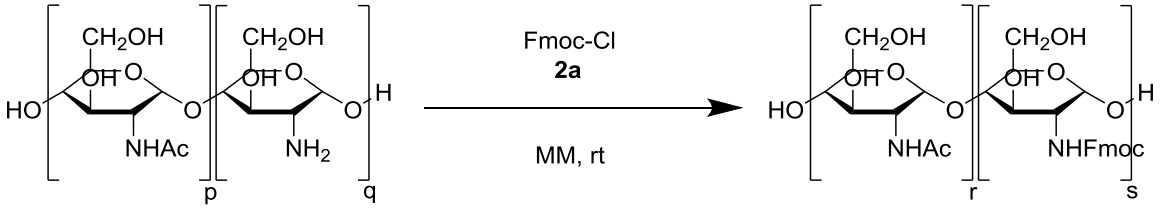

entry	**1a** (mg)	**2a** (equiv)	milling freq (Hz)	milling cycle (n)	milling time (min)	yield (%)
1	30.0	2.0	30	1	60	not significant
2	50.0	2.0	30	1	60	not significant
3	50.0	2.0	25	1 2	60 60	not significant
4	50.0	4.0	30	1	60	16
5	250.0	4.0	30	1	60	4
6	250.0	4.0	30	1	60	3

[a]Using one 10 mm diameter zirconia ball bearing.

Table 3.1 Initial neat/solvent-free ball milling reaction condition screening

energy method traditionally used for mechanochemical mixing (i.e., advanced comminution/particle size reduction[36], see discussions in sections 1.1, p. 4, and 1.3.8, Table 1.1) but one which remains largely unexplored with the perspective of deliberately effecting chemical changes in biomass substrates. At this stage, the most pressing issue was to conduct a methodological investigation to expedite the discovery of a process leading to compound **4** from compound **3**: first, we needed to demonstrate that a neat/solvent-free ball milling methodology represents a viable approach to produce the key and versatile intermediate **4**. To explore the initial operation conditions of the mixer mill, compound **3** and stoichiometric equivalents of 9-fluorenylmethyl chloroformate (starting with 2 equiv) were placed into a 15 mL PTFE Teflon jar along with one zirconia grinding ball of 10 mm diameter (see Table 3.1, entries 1-3). The samples were then ground in a Retsch MM400 grinding mill operating at a frequency of 30 Hz in one increment/segment of 60 min (see Table 3.1, entries 1, 2, 4-6). Initial screening reveals an

optimal loading (milling media-to-sample weight ratio) of 50.0 mg for compound **3** and 4 equiv of 9-fluorenylmethyl chloroformate are needed to afford a yield of 16% (see Table 3.1, entry 4), higher loading levels of 250.0 mg for compound **3** reduced the yield to 3-4% (see Table 3.1, entries 5 and 6) whilst under the conditions of lower loading levels of 30.0 mg for compound **3** (see Table 3.1, entry 1) and/or 2 equiv of 9-fluorenylmethyl chloroformate (including lengthening the reaction time in two increments/segments of 60 min at a frequency of 25 Hz) (see Table 3.1, entries 1-3), the intermediate **4** could still be detected by ^{1}H NMR; however, the amounts of isolated yield were not significant; second, we then turned our efforts to investigate the effect of base additives for neat/solvent-free ball milling reaction condition screening. Addition of a base should be favourable for it would presumably act to neutralize the released HCl byproduct from carbamate moiety formation, as such we investigated the common organic base Et_3N (10 wt% to solid reactants, see Table 3.2, entries 1-3) as well as more economically attractive inorganic bases such as $NaHCO_3$ and Na_2CO_3 (see Table 3.2, entries 4-6). The results of this screening round reveal that under identical milling conditions to those leading to the highest yet attained yield (16%) without any base additive (see Table 3.1, entry 4), the addition of organic base Et_3N lowered the yield to 9% (see Table 3.2, entry 3), and that at 2 equiv of 9-fluorenylmethyl chloroformate (see Table 3.2, entry 2) and/or under LAG liquid-assisted grinding (wet-milling) conditions using dioxane as the solvent (see Table 3.2, entry 1), intermediate **4** was not detected (n.d.) by ^{1}H NMR.

Table 3.2 Base additives for neat/solvent-free ball milling reaction condition screening[a]

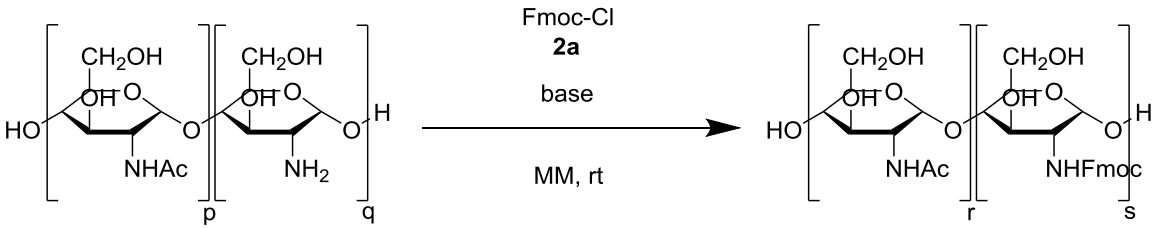

1a **3a**

entry	**1a** (mg)	**2a** (equiv)	base	base (equiv)	milling freq (Hz)	milling time (min)	yield (%)
1	33.8	2.0	Et_3N	10 wt%	30	60	n.d.[b]
2	50.0	2.0	Et_3N	10 wt%	25	60	n.d.
3	50.0	4.0	Et_3N	10 wt%	30	60	9
4	50.0	4.0	$NaHCO_3$	4.0	30	60	49
5	50.0	4.0	Na_2CO_3	4.0	30	60	54
6	50.0	10.0	$NaHCO_3$	4.0	30	60	22

[a]Using one 10 mm diameter zirconia ball bearing. [b]Under LAG liquid-assisted grinding (wet-milling) conditions using dioxane as the solvent.

Table 3.2 Base additives for neat/solvent-free ball milling reaction condition screening

Table 3.3 Influence of milling time for neat/solvent-free ball milling reaction condition screening[a]

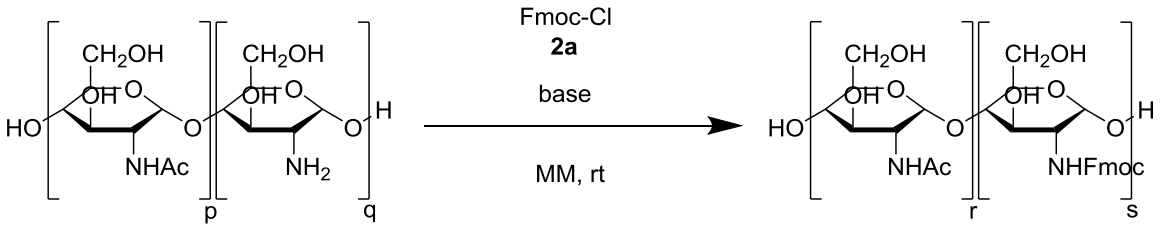

1a **3a**

entry	**1a** (mg)	**2a** (equiv)	milling freq (Hz)	milling cycle (n)	milling time (min)	yield (%)
1	50.0	4.0	30	1	30	20
2	50.0	4.0	30	1	60	49
3	50.0	4.0	30	1 2	30 60	60
4	50.0	4.0	30	1 2	60 60	85

[a]Using one 10 mm diameter zirconia ball bearing, $NaHCO_3$ (4 equiv) as base.

Table 3.3 Influence of milling time for neat/solvent-free ball milling reaction condition screening

Under similar conditions to those leading to the highest yet attained yield (16%) without any base additive (see Table 3.1, entry 4), it was found that by adding 4 equiv of inorganic bases, the yield could be increased to 49% for $NaHCO_3$ (see Table 3.2, entry 4) and to 54% for Na_2CO_3 (see Table 3.2, entry 5); also note that the yields do not differ markedly from each other. Thus, the choice of a base significantly impacts the success of this nucleophilic acyl substitution reaction with inorganic bases $NaHCO_3$ and Na_2CO_3 significantly outperforming organic base Et_3N. Moreover, it is worth noting that inorganic bases, once neutralized into their salt forms, can be conveniently removed by washing away with water. The results are fully consistent with the presumption that a base is needed to neutralize the released HCl byproduct from carbamate formation. It is noteworthy that increasing the amount of 9-fluorenylmethyl chloroformate to 10 equiv decreases the yield to 22% (see Table 3.2, entry 6), clearly a delicate and intricate balance is needed between neutralization, proper stoichiometric ratio between reagents, and an optimal loading level (milling media-to-sample weight ratio); third, with access to reaction conditions

which provide yields in the 49-54% range (see Table 3.2, entries 4 and 5), we then examined the influence of milling time on the yield, and found that diminishing the milling time to 30 min correspondingly decreases the yield to 20% (see Table 3.3, entry 1) whilst lengthening the milling time to 90 min and 120 min increased the yields to 60% and 85% respectively (see Table 3.3, entries 3 and 4); last, we then directed our attention to evaluate the influence of milling media, i.e., number, size, and density/type of milling materials, on the yield as well as exploring the effect of further extending the milling time on the yield.

Table 3.4 Influence of milling media (ball bearing number/size/density) for neat/solvent-free ball milling reaction condition screening[a]

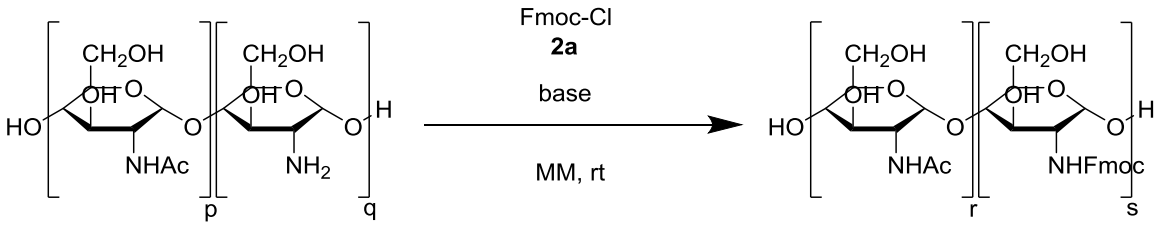

entry	base	base (equiv)	milling freq (Hz)	milling cycle (n)	milling time (min)	yield (%)
1	$NaHCO_3$	4.0	25	1	90	37
				2	90	
2	Na_2CO_3	4.0	25	1	90	28
				2	90	
3	$NaHCO_3$	4.0	25	1	90	22
				2	90	
				3	90	
				4	90	
4	Na_2CO_3	4.0	25	1	90	29
				2	90	
				3	90	
				4	90	

[a]Using four 5 mm diameter stainless steel ball bearing, **1a** (50 mg), **2a** (4 equiv).

Table 3.4 Influence of milling media (ball bearing number/size/density) for neat/solvent-free ball milling reaction condition screening

In this series of experiments, the single zirconia grinding ball (number of milling ball (n_{MB} = 1), diameter (d_{MB} = 10 mm), density (ρ_{MB} = 4.5 g cm^{-3})[38], Knoop index (KI = 1160)[38]) was exchanged for four stainless steel ball bearings (number of milling ball (n_{MB} = 4), diameter (d_{MB} = 5 mm), density (ρ_{MB} = 7.7 g cm^{-3})[38], Knoop index (KI = 138)[38]) and the solid reactants were charged into a 15 mL PTFE Teflon milling/grinding jar and milled in a Retsch MM200 grinding mill operating at a frequency of 25 Hz in two or four increments/segments of 90 min. The Knoop index (KI) being a measure for mechanical hardness[38], we effectively substituted a single larger diameter, less dense but harder zirconia grinding ball bearing with four smaller diameter, more dense but softer stainless steel ball bearings. Under those conditions, the following observations were made: (1) the yields deteriorated to 37% and 28% for $NaHCO_3$ and Na_2CO_3 respectively when the mill was operated for two increments/segments of 90 min (see Table 3.4, entries 1 and 2), (2) similarly, the yields were reduced to 22% and 29% for $NaHCO_3$ and Na_2CO_3 respectively when the mill was operated for four increments/segments of 90 min (see Table 3.4, entries 3 and 4), and most importantly (3) comminution/particle size reduction was more efficient when using four smaller diameter, more dense but softer stainless steel ball bearings (see Table 3.4, entries 1-4) rather than one larger diameter, less dense but harder zirconia grinding ball bearing (see Table 3.1, entries 1-6, Table 3.2, entries 1-6, Table 3.3, entries 1-4). Whilst one may regrettably conclude that further extending the milling time from two increments/segments of 60 min to two or four increments/segments of 90 min did not have a positive effect on the yield (see Table 3.4, entries 1-4), nevertheless, owing to the need to expose intermediate **4** to further functionalization (*vide infra*), i.e., it isn't the final desired product, the process outcome of generating smaller particle size (albeit at a lower yield) was experimentally proven to be determinant and vital to the success of subsequent functionalization steps. Indeed, the use of four smaller diameter, more dense but softer stainless steel ball bearings importantly improved mixing for further functionalization, which in turn allowed superior solid-solid contacts between reagents considered essential to initiate solid-solid transformations[41], and the resulting smaller particle size of the intermediate **4** provides a means to sidestep the known problems or limitations associated with particle segregation (inhomogeneous mixture) which lead to poorer reactivity, i.e., particle segregation occurring as a result of difference in size and density between solid reagents, and the propensity of larger particles to segregate readily from smaller ones, in which case, further shaking results not in improved mixing but rather in enhanced segregation[41]. Thus,

forgoing the higher attainable yield of 85% (see Table 3.3, entry 4) which generates larger particle size, the free primary amine of **3** was converted to a carbamate group upon exposure to 9-fluorenylmethyl chloroformate and Na_2CO_3 to afford **4** in 29% yield (see Table 3.4, entry 4, and Figure 2.10).

^{1}H NMR (500 MHz, DMSO-d_6 at 90 °C): δ = 7.87-7.78 (m), 7.74-7.67 (m), 7.44-7.28 (m), 6.98 (br s), 6.22 (s), 4.58-4.42 (m), 4.39-4.18 (m), 3.85-3.19 (m) ppm.

NMR spectrum for compound **4** is shown in Figure 3.3.

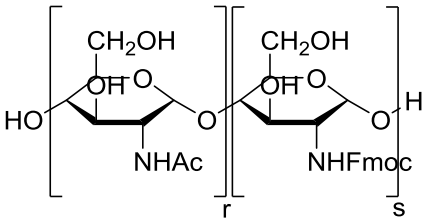

Compound 4

^{1}H NMR (500 MHz, DMSO-d_6 at 90 °C)

proton integration omitted due to limited solubility

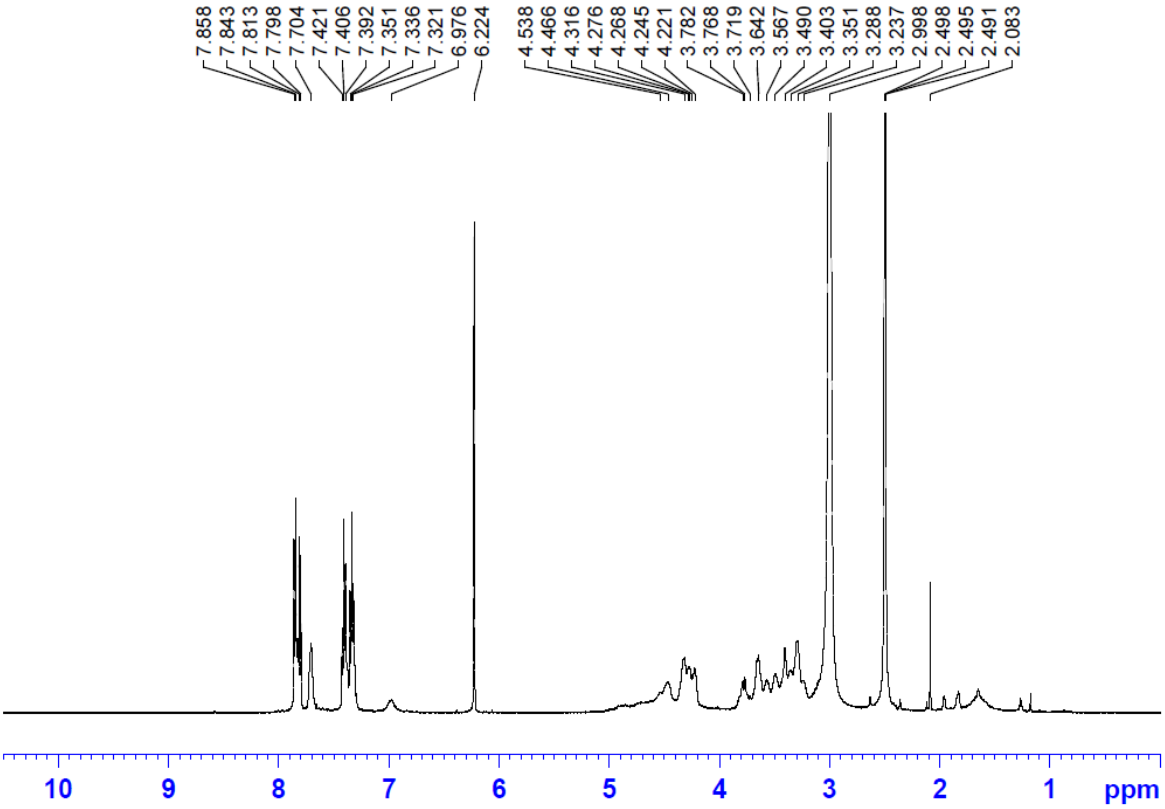

Figure 3.3 ^{1}H NMR spectra of compound **4**

Having successfully installed a carbamate moiety in the corresponding Fmoc-N-protected highly deacetylated chitosan oligosaccharides (COS) **4**, we turned our attention to construct the propargylated and brominated heterobifunctional tetraethylene glycol-based spacer/linker 1-bromo-3,6,9,12-tetraoxapentadec-14-yne **7**. The sequence begins with treating tetraethylene glycol **5** with NaH, a catalytic amount of Bu_4NI, and propargyl bromide in anhydrous THF under argon atmosphere to form *O*-propargyltetra(ethylene glycol) or 3,6,9,12-tetraoxapentadec-14-yn-1-ol **6** in 63% yield (see Figure 2.12).

^{1}H NMR (500 MHz, $CDCl_3$): δ = 4.10 (d, J = 2.4 Hz, 2H), 3.63-3.54 (m, 14H), 3.49 (t, J = 4.4 Hz, 2H), 3.16 (br s, 1H), 2.40 (t, J = 2.4 Hz, 1H) ppm.

^{13}C NMR (125 MHz, $CDCl_3$): δ = 79.6, 74.7, 72.5, 70.4, 70.2, 69.0, 61.5, 58.3 ppm.

NMR spectra for compound **6** are shown in Figures 3.4 and 3.5.

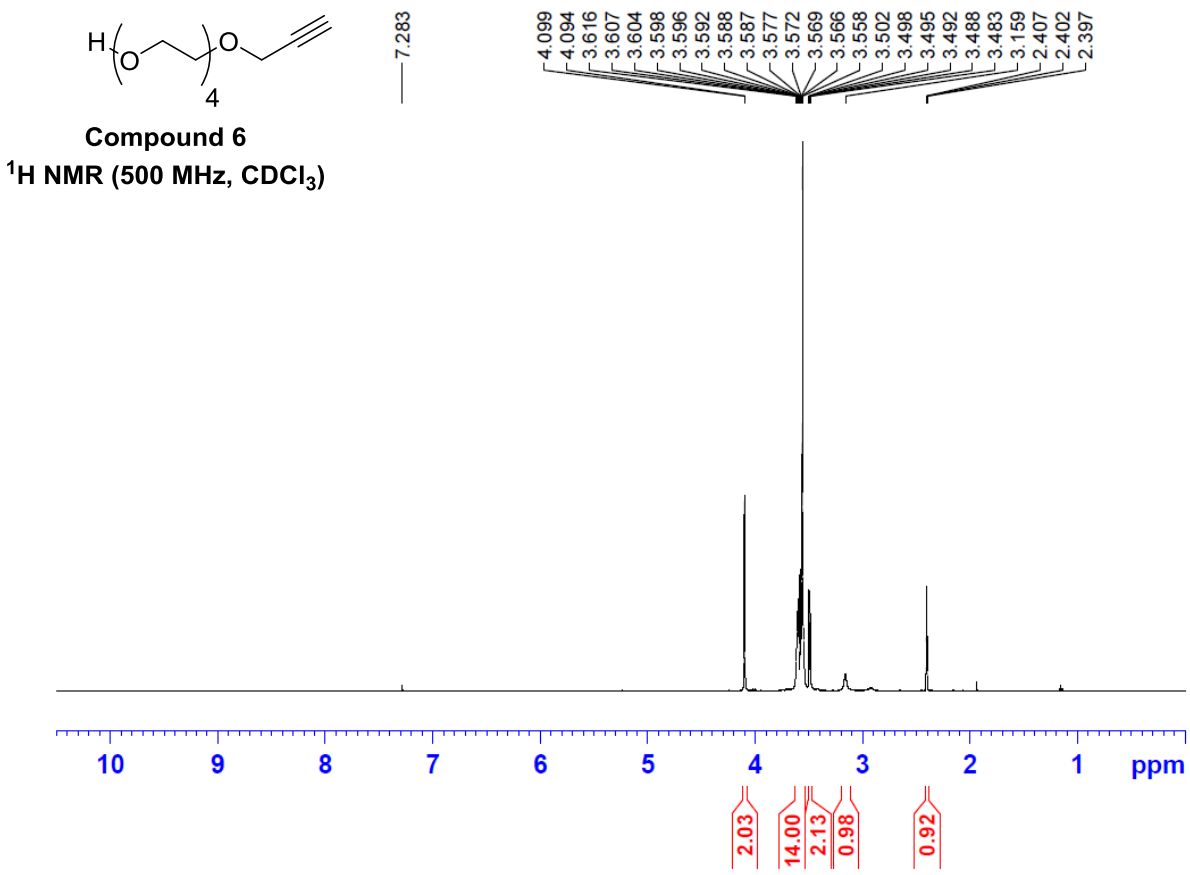

Figure 3.4 ^{1}H NMR spectra of compound **6**

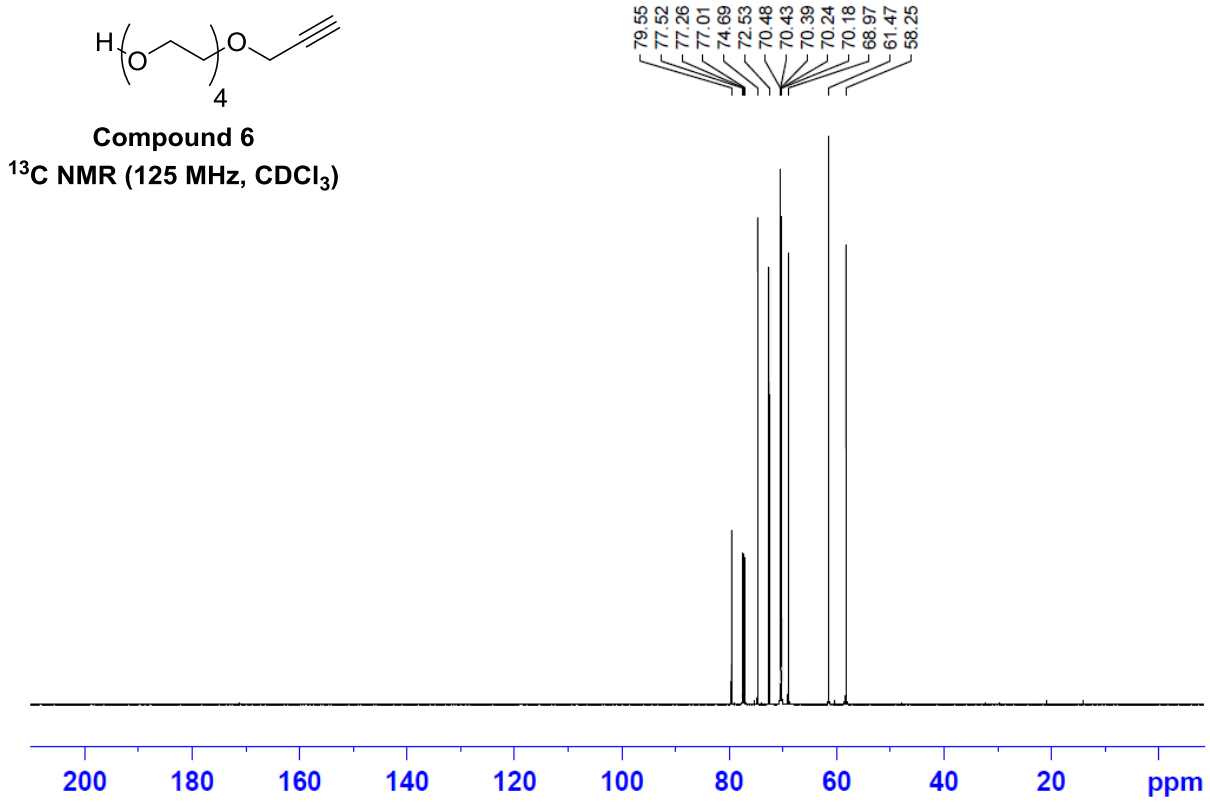

Figure 3.5 ^{13}C NMR spectra of compound **6**

Next, the remaining primary hydroxyl of **6** was brominated using PBr_3 dissolved anhydrous $CHCl_2$ to give the anticipated propargylated and brominated heterobifunctional tetraethylene glycol-based spacer/linker 1-bromo-3,6,9,12-tetraoxapentadec-14-yne **7** in 54% yield (see Figure 2.14).

^{1}H NMR (500 MHz, $CDCl_3$): δ = 4.23 (d, J = 2.4 Hz, 2H), 3.84 (t, J = 6.4 Hz, 2H), 3.75-3.67 (m, 12H), 3.50 (t, J = 6.4 Hz, 2H), 2.45 (t, J = 2.4 Hz, 1H) ppm.

^{13}C NMR (125 MHz, $CDCl_3$): δ = 79.7, 74.5, 71.2, 70.7, 70.6, 70.4, 69.1, 58.4, 30.3 ppm.

NMR spectra for compound **7** are shown in Figures 3.6 and 3.7.

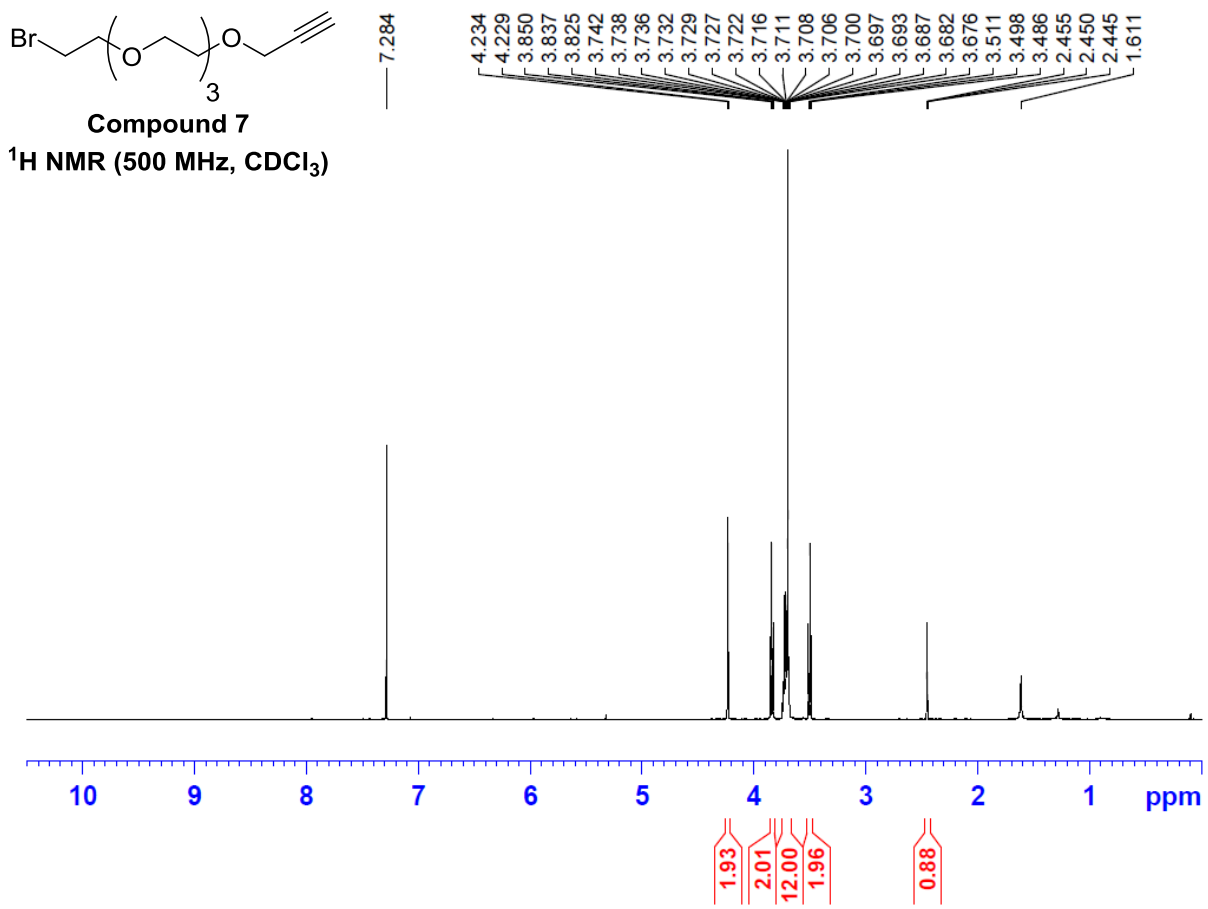

Figure 3.6 ^{1}H NMR spectra of compound **7**

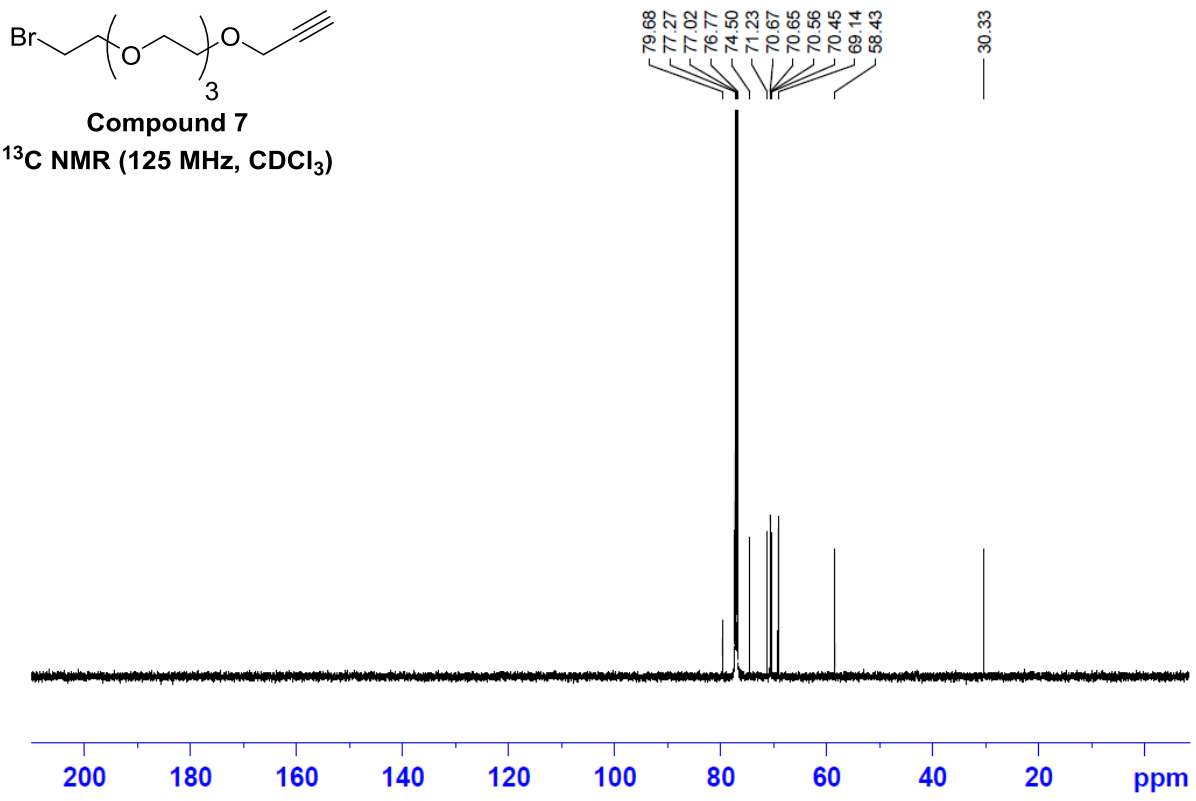

Figure 3.7 ^{13}C NMR spectra of compound **7**

With access to the heterobifunctional tetraethylene glycol-based spacer/linker **7,** we proceeded to the functionalization of the 7-Amino-4-methylcoumarin substrate **8** as required for the subsequent functionalization reaction (*vide infra*). To this end, the classical Sandmeyer reaction provides a convenient route for the conversion of arene diazonium salts which react with azide ions without Cu(I) catalyst[201] to the corresponding arene azide[201-203]. An azide group was introduced into **8** by treatment with concentrated HCl and $NaNO_2$ in aqueous solution, followed by NaN_3 in aqueous solution, provided 7-azido-4-methyl-2*H*-chromen-2-one **9** in a 84% combined yield over two-steps in one-pot (see Figure 2.16).

^{1}H NMR (500 MHz, $CDCl_3$): δ = 7.60 (d, J = 8.4 Hz, 1H), 7.02-6.96 (m, 2H), 6.26 (q, 1H), 2.45 (d, J = 1.2 Hz, 3H) ppm.

^{13}C NMR (125 MHz, $CDCl_3$): δ = 160.4, 154.7, 151.9, 143.9, 126.0, 117.1, 115.3, 114.0, 107.2, 18.7 ppm.

NMR spectra for compound **9** are shown in Figures 3.8 and 3.9.

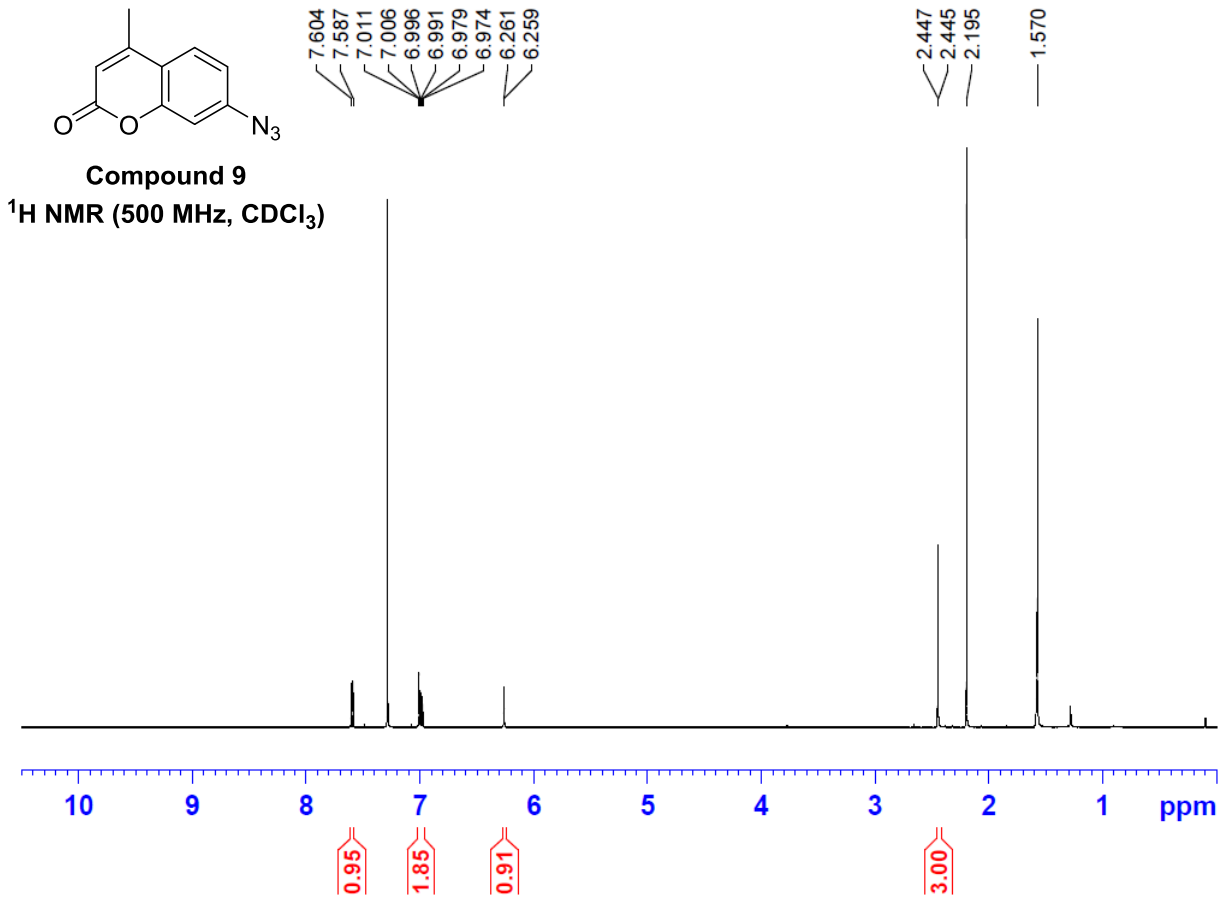

Figure 3.8 ^{1}H NMR spectra of compound **9**

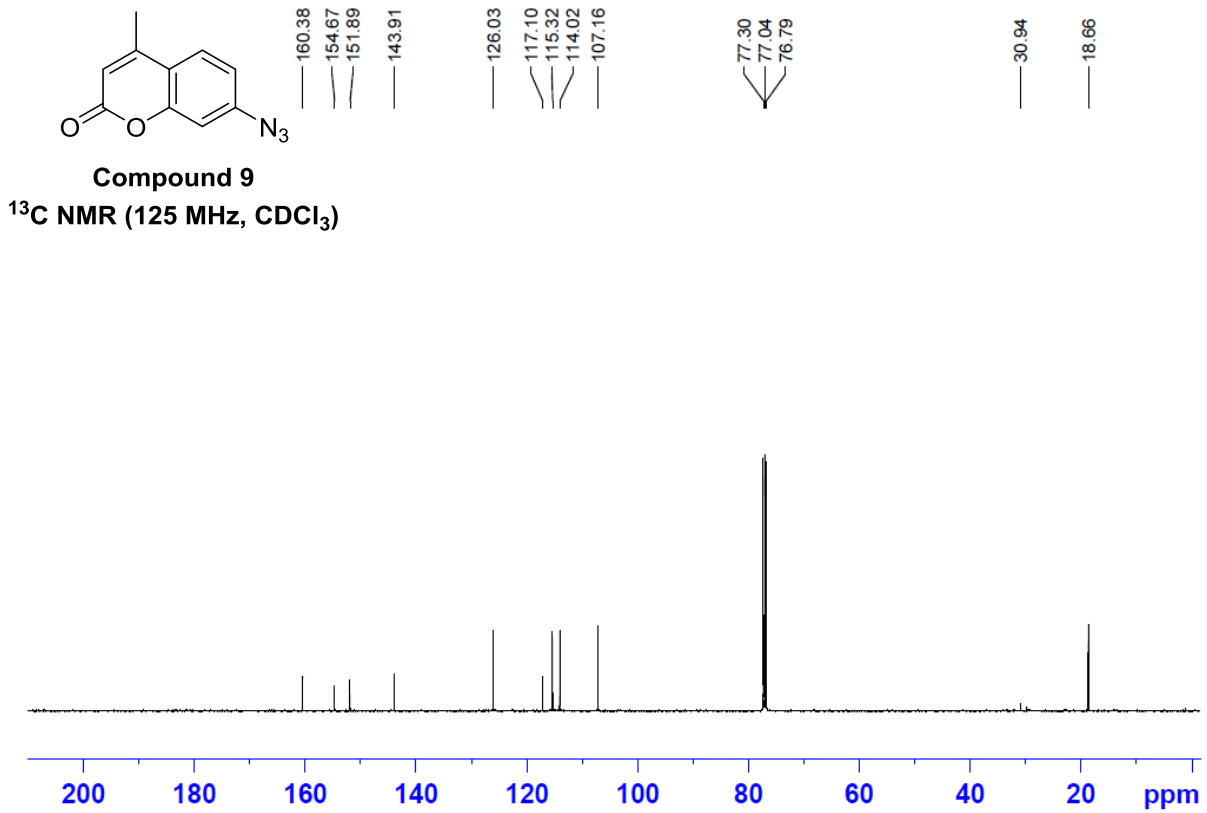

Figure 3.9 ^{13}C NMR spectra of compound **9**

With the two required fragments in hand, their assembly to a medicinally/therapeutically relevant 1,4-disubstituted 1,2,3-triazole heterocycle via Cu(I)-catalyzed Huisgen 1,3-dipolar cycloaddition was undertaken. Nitrogen-containing heterocycles are an important class of structures and form an integral part of therapeutically interesting compounds which display diverse biological activities, i.e., their structural subunits exist in many natural products (ubiquitous in nature) such as vitamins, hormones, antibiotics, alkaloids, pharmaceuticals, herbicides, and dyes[59]. In particular, the triazole moiety has been shown to act as a non-classical bioisostere surrogate to potentially labile functional groups (e.g., esters, amides); its stable heterocyclic ring mimics similar electrostatic potential map, thus it has the bioisosteric potential to mimic the amide of a peptide bond, i.e., act as an amide bond surrogate in peptidomimetic structures without the lability of the latter to acidic or basic hydrolysis[204]. Moreover, 1,2,3-triazoles subunits are of interest for their excellent PK characteristics, favourable safety profiles, latent ability for hydrogen bond formation, moderate dipole character, rigidity and stability under *in vivo* conditions[159]. Furthermore, it was reported that novobiocin (an aminocoumarin antibiotic[179] which selectively inhibits bacterial topoisomerase[205], i.e., novobiocin's antibacterial activity and its inhibition of the supercoiling activity of *E. coli* DNA gyrase[206]) analogs with 1,2,3-triazole conjugated at the 7th position exhibited obvious anticancer activity by inducing cell line apoptosis[159] (see discussion in section 1.3.10, p. 28). The functionalized alkyne **7** and azide **9** precursors were subjected to Cu(I)-catalyzed Huisgen 1,3-dipolar cycloaddition conditions to construct a 1,4-disubstituted 1,2,3-triazole heterocycle **10** in 52% yield (68% NMR yield, mesitylene as internal standard, see Figure 2.18).

^{1}H NMR (500 MHz, $CDCl_3$): δ = 8.17 (s, $1H_a$), 7.82 (dd, J = 8.6, 2.0 Hz, $1H_b$), 7.77 (d, J = 8.6 Hz, $1H_c$), 7.72 (d, J = 2.0 Hz, $1H_d$), 6.37 (q, $1H_e$), 4.82 (s, $2H_f$), 3.84-3.76 (m, $4H_g$), 3.76-3.64 (m, $10H_h$), 3.47 (t, J = 6.3 Hz, $2H_i$), 2.50 (d, J = 1.25 Hz, $3H_j$) ppm.

^{13}C NMR (125 MHz, $CDCl_3$): δ = 159.9, 154.2, 151.5, 139.1, 126.3, 120.8, 119.9, 115.9, 115.6, 108.3, 71.1, 70.7, 70.6, 70.5, 70.1, 64.6, 30.4, 18.7 ppm.

NMR spectra for compound **10** are shown in Figures 3.10 (proton labelled) and 3.11.

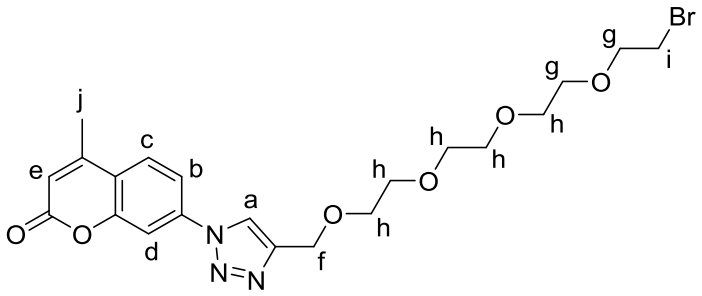

Compound 10

^{1}H NMR (500 MHz, $CDCl_3$) (proton labelled)

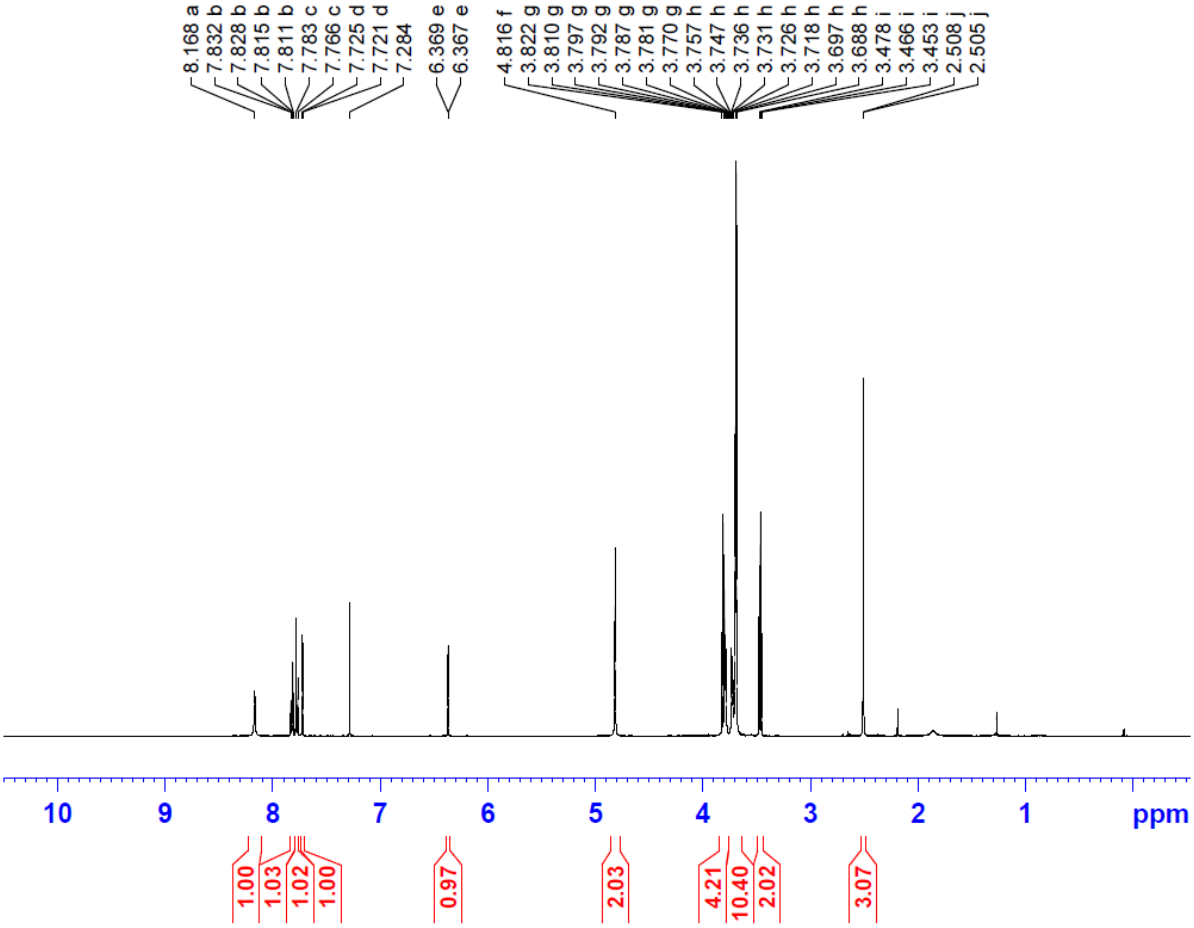

Figure 3.10 ^{1}H NMR spectra of compound **10** (proton labelled)

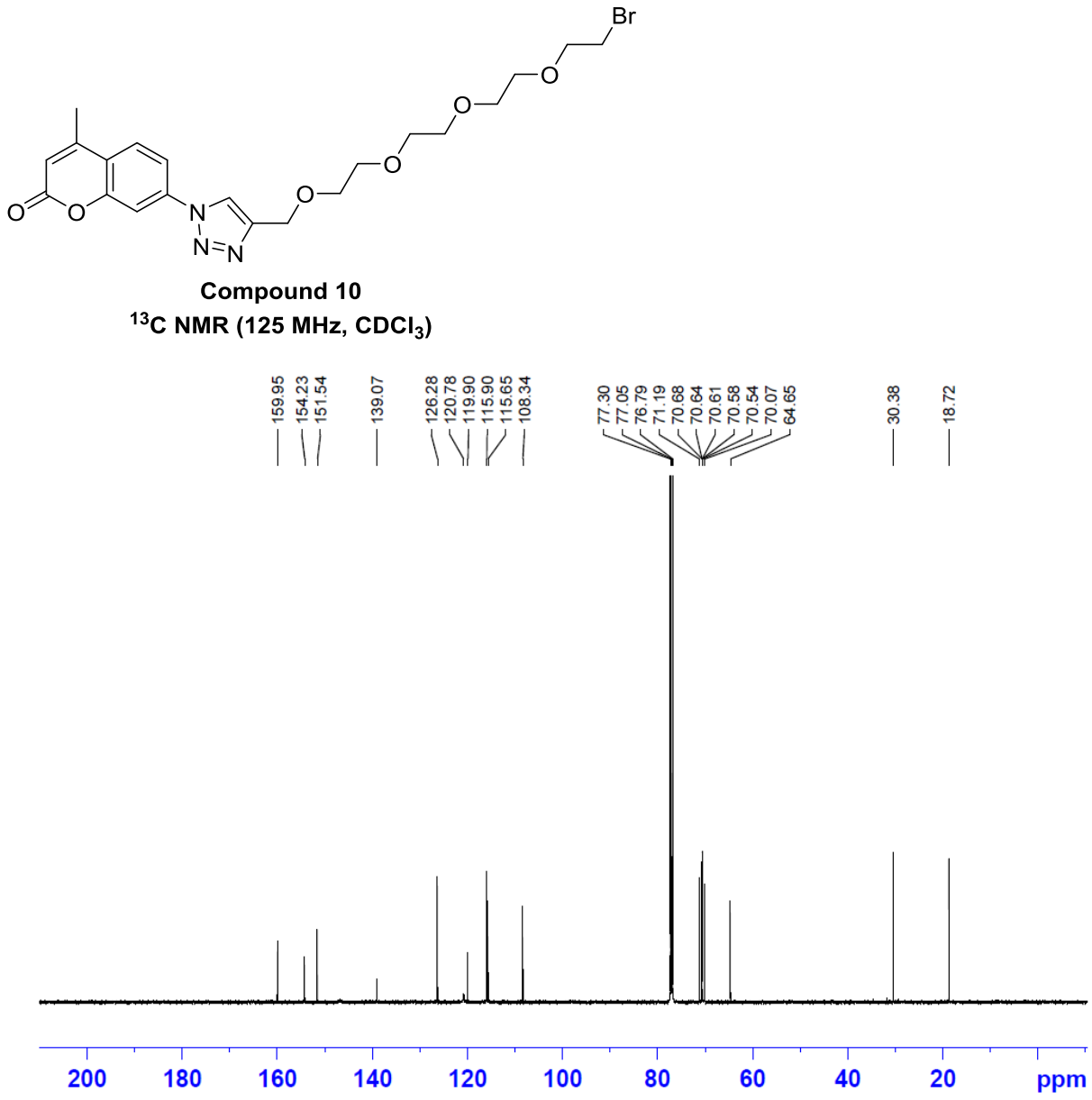

Figure 3.11 ^{13}C NMR spectra of compound **10**

To *aid* the readers who are not familiar with the chemical literature, peak assignments refer to protons labelled in Figure 3.10. However, this is done so only for this novel structure as peak assignments have been extensively described for the known structures of precursors. Note that proton labelling in peak assignments is uncommon for small molecules unless the focus is on studying key mechanistic aspects of a novel reaction or to gain structural information on complex formation involving cations, see references[207,208]. If peak assignments of broad polymer peaks (but proton labelled) is of interest to the reader, the following references could be consulted, FTIR spectra for coordination polymer, metal-organic frameworks (MOFs)[209] and macromolecular (co)polymeric architectures, e.g., photo-cross-linking acrylated *star*-poly(ε-caprolactone-*co*-D,L-lactide), *star*-poly(D,L-lactide), *star*-poly(ε-caprolactone), *star*-poly(ε-caprolactone-co-D,L-lactide), terminus-acrylated *star*-poly(ε-caprolactone-co-D,L-lactide)[210] .

To complete the overall modification, the functionalized side chain was introduced by submitting Fmoc-N-protected highly deacetylated chitosan oligosaccharides (COS) **4** to 1,4-disubstituted 1,2,3-triazole heterocycle **10** and 1,4-diazabicyclo[2.2.2]octane under neat/solvent-free ball milling conditions to deliver Fmoc-N-protected O-TEGylated spacer/linker 1,4-disubstituted 1,2,3-triazole heterocycle/coumarin functionalized highly deacetylated chitosan oligosaccharides (COS) **11** in 30% yield (see Figure 2.20). Admittedly, this approach required a 4 equiv large excess of **10**, a valuable and hard-won intermediate that had to be sacrificed in order to allow the reaction to proceed to completion. Whilst it is unsurprising that **4** was proven to be a challenging/recalcitrant biomass-derived substrate as illustrated by the current and final step which only gave 30% yield, it is worth keeping in mind that main objective of this work was to find a practical and workable route from **1** to **11**. Optimizing the overall yield and each of the stepwise yield were secondary concerns, surely attempted but definitely not the primary focus of this work.

^{1}H NMR (500 MHz, DMSO-d_6 at 90 °C): δ = 8.88-8.85 (m), 7.98-7.93 (m), 7.87-7.78 (m), 7.74-7.67 (m), 7.44-7.28 (m), 6.98 (br s), 6.43 (s), 6.22 (s), 4.68 (s), 4.58-4.42 (m), 4.39-4.18 (m), 3.85-3.19 (m), 2.63 (s) ppm.

NMR spectrum for compound **11** is shown in Figure 3.12.

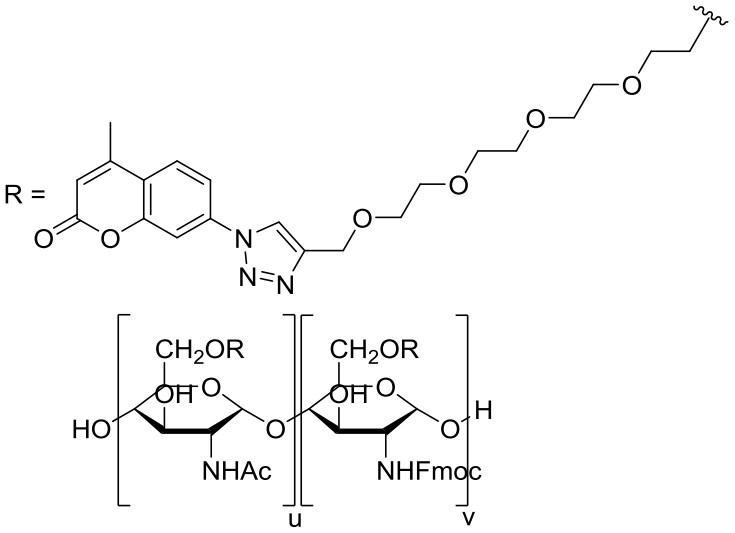

Compound 11
1H NMR (500 MHz, DMSO-d_6 at 90 °C)
proton integration omitted due to limited solubility

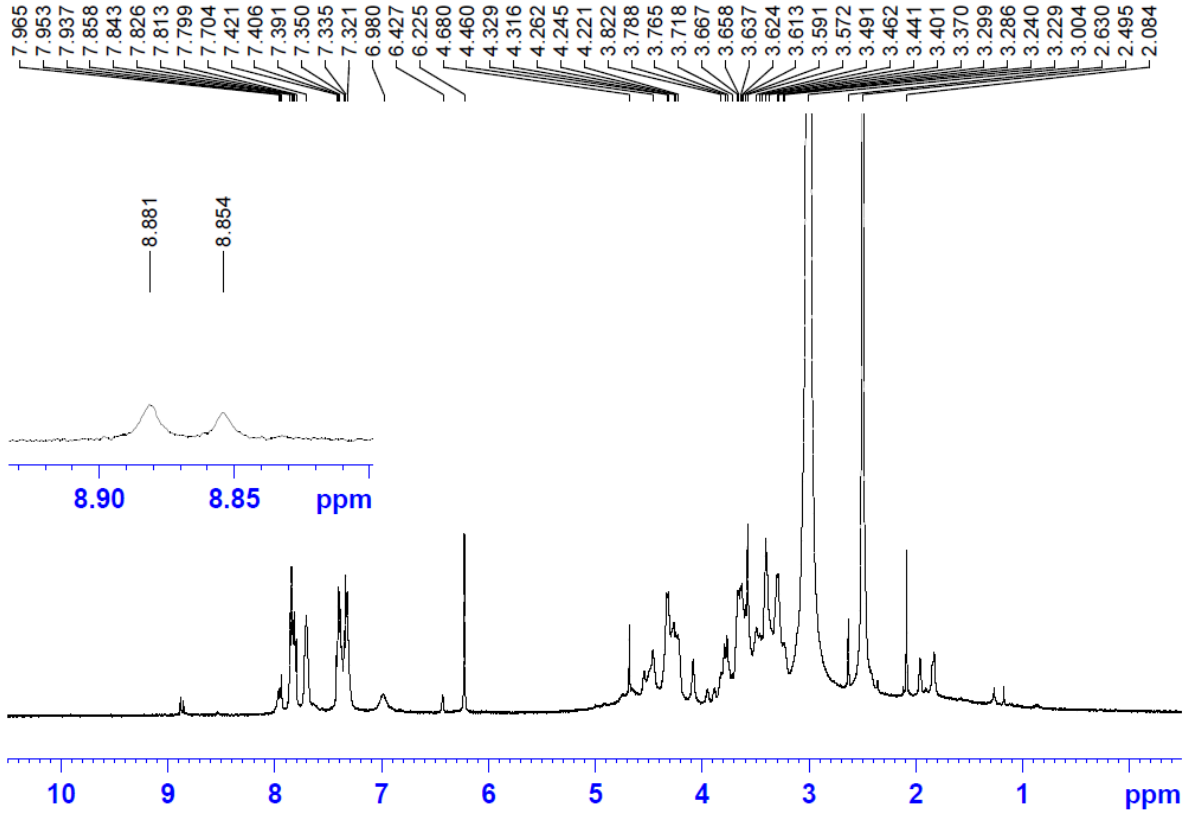

Figure 3.12 ^{1}H NMR spectra of compound **11**

The next chapter closes with some general conclusions about the demonstrated concept of employing HSBM methodology in this work for the practical transformation of recalcitrant biomass oligosaccharides in view of preparing useful new materials and platform molecules along with a brief discussion about possible future work or research directions.

CHAPTER 4
CONCLUSION

In summary, we demonstrated that high-value oligosaccharide biomaterials could be prepared from abundant and renewable biomass carbohydrate residues (shellfish waste) which are inherently biodegradable, as a sustainable carbon based feedstock, hence entirely consonant with the concept of a waste-based biorefinery.

To this end, we have developed a novel method leading to the modification of recalcitrant biomass oligosaccharides where hitherto traditional solution-based methodologies typically involve harsh conditions such as elevated temperature, long reaction times, excess and concentrated acids or bases; under such conditions, carbohydrates readily undergo problematic side reactions, thus forming myriad complex compounds. The key design aspect of our strategy was to recognize the potential for the deliberate employment of mechanical force and energy by means of high speed ball milling (HSBM) to effect productive and purposeful chemical transformations of recalcitrant oligosaccharides for the preparation of useful new materials and platform molecules. HSBM is a method conventionally used in material science and engineering for mechanochemical mixing (i.e., advanced comminution/particle size reduction, see discussions in sections 1.1, p. 4, and 1.3.8, Table 1.1) but one which remains largely unexplored with the perspective of deliberately effecting constructive chemical changes in recalcitrant biomass substrates. In light of the difficulties and harsh conditions associated with classical solution-based methodologies, HSBM as a non-thermal method and operationally simple process provides numerous advantages for the practical transformation of recalcitrant biomass oligosaccharides, namely mild processing (room temperature, ambient air, shorter reaction times) and solvent-free (absence of toxic or carcinogenic high boiling polar aprotic solvents such as pyridine, DMF, DMSO) conditions (see discussion in section 1.2, p. 10). In this work, HSBM was proven to be particularly beneficial as it provides access to complex carbohydrate structures that could not be readily obtained by other methods or means, namely solution-based (peptide synthesis protocols) and alternative energy methodologies such as microwave-assisted and ultrasonic (sonochemistry) irradiation. In short, the methodology reported herein provides access to challenging modifications in a mild manner and to otherwise difficult-to-access structurally

complex products using conventional solution-based methodologies or by the aforementioned alternative energy approaches.

Furthermore, the late-stage incorporation of a medicinally/therapeutically relevant side chain with potential anticancer, antitumour, and/or antitubercular profiles (see discussions in sections 1.3.10, p. 29, 1.3.11, p. 29, 1.3.12, p. 30, and Chapter 3, p. 79) to a key intermediate oligosaccharide-based scaffold (see discussion in section 1.2, p. 12) or support or carrier produced from renewable and functionalized feedstock biomass demonstrates the generality, modularity, and applicability to complex biomass-derived substrates for late-stage diversification of the HSBM methodology, and offers a glimpse/hint at the potential and possibilities (future work) for the versatile preparation of a wide range and/or new classes of compounds or derivatives or variants tailored for medicinal chemistry, materials chemistry, biosensing and other applications as well as for the practical process conversion and scale-up from laboratory-scale shaker/mixer mill into readily available and industrially utilized large-sized planetary mills. As alluded to in section 1.2, p. 12, future work could focus on harnessing HSBM solvent-free methodologies for the chemical modification of oligosaccharide residues intended to function as carriers for several pharmaceutical applications, including therapeutic deliveries of DNA, drugs, growth factors or as pH-sensitive coating agents for tumour-specific drug delivery. For pharmaceutical applications, it is worth re-emphasizing that the ability to chemically modify oligosaccharide residues in mild temperature conditions (ca. 7-12 °C above room temperature, see discussion in section 1.2, p. 8, which is a very negligible temperature increase compared to the harsh elevated temperature range used in the traditional solution-based methodologies for monosaccharide, oligosaccharide, and polysaccharide modifications) in the absence of toxic or carcinogenic high boiling polar aprotic solvents and without the use of concentrated or excessive amounts of harsh acids or bases (see discussion in section 1.2, p. 10) proves to be very advantageous and valuable as does the design choice of utilizing oligosaccharide residues which have been widely reported to possess lower haemolytic, hepatotropic, and cytotoxicity profiles (important considerations for the pharmaceutical field) than their polymeric polysaccharide counterparts (see discussion in section 1.2, p. 12). Similarly, the above properties would undeniably also be desirable for biosensing applications (see discussion in section 1.2, p. 13).

The long-term implications for the mechanochemistry, green chemistry, medicinal chemistry, pharmaceutical and biomedical (drug carrier, hydrogels, scaffolds, etc) fields from the HSBM solvent-free methodology developed in this thesis is that a modern 21st century greener alternative approach to the early 1990s era polymer cross-linking one is now viable to sidestep the known and extensively documented cytotoxicity aspects related to the cross-linking paradigm (see discussion in section 1.3.7, p. 18); an early 1990s era where the environmental damage, hazards and costs of remediation (copious organic (co-)solvent(s) and distilled/deionized water usage in polymer methodologies and protocols, e.g., repeated wash and/or solvent exchange cycles which generate large volume of effluent wastewater containing mixtures of chemicals and organic solvents, see discussions in section 1.3.2, p. 14 and references in section 1.3.3, p. 15) are not taken into account in the production of chemically modified and useful materials (important considerations in contemporary 21st century, see discussion in section 1.1, p. 4). Lastly, the HSBM solvent-free methodology developed in this thesis, unlike the early 1990s era polymer cross-linking paradigm (see discussion in section 1.3.7, p. 20), is one that can accommodate crystalline and recalcitrant biomass for the purposeful chemical modification of oligosaccharide residues under solvent-free and mild temperature conditions (as demonstrated in this thesis, whereas previously ball milling was merely used as a physical pretreatment method for biomass comminution or reduction in particle size and/or crystallinity, see discussions in sections 1.1, p. 4, and 1.3.8, Table 1.1, mechanical comminution including ball milling), which are arguably, the only remaining readily available carbon feedstock (most importantly, renewable long-term source of organic carbon, see discussion in section 1.1, p. 3) for the production of valuable platform chemicals and fuels moving forward late into the 21st century.

REFERENCES

1. Sheldon, R. A. Green and sustainable manufacture of chemicals from biomass: state of the art. *Green Chem.* **16**, 950-963 (2014).

2. Lin, C. S. K. *et al.* Food waste as a valuable resource for the production of chemicals, materials and fuels. Current situation and global perspective. *Energy Environ. Sci.* **6**, 426-464 (2013).

3. Van den Bosch, S. *et al.* Reductive lignocellulose fractionation into soluble lignin-derived phenolic monomers and dimers and processable carbohydrate pulps. *Energy Environ. Sci.* **8**, 1748-1763 (2015).

4. Farrán, A. *et al.* Green Solvents in Carbohydrate Chemistry: From Raw Materials to Fine Chemicals. *Chem. Rev.* **115**, 6811-6853 (2015).

5. Zakzeski, J., Bruijnincx, P. C. A., Jongerius, A. L. & Weckhuysen, B. M. The Catalytic Valorization of Lignin for the Production of Renewable Chemicals. *Chem. Rev.* **110**, 3552-3599 (2010).

6. Van de Vyver, S., Geboers, J., Jacobs, P. A. & Sels, B. F. Recent Advances in the Catalytic Conversion of Cellulose. *ChemCatChem* **3**, 82-94 (2011).

7. Chen, X., Yang, H., Zhong, Z. & Yan, N. Base-catalysed, one-step mechanochemical conversion of chitin and shrimp shells into low molecular weight chitosan. *Green Chem.* **19**, 2783-2792 (2017).

8. Chen, X., Yang, H. & Yan, N. Shell Biorefinery: Dream or Reality? *Chem. Eur. J.* **22**, 13402-13421 (2016).

9. Szabolcs, A., Molnar, M., Dibo, G. & Mika, L. T. Microwave-assisted conversion of carbohydrates to levulinic acid: an essential step in biomass conversion. *Green Chem.* **15**, 439-445 (2013).

10. Alonso, D. M., Bond, J. Q. & Dumesic, J. A. Catalytic conversion of biomass to biofuels. *Green Chem.* **12**, 1493-1513 (2010).

11. Song, J., Fan, H., Ma, J. & Han, B. Conversion of glucose and cellulose into value-added products in water and ionic liquids. *Green Chem.* **15**, 2619-2635 (2013).

12. Sheldon, R. A. The E factor 25 years on: the rise of green chemistry and sustainability. *Green Chem.* **19**, 18-43 (2017).

13. Chatel, G., De Oliveira Vigier, K. & Jérôme, F. Sonochemistry: What Potential for Conversion of Lignocellulosic Biomass into Platform Chemicals? *ChemSusChem* **7**, 2774-2787 (2014).

14. Zhang, Y., Pidko, E. A. & Hensen, E. J. M. Molecular Aspects of Glucose Dehydration by Chromium Chlorides in Ionic Liquids. *Chem. Eur. J.* **17**, 5281-5288 (2011).

15. Yan, N. & Chen, X. Sustainability: Don't waste seafood waste. *Nature* **524**, 155-157 (2015).

16. Kerton, F. M., Liu, Y., Omari, K. W. & Hawboldt, K. Green chemistry and the ocean-based biorefinery. *Green Chem.* **15**, 860-871 (2013).

17. Kaur, S. & Dhillon, G. S. Recent trends in biological extraction of chitin from marine shell wastes: a review. *Crit. Rev. Biotechnol.* **35**, 44-61 (2015).

18. Tuck, C. O., Pérez, E., Horváth, I. T., Sheldon, R. A. & Poliakoff, M. Valorization of Biomass: Deriving More Value from Waste. *Science* **337**, 695-699 (2012).

19. Margoutidis, G., Parsons, V. H., Bottaro, C. S., Yan, N. & Kerton, F. M. Mechanochemical Amorphization of α-Chitin and Conversion into Oligomers of N-Acetyl-d-glucosamine. *ACS Sustainable Chem. Eng.* **6**, 1662-1669 (2018).

20. Tabasso, S., Carnaroglio, D., Calcio Gaudino, E. & Cravotto, G. Microwave, ultrasound and ball mill procedures for bio-waste valorisation. *Green Chem.* **17**, 684-693 (2015).

21. Huang, Y.-B. & Fu, Y. Hydrolysis of cellulose to glucose by solid acid catalysts. *Green Chem.* **15**, 1095-1111 (2013).

22. Dusselier, M., Van Wouwe, P., Dewaele, A., Makshina, E. & Sels, B. F. Lactic acid as a platform chemical in the biobased economy: the role of chemocatalysis. *Energy Environ. Sci.* **6**, 1415-1442 (2013).

23. Bozell, J. J. & Petersen, G. R. Technology development for the production of biobased products from biorefinery carbohydrates-the US Department of Energy's "Top 10" revisited. *Green Chem.* **12**, 539-554 (2010).

24. Sheldon, R. A. Fundamentals of green chemistry: efficiency in reaction design. *Chem. Soc. Rev.* **41**, 1437-1451 (2012).

25. Wahlstrom, R. M. & Suurnakki, A. Enzymatic hydrolysis of lignocellulosic polysaccharides in the presence of ionic liquids. *Green Chem.* **17**, 694-714 (2015).

26. Zhang, Q. & Jérôme, F. Mechanocatalytic Deconstruction of Cellulose: An Emerging Entry into Biorefinery. *ChemSusChem* **6**, 2042-2044 (2013).

27. Nakagawa, Y. S., Eijsink, V. G. H., Totani, K. & Vaaje-Kolstad, G. Conversion of α-Chitin Substrates with Varying Particle Size and Crystallinity Reveals Substrate Preferences of the Chitinases and Lytic Polysaccharide Monooxygenase of Serratia marcescens. *J. Agric. Food Chem.* **61**, 11061-11066 (2013).

28. Meine, N., Rinaldi, R. & Schüth, F. Solvent‐Free Catalytic Depolymerization of Cellulose to Water‐Soluble Oligosaccharides. *ChemSusChem* **5**, 1449-1454 (2012).

29. Hilgert, J., Meine, N., Rinaldi, R. & Schüth, F. Mechanocatalytic depolymerization of cellulose combined with hydrogenolysis as a highly efficient pathway to sugar alcohols. *Energy Environ. Sci.* **6**, 92-96 (2013).

30. Chen, X., Chew, S. L., Kerton, F. M. & Yan, N. Direct conversion of chitin into a N-containing furan derivative. *Green Chem.* **16**, 2204-2212 (2014).

31. Carrasquillo-Flores, R., Käldström, M., Schüth, F., Dumesic, J. A. & Rinaldi, R. Mechanocatalytic Depolymerization of Dry (Ligno)cellulose As an Entry Process for High-Yield Production of Furfurals. *ACS Catal.* **3**, 993-997 (2013).

32. S. Ribeiro, L., Orfao, J. J. M. & R. Pereira, M. F. Enhanced direct production of sorbitol by cellulose ball-milling. *Green Chem.* **17**, 2973-2980 (2015).

33. Yabushita, M., Kobayashi, H., Kuroki, K., Ito, S. & Fukuoka, A. Catalytic Depolymerization of Chitin with Retention of N‐Acetyl Group. *ChemSusChem* **8**, 3760-3763 (2015).

34. Kralisch, D., Ott, D. & Gericke, D. Rules and benefits of Life Cycle Assessment in green chemical process and synthesis design: a tutorial review. *Green Chem.* **17**, 123-145 (2015).

35. Kleine, T., Buendia, J. & Bolm, C. Mechanochemical degradation of lignin and wood by solvent-free grinding in a reactive medium. *Green Chem.* **15**, 160-166 (2013).

36. Hernández, J. G. & Bolm, C. Altering Product Selectivity by Mechanochemistry. *J. Org. Chem.* **82**, 4007-4019 (2017).

37. James, S. L. *et al.* Mechanochemistry: opportunities for new and cleaner synthesis. *Chem. Soc. Rev.* **41**, 413-447 (2012).

38. Tan, D. & Friščić, T. Mechanochemistry for Organic Chemists: An Update. *Eur. J. Org. Chem.* **2018**, 18-33 (2018).

39. Strukil, V. *et al.* A model for a solvent-free synthetic organic research laboratory: click-mechanosynthesis and structural characterization of thioureas without bulk solvents. *Green Chem.* **14**, 2462-2473 (2012).

40. Friščić, T. Supramolecular concepts and new techniques in mechanochemistry: cocrystals, cages, rotaxanes, open metal-organic frameworks. *Chem. Soc. Rev.* **41**, 3493-3510 (2012).

41. Boldyreva, E. Mechanochemistry of inorganic and organic systems: what is similar, what is different? *Chem. Soc. Rev.* **42**, 7719-7738 (2013).

42. Kaldstrom, M., Meine, N., Fares, C., Rinaldi, R. & Schüth, F. Fractionation of 'water-soluble lignocellulose' into C5/C6 sugars and sulfur-free lignins. *Green Chem.* **16**, 2454-2462 (2014).

43. Stolle, A., Szuppa, T., Leonhardt, S. E. S. & Ondruschka, B. Ball milling in organic synthesis: solutions and challenges. *Chem. Soc. Rev.* **40**, 2317-2329 (2011).

44. Zhu, S.-E., Li, F. & Wang, G.-W. Mechanochemistry of fullerenes and related materials. *Chem. Soc. Rev.* **42**, 7535-7570 (2013).

45. Rightmire, N. R. & Hanusa, T. P. Advances in organometallic synthesis with mechanochemical methods. *Dalton Trans.* **45**, 2352-2362 (2016).

46. Takacs, L. The historical development of mechanochemistry. *Chem. Soc. Rev.* **42**, 7649-7659 (2013).

47. Friščić, T. *et al.* Real-time and in situ monitoring of mechanochemical milling reactions. *Nat. Chem.* **5**, 66-73 (2013).

48. Cravotto, G., Gaudino, E. C. & Cintas, P. On the mechanochemical activation by ultrasound. *Chem. Soc. Rev.* **42**, 7521-7534 (2013).

49. Balaz, P. *et al.* Hallmarks of mechanochemistry: from nanoparticles to technology. *Chem. Soc. Rev.* **42**, 7571-7637 (2013).

50. Tan, D., Loots, L. & Friščić, T. Towards medicinal mechanochemistry: evolution of milling from pharmaceutical solid form screening to the synthesis of active pharmaceutical ingredients (APIs). *Chem. Commun.* **52**, 7760-7781 (2016).

51. Jones, W. & Eddleston, M. D. Introductory Lecture: Mechanochemistry, a versatile synthesis strategy for new materials. *Faraday Discuss.* **170**, 9-34 (2014).

52. Kaldstrom, M., Meine, N., Fares, C., Schüth, F. & Rinaldi, R. Deciphering 'water-soluble lignocellulose' obtained by mechanocatalysis: new insights into the chemical processes leading to deep depolymerization. *Green Chem.* **16**, 3528-3538 (2014).

53. Užarević, K. *et al.* Exploring the Effect of Temperature on a Mechanochemical Reaction by in Situ Synchrotron Powder X-ray Diffraction. *Cryst. Growth Des.* **16**, 2342-2347 (2016).

54. Bowmaker, G. A. Solvent-assisted mechanochemistry. *Chem. Commun.* **49**, 334-348 (2013).

55. Schmidt, R. *et al.* Fast, Ligand‐ and Solvent‐Free Synthesis of 1,4‐Substituted Buta‐1,3‐diynes by Cu‐Catalyzed Homocoupling of Terminal Alkynes in a Ball Mill. *Chem. Eur. J.* **17**, 8129-8138 (2011).

56. Paveglio, G. C. *et al.* How Mechanical and Chemical Features Affect the Green Synthesis of 1H-Pyrazoles in a Ball Mill. *ACS Sustainable Chem. Eng.* **2**, 1895-1901 (2014).

57. Wang, G.-W. Mechanochemical organic synthesis. *Chem. Soc. Rev.* **42**, 7668-7700 (2013).

58. Štrukil, V., Gracin, D., Magdysyuk, O. V., Dinnebier, R. E. & Friščić, T. Trapping Reactive Intermediates by Mechanochemistry: Elusive Aryl N‐Thiocarbamoylbenzotriazoles as Bench‐Stable Reagents. *Angew. Chem. Int. Ed.* **54**, 8440-8443 (2015).

59. Baig, R. B. N. & Varma, R. S. Alternative energy input: mechanochemical, microwave and ultrasound-assisted organic synthesis. *Chem. Soc. Rev.* **41**, 1559-1584 (2012).

60. Jérôme, F., Chatel, G. & De Oliveira Vigier, K. Depolymerization of cellulose to processable glucans by non-thermal technologies. *Green Chem.* **18**, 3903-3913 (2016).

61. Pierson, Y., Chen, X., Bobbink, F. D., Zhang, J. & Yan, N. Acid-Catalyzed Chitin Liquefaction in Ethylene Glycol. *ACS Sustainable Chem. Eng.* **2**, 2081-2089 (2014).

62. Dutta, S., De, S., Alam, M. I., Abu-Omar, M. M. & Saha, B. Direct conversion of cellulose and lignocellulosic biomass into chemicals and biofuel with metal chloride catalysts. *J. Catal.* **288**, 8-15 (2012).

63. Ravalico, F., James, S. L. & Vyle, J. S. Synthesis of nucleoside analogues in a ball mill: fast, chemoselective and high yielding acylation without undesirable solvents. *Green Chem.* **13**, 1778-1783 (2011).

64. Osada, M. *et al.* Non-catalytic synthesis of Chromogen I and III from N-acetyl-d-glucosamine in high-temperature water. *Green Chem.* **15**, 2960-2966 (2013).

65. Shen, X., Shamshina, J. L., Berton, P., Gurau, G. & Rogers, R. D. Hydrogels based on cellulose and chitin: fabrication, properties, and applications. *Green Chem.* **18**, 53-75 (2016).

66. Virkutyte, J. & Varma, R. S. Green synthesis of metal nanoparticles: Biodegradable polymers and enzymes in stabilization and surface functionalization. *Chem. Sci.* **2**, 837-846 (2011).

67. Kuhbeck, D., Saidulu, G., Reddy, K. R. & Diaz, D. D. Critical assessment of the efficiency of chitosan biohydrogel beads as recyclable and heterogeneous organocatalyst for C-C bond formation. *Green Chem.* **14**, 378-392 (2012).

68. Park, J. H., Saravanakumar, G., Kim, K. & Kwon, I. C. Targeted delivery of low molecular drugs using chitosan and its derivatives. *Adv. Drug Delivery Rev.* **62**, 28-41 (2010).

69. Hamed, I., Özogul, F. & Regenstein, J. M. Industrial applications of crustacean by-products (chitin, chitosan, and chitooligosaccharides): A review. *Trends Food Sci. Technol.* **48**, 40-50 (2016).

70. Duceppe, N. & Tabrizian, M. Factors influencing the transfection efficiency of ultra low molecular weight chitosan/hyaluronic acid nanoparticles. *Biomaterials* **30**, 2625-2631 (2009).

71. Vela Gurovic, M. S. *et al.* Chitooligosaccharides as novel ingredients of fermented foods. *Food Funct.* **6**, 3437-3443 (2015).

72. Zou, P. *et al.* Advances in characterisation and biological activities of chitosan and chitosan oligosaccharides. *Food Chem.* **190**, 1174-1181 (2016).

73. Fernandes, J. C. *et al.* Antimicrobial effects of chitosans and chitooligosaccharides, upon Staphylococcus aureus and Escherichia coli, in food model systems. *Food Microbiol.* **25**, 922-928 (2008).

74. Wang, Y. *et al.* Low molecular weight chitosan is an effective antifungal agent against Botryosphaeria sp. and preservative agent for pear (Pyrus) fruits. *Int. J. Biol. Macromol.* **95**, 1135-1143 (2017).

75. Richardson, S. C. W., Kolbe, H. V. J. & Duncan, R. Potential of low molecular mass chitosan as a DNA delivery system: biocompatibility, body distribution and ability to complex and protect DNA. *Int. J. Pharm.* **178**, 231-243 (1999).

76. Kean, T. & Thanou, M. Biodegradation, biodistribution and toxicity of chitosan. *Adv. Drug Delivery Rev.* **62**, 3-11 (2010).

77. Bernkop-Schnürch, A. & Dünnhaupt, S. Chitosan-based drug delivery systems. *Eur. J. Pharm. Biopharm.* **81**, 463-469 (2012).

78. Kumar, M. N. V. R., Muzzarelli, R. A. A., Muzzarelli, C., Sashiwa, H. & Domb, A. J. Chitosan Chemistry and Pharmaceutical Perspectives. *Chem. Rev.* **104**, 6017-6084 (2004).

79. Guang Liu, W. & De Yao, K. Chitosan and its derivatives—a promising non-viral vector for gene transfection. *J. Controlled Release* **83**, 1-11 (2002).

80. Amarnath, L. P., Srinivas, A. & Ramamurthi, A. In vitro hemocompatibility testing of UV-modified hyaluronan hydrogels. *Biomaterials* **27**, 1416-1424 (2006).

81. Davis, A. P. & Wareham, R. S. Carbohydrate Recognition through Noncovalent Interactions: A Challenge for Biomimetic and Supramolecular Chemistry. *Angew. Chem. Int. Ed.* **38**, 2978-2996 (1999).

82. van Rantwijk, F. & Sheldon, R. A. Biocatalysis in Ionic Liquids. *Chem. Rev.* **107**, 2757-2785 (2007).

83. Mahal, L. K., Yarema, K. J. & Bertozzi, C. R. Engineering Chemical Reactivity on Cell Surfaces Through Oligosaccharide Biosynthesis. *Science* **276**, 1125-1128 (1997).

84. Zalipsky, S. Functionalized Poly(ethylene glycols) for Preparation of Biologically Relevant Conjugates. *Bioconjugate Chem.* **6**, 150-165 (1995).

85. Zalipsky, S. Chemistry of polyethylene glycol conjugates with biologically active molecules. *Adv. Drug Delivery Rev.* **16**, 157-182 (1995).

86. Mar, G. J., Barrington, M. J. & McGuirk, B. R. Acute compartment syndrome of the lower limb and the effect of postoperative analgesia on diagnosis†. *Br. J. Anaesth.* **102**, 3-11 (2009).

87. Zhang, H., Jin, Y., Deng, Y., Wang, D. & Zhao, Y. Production of chitin from shrimp shell powders using Serratia marcescens B742 and Lactobacillus plantarum ATCC 8014 successive two-step fermentation. *Carbohydr. Res.* **362**, 13-20 (2012).

88. Sedaghat, F., Yousefzadi, M., Toiserkani, H. & Najafipour, S. Chitin from Penaeus merguiensis via microbial fermentation processing and antioxidant activity. *Int. J. Biol. Macromol.* **82**, 279-283 (2016).

89. Mao, X., Guo, N., Sun, J. & Xue, C. Comprehensive utilization of shrimp waste based on biotechnological methods: A review. *J. Cleaner Prod.* **143**, 814-823 (2017).

90. Shamshina, J. L., Barber, P. S., Gurau, G., Griggs, C. S. & Rogers, R. D. Pulping of Crustacean Waste Using Ionic Liquids: To Extract or Not To Extract. *ACS Sustainable Chem. Eng.* **4**, 6072-6081 (2016).

91. Barber, P. S., Kelley, S. P., Griggs, C. S., Wallace, S. & Rogers, R. D. Surface modification of ionic liquid-spun chitin fibers for the extraction of uranium from seawater: seeking the strength of chitin and the chemical functionality of chitosan. *Green Chem.* **16**, 1828-1836 (2014).

92. Qin, Y., Lu, X., Sun, N. & Rogers, R. D. Dissolution or extraction of crustacean shells using ionic liquids to obtain high molecular weight purified chitin and direct production of chitin films and fibers. *Green Chem.* **12**, 968-971 (2010).

93. Lamarque, G., Viton, C. & Domard, A. Comparative Study of the First Heterogeneous Deacetylation of α- and β-Chitins in a Multistep Process. *Biomacromolecules* **5**, 992-1001 (2004).

94. Popa-Nita, S., Lucas, J.-M., Ladavière, C., David, L. & Domard, A. Mechanisms Involved During the Ultrasonically Induced Depolymerization of Chitosan: Characterization and Control. *Biomacromolecules* **10**, 1203-1211 (2009).

95. Khor, E. & Lim, L. Y. Implantable applications of chitin and chitosan. *Biomaterials* **24**, 2339-2349 (2003).

96. Fatimi, A. *et al.* A new injectable radiopaque chitosan-based sclerosing embolizing hydrogel for endovascular therapies. *Acta Biomater.* **8**, 2712-2721 (2012).

97. Nagahama, H. *et al.* Preparation of biodegradable chitin/gelatin membranes with GlcNAc for tissue engineering applications. *Carbohydr. Polym.* **73**, 456-463 (2008).

98. Ruel-Gariépy, E. *et al.* A thermosensitive chitosan-based hydrogel for the local delivery of paclitaxel. *Eur. J. Pharm. Biopharm.* **57**, 53-63 (2004).

99. Tikhonov, V. E. *et al.* Bactericidal and antifungal activities of a low molecular weight chitosan and its N-/2(3)-(dodec-2-enyl)succinoyl/-derivatives. *Carbohydr. Polym.* **64**, 66-72 (2006).

100. Muzzarelli, R. A. A., Greco, F., Busilacchi, A., Sollazzo, V. & Gigante, A. Chitosan, hyaluronan and chondroitin sulfate in tissue engineering for cartilage regeneration: A review. *Carbohydr. Polym.* **89**, 723-739 (2012).

101. Monette, A., Ceccaldi, C., Assaad, E., Lerouge, S. & Lapointe, R. Chitosan thermogels for local expansion and delivery of tumor-specific T lymphocytes towards enhanced cancer immunotherapies. *Biomaterials* **75**, 237-249 (2016).

102. Moreau, J. L. & Xu, H. H. K. Mesenchymal stem cell proliferation and differentiation on an injectable calcium phosphate – Chitosan composite scaffold. *Biomaterials* **30**, 2675-2682 (2009).

103. Muzzarelli, R. A. A. *et al.* The biocompatibility of dibutyryl chitin in the context of wound dressings. *Biomaterials* **26**, 5844-5854 (2005).

104. Guo, T. *et al.* Porous chitosan-gelatin scaffold containing plasmid DNA encoding transforming growth factor-β1 for chondrocytes proliferation. *Biomaterials* **27**, 1095-1103 (2006).

105. Ma, L. *et al.* Collagen/chitosan porous scaffolds with improved biostability for skin tissue engineering. *Biomaterials* **24**, 4833-4841 (2003).

106. Shalumon, K. T. *et al.* Electrospinning of carboxymethyl chitin/poly(vinyl alcohol) nanofibrous scaffolds for tissue engineering applications. *Carbohydr. Polym.* **77**, 863-869 (2009).

107. Chatelet, C., Damour, O. & Domard, A. Influence of the degree of acetylation on some biological properties of chitosan films. *Biomaterials* **22**, 261-268 (2001).

108. Yang, Y. *et al.* Nerve conduits based on immobilization of nerve growth factor onto modified chitosan by using genipin as a crosslinking agent. *Eur. J. Pharm. Biopharm.* **79**, 519-525 (2011).

109. Cooper, A., Jana, S., Bhattarai, N. & Zhang, M. Aligned chitosan-based nanofibers for enhanced myogenesis. *J. Mater. Chem.* **20**, 8904-8911 (2010).

110. Cooper, A., Bhattarai, N. & Zhang, M. Fabrication and cellular compatibility of aligned chitosan–PCL fibers for nerve tissue regeneration. *Carbohydr. Polym.* **85**, 149-156 (2011).

111. Lin-Gibson, S., Walls, H. J., Kennedy, S. B. & Welsh, E. R. Reaction kinetics and gel properties of blocked diisocyinate crosslinked chitosan hydrogels. *Carbohydr. Polym.* **54**, 193-199 (2003).

112. Huang, Y., Onyeri, S., Siewe, M., Moshfeghian, A. & Madihally, S. V. In vitro characterization of chitosan–gelatin scaffolds for tissue engineering. *Biomaterials* **26**, 7616-7627 (2005).

113. Wang, Z. *et al.* A novel and simple procedure to synthesize chitosan-graft-polycaprolactone in an ionic liquid. *Carbohydr. Polym.* **94**, 505-510 (2013).

114. Liu, T.-Y. & Lin, Y.-L. Novel pH-sensitive chitosan-based hydrogel for encapsulating poorly water-soluble drugs. *Acta Biomater.* **6**, 1423-1429 (2010).

115. Almeida, E. V. R., Frollini, E., Castellan, A. & Coma, V. Chitosan, sisal cellulose, and biocomposite chitosan/sisal cellulose films prepared from thiourea/NaOH aqueous solution. *Carbohydr. Polym.* **80**, 655-664 (2010).

116. Qin, Y. *et al.* Synthesis and antifungal evaluation of (1,2,3-triazol-4-yl)methyl nicotinate chitosan. *Int. J. Biol. Macromol.* **61**, 58-62 (2013).

117. Zhang, J. & Yan, N. Formic acid-mediated liquefaction of chitin. *Green Chem.* **18**, 5050-5058 (2016).

118. Ruel-Gariépy, E. & Leroux, J.-C. In situ-forming hydrogels—review of temperature-sensitive systems. *Eur. J. Pharm. Biopharm.* **58**, 409-426 (2004).

119. Hollister, S. J. Porous scaffold design for tissue engineering. *Nat. Mater.* **4**, 518-524 (2005).

120. Bhattarai, N., Gunn, J. & Zhang, M. Chitosan-based hydrogels for controlled, localized drug delivery. *Adv. Drug Delivery Rev.* **62**, 83-99 (2010).

121. Dash, M., Chiellini, F., Ottenbrite, R. M. & Chiellini, E. Chitosan—A versatile semi-synthetic polymer in biomedical applications. *Prog. Polym. Sci.* **36**, 981-1014 (2011).

122. He, M. *et al.* Biocompatible and Biodegradable Bioplastics Constructed from Chitin via a "Green" Pathway for Bone Repair. *ACS Sustainable Chem. Eng.* **5**, 9126-9135 (2017).

123. Kim, I.-Y. *et al.* Chitosan and its derivatives for tissue engineering applications. *Biotechnol. Adv.* **26**, 1-21 (2008).

124. Zhao, L. *et al.* Fatigue and human umbilical cord stem cell seeding characteristics of calcium phosphate–chitosan–biodegradable fiber scaffolds. *Biomaterials* **31**, 840-847 (2010).

125. Busilacchi, A., Gigante, A., Mattioli-Belmonte, M., Manzotti, S. & Muzzarelli, R. A. A. Chitosan stabilizes platelet growth factors and modulates stem cell differentiation toward tissue regeneration. *Carbohydr. Polym.* **98**, 665-676 (2013).

126. Yang, Y. *et al.* Biocompatibility evaluation of silk fibroin with peripheral nerve tissues and cells in vitro. *Biomaterials* **28**, 1643-1652 (2007).

127. Yao, C.-H., Liu, B.-S., Hsu, S.-H. & Chen, Y.-S. Calvarial bone response to a tricalcium phosphate-genipin crosslinked gelatin composite. *Biomaterials* **26**, 3065-3074 (2005).

128. Geiger, M., Li, R. H. & Friess, W. Collagen sponges for bone regeneration with rhBMP-2. *Adv. Drug Delivery Rev.* **55**, 1613-1629 (2003).

129. Elbert, D. L. & Hubbell, J. A. Surface Treatments of Polymers for Biocompatibility. *Annu. Rev. Mater. Sci.* **26**, 365-394 (1996).

130. Ma, S. *et al.* Asymmetric Collagen/chitosan Membrane Containing Minocycline-loaded Chitosan Nanoparticles for Guided Bone Regeneration. *Sci. Rep.* **6**, 31822-31832 (2016).

131. Jin, J., Song, M. & Hourston, D. J. Novel Chitosan-Based Films Cross-Linked by Genipin with Improved Physical Properties. *Biomacromolecules* **5**, 162-168 (2004).

132. Tibbitt, M. W., Dahlman, J. E. & Langer, R. Emerging Frontiers in Drug Delivery. *J. Am. Chem. Soc.* **138**, 704-717 (2016).

133. Gokarn, Y. R. *et al.* Effective charge measurements reveal selective and preferential accumulation of anions, but not cations, at the protein surface in dilute salt solutions. *Protein Sci.* **20**, 580-587 (2011).

134. Dautzenberg, H. & Kriz, J. Response of Polyelectrolyte Complexes to Subsequent Addition of Salts with Different Cations. *Langmuir* **19**, 5204-5211 (2003).

135. Zintchenko, A., Dautzenberg, H., Tauer, K. & Khrenov, V. Polyelectrolyte Complex Formation with Double Hydrophilic Block Polyelectrolytes: Effects of the Amount and Length of the Neutral Block. *Langmuir* **18**, 1386-1393 (2002).

136. Burkhardt, M. *et al.* Water-Soluble Interpolyelectrolyte Complexes of Polyisobutylene-block-Poly(methacrylic acid) Micelles: Formation and Properties. *Langmuir* **24**, 1769-1777 (2008).

137. Rowland, C. R., Lennon, D. P., Caplan, A. I. & Guilak, F. The effects of crosslinking of scaffolds engineered from cartilage ECM on the chondrogenic differentiation of MSCs. *Biomaterials* **34**, 5802-5812 (2013).

138. Gunn, J. & Zhang, M. Polyblend nanofibers for biomedical applications: perspectives and challenges. *Trends Biotechnol.* **28**, 189-197 (2010).

139. Yuan, Y. *et al.* The effect of cross-linking of chitosan microspheres with genipin on protein release. *Carbohydr. Polym.* **68**, 561-567 (2007).

140. Tonda-Turo, C. *et al.* Comparative analysis of gelatin scaffolds crosslinked by genipin and silane coupling agent. *Int. J. Biol. Macromol.* **49**, 700-706 (2011).

141. Sisson, K., Zhang, C., Farach-Carson, M. C., Chase, D. B. & Rabolt, J. F. Evaluation of Cross-Linking Methods for Electrospun Gelatin on Cell Growth and Viability. *Biomacromolecules* **10**, 1675-1680 (2009).

142. Jayakumar, R., Prabaharan, M., Sudheesh Kumar, P. T., Nair, S. V. & Tamura, H. Biomaterials based on chitin and chitosan in wound dressing applications. *Biotechnol. Adv.* **29**, 322-337 (2011).

143. Williams, D. F. On the mechanisms of biocompatibility. *Biomaterials* **29**, 2941-2953 (2008).

144. Mi, F.-L., Tan, Y.-C., Liang, H.-C., Huang, R.-N. & Sung, H.-W. In vitro evaluation of a chitosan membrane cross-linked with genipin. *J. Biomater. Sci., Polym. Ed.* **12**, 835-850 (2001).

145. Singh, R., Krishna, B. B., Kumar, J. & Bhaskar, T. Opportunities for utilization of non-conventional energy sources for biomass pretreatment. *Bioresour. Technol.* **199**, 398-407 (2016).

146. Akhtar, N., Gupta, K., Goyal, D. & Goyal, A. Recent advances in pretreatment technologies for efficient hydrolysis of lignocellulosic biomass. *Environ. Prog. Sustainable Energy* **35**, 489-511 (2016).

147. Zabed, H., Sahu, J. N., Boyce, A. N. & Faruq, G. Fuel ethanol production from lignocellulosic biomass: An overview on feedstocks and technological approaches. *Renewable Sustainable Energy Rev.* **66**, 751-774 (2016).

148. Chen, H. *et al.* A review on the pretreatment of lignocellulose for high-value chemicals. *Fuel Process. Technol.* **160**, 196-206 (2017).

149. Nocentini, A. *et al.* Discovery of New Sulfonamide Carbonic Anhydrase IX Inhibitors Incorporating Nitrogenous Bases. *ACS Med. Chem. Lett.* **8**, 1314-1319 (2017).

150. Yadav, P. *et al.* Green synthesis and anticancer potential of chalcone linked-1,2,3-triazoles. *Eur. J. Med. Chem.* **126**, 944-953 (2017).

151. Zhang, S. *et al.* Triazole derivatives and their anti-tubercular activity. *Eur. J. Med. Chem.* **138**, 501-513 (2017).

152. Wang, X.-L., Wan, K. & Zhou, C.-H. Synthesis of novel sulfanilamide-derived 1,2,3-triazoles and their evaluation for antibacterial and antifungal activities. *Eur. J. Med. Chem.* **45**, 4631-4639 (2010).

153. Kraljević, T. G. *et al.* Synthesis, in vitro anticancer and antibacterial activities and in silico studies of new 4-substituted 1,2,3-triazole–coumarin hybrids. *Eur. J. Med. Chem.* **124**, 794-808 (2016).

154. Patpi, S. R. *et al.* Design, Synthesis, and Structure–Activity Correlations of Novel Dibenzo[b,d]furan, Dibenzo[b,d]thiophene, and N-Methylcarbazole Clubbed 1,2,3-Triazoles as Potent Inhibitors of Mycobacterium tuberculosis. *J. Med. Chem.* **55**, 3911-3922 (2012).

155. Zhuang, C. *et al.* Chalcone: A Privileged Structure in Medicinal Chemistry. *Chem. Rev.* **117**, 7762-7810 (2017).

156. Kant, R. *et al.* Synthesis of newer 1,2,3-triazole linked chalcone and flavone hybrid compounds and evaluation of their antimicrobial and cytotoxic activities. *Eur. J. Med. Chem.* **113**, 34-49 (2016).

157. Hu, Y.-Q. *et al.* Recent developments of coumarin-containing derivatives and their anti-tubercular activity. *Eur. J. Med. Chem.* **136**, 122-130 (2017).

158. Duan, Y.-C. *et al.* Design and synthesis of novel 1,2,3-triazole-dithiocarbamate hybrids as potential anticancer agents. *Eur. J. Med. Chem.* **62**, 11-19 (2013).

159. Lipeeva, A. V. *et al.* Synthesis of 1H-1,2,3-triazole linked aryl(arylamidomethyl) – dihydrofurocoumarin hybrids and analysis of their cytotoxicity. *Eur. J. Med. Chem.* **100**, 119-128 (2015).

160. Xu, Z., Song, X.-F., Hu, Y.-Q., Qiang, M. & Lv, Z.-S. Azide-alkyne cycloaddition towards 1H-1,2,3-triazole-tethered gatifloxacin and isatin conjugates: Design, synthesis and in vitro anti-mycobacterial evaluation. *Eur. J. Med. Chem.* **138**, 66-71 (2017).

161. Carradori, S., Secci, D. & Petzer, J. P. MAO inhibitors and their wider applications: a patent review. *Expert Opin. Ther. Pat.* **28**, 211-226 (2018).

162. Wang, W., Peng, X., Wei, F., Tung, C.-H. & Xu, Z. Copper(I)-Catalyzed Interrupted Click Reaction: Synthesis of Diverse 5-Hetero-Functionalized Triazoles. *Angew. Chem. Int. Ed.* **55**, 649-653 (2016).

163. Ley, S. V. *et al.* Multi-step organic synthesis using solid-supported reagents and scavengers: a new paradigm in chemical library generation. *J. Chem. Soc., Perkin Trans. 1*, 3815-4195 (2000).

164. Balkenhohl, F., von dem Bussche-Hünnefeld, C., Lansky, A. & Zechel, C. Combinatorial Synthesis of Small Organic Molecules. *Angew. Chem., Int. Ed. Engl.* **35**, 2288-2337 (1996).

165. Sletten, E. M. & Bertozzi, C. R. Bioorthogonal Chemistry: Fishing for Selectivity in a Sea of Functionality. *Angew. Chem. Int. Ed.* **48**, 6974-6998 (2009).

166. Lutz, J.-F. 1,3-Dipolar Cycloadditions of Azides and Alkynes: A Universal Ligation Tool in Polymer and Materials Science. *Angew. Chem. Int. Ed.* **46**, 1018-1025 (2007).

167. Rostovtsev, V. V., Green, L. G., Fokin, V. V. & Sharpless, K. B. A Stepwise Huisgen Cycloaddition Process: Copper(I)-Catalyzed Regioselective "Ligation" of Azides and Terminal Alkynes. *Angew. Chem. Int. Ed.* **41**, 2596-2599 (2002).

168. Angell, Y. L. & Burgess, K. Peptidomimetics via copper-catalyzed azide–alkyne cycloadditions. *Chem. Soc. Rev.* **36**, 1674-1689 (2007).

169. Jewett, J. C. & Bertozzi, C. R. Cu-free click cycloaddition reactions in chemical biology. *Chem. Soc. Rev.* **39**, 1272-1279 (2010).

170. Kolb, H. C., Finn, M. G. & Sharpless, K. B. Click Chemistry: Diverse Chemical Function from a Few Good Reactions. *Angew. Chem. Int. Ed.* **40**, 2004-2021 (2001).

171. Helfrich, E. J. N. & Piel, J. Biosynthesis of polyketides by trans-AT polyketide synthases. *Nat. Prod. Rep.* **33**, 231-316 (2016).

172. Melagraki, G. *et al.* Synthesis and evaluation of the antioxidant and anti-inflammatory activity of novel coumarin-3-aminoamides and their alpha-lipoic acid adducts. *Eur. J. Med. Chem.* **44**, 3020-3026 (2009).

173. Detsi, A., Kontogiorgis, C. & Hadjipavlou-Litina, D. Coumarin derivatives: an updated patent review (2015-2016). *Expert Opin. Ther. Pat.* **27**, 1201-1226 (2017).

174. Basanagouda, M. *et al.* Synthesis, structure–activity relationship of iodinated-4-aryloxymethyl-coumarins as potential anti-cancer and anti-mycobacterial agents. *Eur. J. Med. Chem.* **74**, 225-233 (2014).

175. Darandale, S. N., Mulla, N. A., Pansare, D. N., Sangshetti, J. N. & Shinde, D. B. A novel amalgamation of 1,2,3-triazoles, piperidines and thieno pyridine rings and evaluation of their antifungal activity. *Eur. J. Med. Chem.* **65**, 527-532 (2013).

176. da Silva, F. d. C. *et al.* Synthesis, HIV-RT inhibitory activity and SAR of 1-benzyl-1H-1,2,3-triazole derivatives of carbohydrates. *Eur. J. Med. Chem.* **44**, 373-383 (2009).

177. Heller, J. *et al.* Use of poly(ortho esters) for the controlled release of 5-fluorouracyl and a LHRH analogue. *J. Controlled Release* **6**, 217-224 (1987).

178. Banerjee, A. *et al.* Strategies for targeted drug delivery in treatment of colon cancer: current trends and future perspectives. *Drug Discovery Today* **22**, 1224-1232 (2017).

179. Kontogiorgis, C., Detsi, A. & Hadjipavlou-Litina, D. Coumarin-based drugs: a patent review (2008 – present). *Expert Opin. Ther. Pat.* **22**, 437-454 (2012).

180. Farney, E. P., Feng, S. S., Schäfers, F. & Reisman, S. E. Total Synthesis of (+)-Pleuromutilin. *J. Am. Chem. Soc.* **140**, 1267-1270 (2018).

181. da Costa Lopes, A. M., Brenner, M., Falé, P., Roseiro, L. B. & Bogel-Łukasik, R. Extraction and Purification of Phenolic Compounds from Lignocellulosic Biomass Assisted by Ionic Liquid, Polymeric Resins, and Supercritical CO2. *ACS Sustainable Chem. Eng.* **4**, 3357-3367 (2016).

182. Chuang, H.-Y. *et al.* Synthesis and Vaccine Evaluation of the Tumor-Associated Carbohydrate Antigen RM2 from Prostate Cancer. *J. Am. Chem. Soc.* **135**, 11140-11150 (2013).

183. Clarke, C. J., Tu, W.-C., Levers, O., Bröhl, A. & Hallett, J. P. Green and Sustainable Solvents in Chemical Processes. *Chem. Rev.* **118**, 747-800 (2018).

184. Garci, A. *et al.* Efficient and Rapid Mechanochemical Assembly of Platinum(II) Squares for Guanine Quadruplex Targeting. *J. Am. Chem. Soc.* **139**, 16913-16922 (2017).

185. Zhang, Z., Song, J. & Han, B. Catalytic Transformation of Lignocellulose into Chemicals and Fuel Products in Ionic Liquids. *Chem. Rev.* **117**, 6834-6880 (2017).

186. Rege, P. R. & Block, L. H. Chitosan processing: influence of process parameters during acidic and alkaline hydrolysis and effect of the processing sequence on the resultant chitosan's properties. *Carbohydr. Res.* **321**, 235-245 (1999).

187. Jervis, P. J. *et al.* Towards multivalent CD1d ligands: synthesis and biological activity of homodimeric α-galactosyl ceramide analogues. *Carbohydr. Res.* **356**, 152-162 (2012).

188. Schönenberg, L. & Ritter, H. From Old to New: Polymers from Mono-α-Alkylated N-vinylcaprolactam. *Macromol. Chem. Phys.* **216**, 69-76 (2014).

189. Zhu, Z. *et al.* Multi-Fluorinated Azido Coumarins for Rapid and Selective Detection of Biological H2S in Living Cells. *Chem. - Asian J.* **11**, 68-71 (2016).

190. Thorson, M. K., Majtan, T., Kraus, J. P. & Barrios, A. M. Identification of Cystathionine β-Synthase Inhibitors Using a Hydrogen Sulfide Selective Probe. *Angew. Chem.* **125**, 4739-4742 (2013).

191. Sivakumar, K. *et al.* A Fluorogenic 1,3-Dipolar Cycloaddition Reaction of 3-Azidocoumarins and Acetylenes. *Org. Lett.* **6**, 4603-4606 (2004).

192. Rahimi, A., Ulbrich, A., Coon, J. J. & Stahl, S. S. Formic-acid-induced depolymerization of oxidized lignin to aromatics. *Nature* **515**, 249-252 (2014).

193. Kobayashi, H., Techikawara, K. & Fukuoka, A. Hydrolytic hydrogenation of chitin to amino sugar alcohol. *Green Chem.* **19**, 3350-3356 (2017).

194. Rinaldi, R., Palkovits, R. & Schüth, F. Depolymerization of Cellulose Using Solid Catalysts in Ionic Liquids. *Angew. Chem. Int. Ed.* **47**, 8047-8050 (2008).

195. Rinaldi, R., Meine, N., vom Stein, J., Palkovits, R. & Schüth, F. Which Controls the Depolymerization of Cellulose in Ionic Liquids: The Solid Acid Catalyst or Cellulose? *ChemSusChem* **3**, 266-276 (2010).

196. Katahira, R. *et al.* Base-Catalyzed Depolymerization of Biorefinery Lignins. *ACS Sustainable Chem. Eng.* **4**, 1474-1486 (2016).

197. Schutyser, W. *et al.* Chemicals from lignin: an interplay of lignocellulose fractionation, depolymerisation, and upgrading. *Chem. Soc. Rev.* **47**, 852-908 (2018).

198. Linger, J. G. *et al.* Lignin valorization through integrated biological funneling and chemical catalysis. *Proc. Natl. Acad. Sci. U. S. A.* **111**, 12013-12018 (2014).

199. Ruvinov, E. & Cohen, S. Alginate biomaterial for the treatment of myocardial infarction: Progress, translational strategies, and clinical outlook: From ocean algae to patient bedside. *Adv. Drug Delivery Rev.* **96**, 54-76 (2016).

200. Pickenhahn, V. D. *et al.* Regioselective thioacetylation of chitosan end-groups for nanoparticle gene delivery systems. *Chem. Sci.* **6**, 4650-4664 (2015).

201. Bräse, S., Gil, C., Knepper, K. & Zimmermann, V. Organic Azides: An Exploding Diversity of a Unique Class of Compounds. *Angew. Chem. Int. Ed.* **44**, 5188-5240 (2005).

202. Krause, N. & Gerold, A. Regio- and Stereoselective Syntheses with Organocopper Reagents. *Angew. Chem., Int. Ed. Engl.* **36**, 186-204 (1997).

203. Iqbal, J., Bhatia, B. & Nayyar, N. K. Transition Metal-Promoted Free-Radical Reactions in Organic Synthesis: The Formation of Carbon-Carbon Bonds. *Chem. Rev.* **94**, 519-564 (1994).

204. Tron, G. C. *et al.* Click chemistry reactions in medicinal chemistry: Applications of the 1,3-dipolar cycloaddition between azides and alkynes. *Med. Res. Rev.* **28**, 278-308 (2008).

205. Tanitame, A. *et al.* Synthesis and Antibacterial Activity of a Novel Series of Potent DNA Gyrase Inhibitors. Pyrazole Derivatives. *J. Med. Chem.* **47**, 3693-3696 (2004).

206. Laurin, P. *et al.* Structure-activity relationship in two series of aminoalkyl substituted coumarin inhibitors of gyrase B. *Bioorg. Med. Chem. Lett.* **9**, 2875-2880 (1999).

207. Ho, I. T. *et al.* Design and synthesis of triazolyl coumarins as Hg2+ selective fluorescent chemosensors. *Analyst* **137**, 5770-5776 (2012).

208. Olivier-Bourbigou, H., Magna, L. & Morvan, D. Ionic liquids and catalysis: Recent progress from knowledge to applications. *Appl. Catal., A* **373**, 1-56 (2010).

209. Howarth, A. J. *et al.* Best Practices for the Synthesis, Activation, and Characterization of Metal–Organic Frameworks. *Chem. Mater.* **29**, 26-39 (2017).

210. Amsden, B. G., Tse, M. Y., Turner, N. D., Knight, D. K. & Pang, S. C. In Vivo Degradation Behavior of Photo-Cross-Linked star-Poly(ε-caprolactone-co-d,l-lactide) Elastomers. *Biomacromolecules* **7**, 365-372 (2006).

A. APPENDICES

A.1MALDI-MS spectra

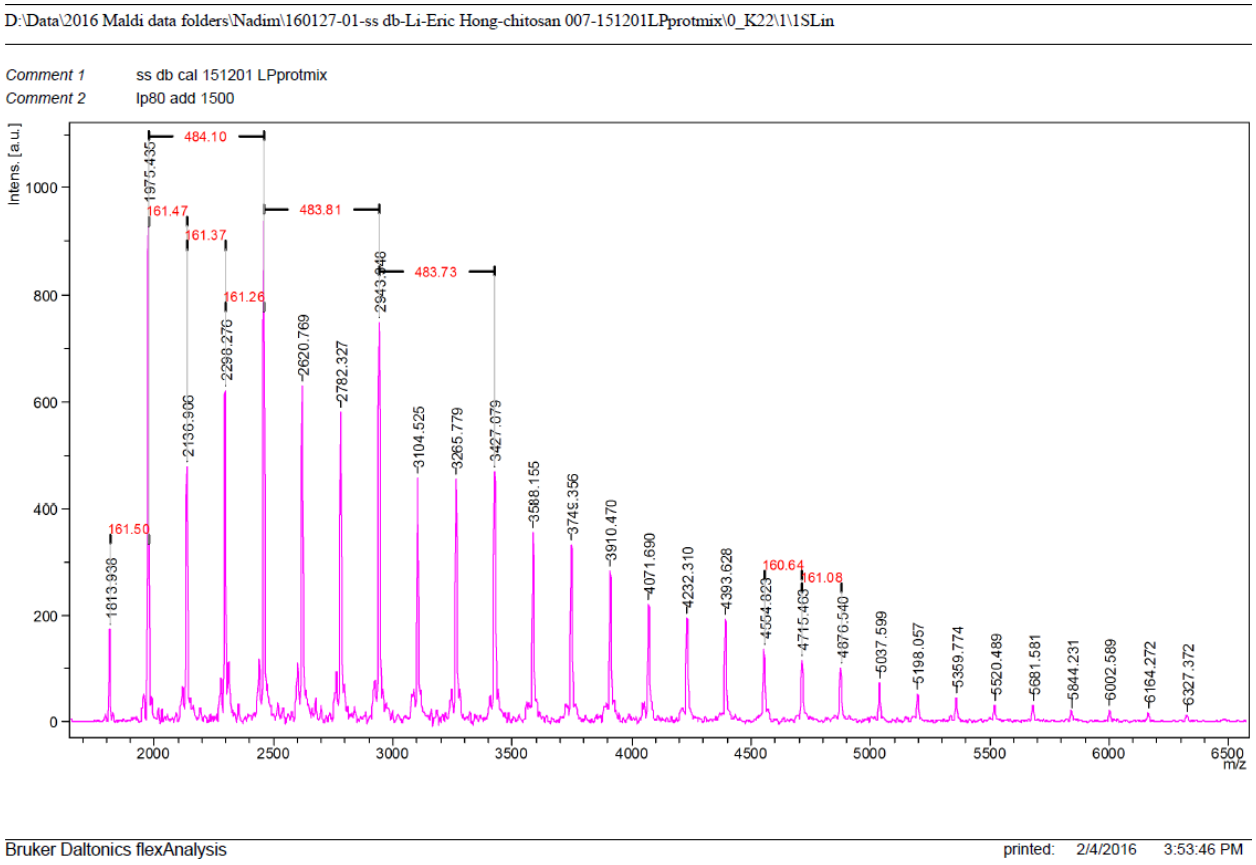

Figure A.1 MALDI-MS spectra of highly deacetylated chitosan oligosaccharides (COS)

polytool Date: 02/04/2016 Time: 15:52

FileName: ...osan 007-151201LPprotmix\0_K22\1\1SLin\pdata\1\peaklist.xml
peak integrals - ss db cal 151201 LPprotmix
lp80 add 1500

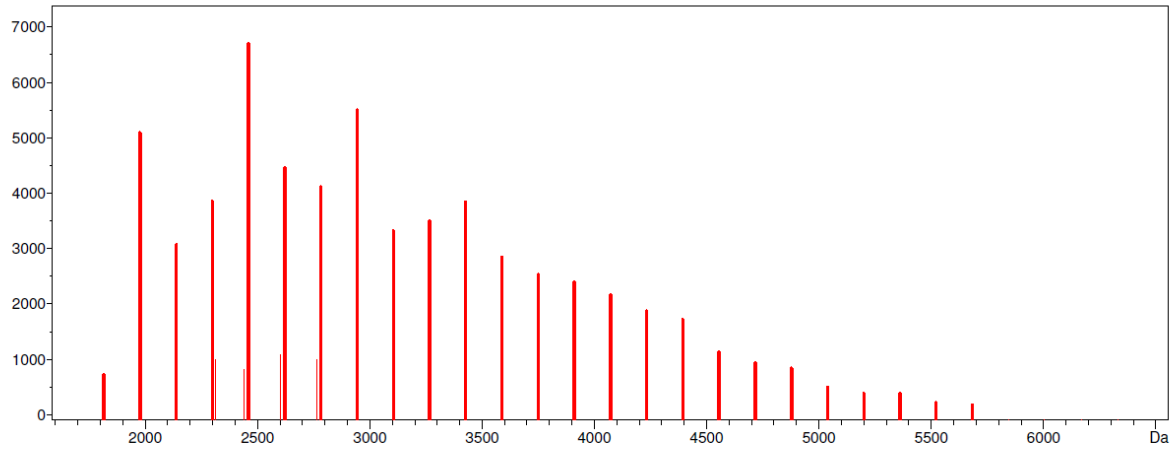

n	ser.	rep.unit	resid.	end1	end2	cation	Mn	Mw	pd	DP	% I.	cnt
1	1	161.000	4.70897	OH	H	Na	3105.20	3344.72	1.07714	19.2870	93.8	25

Figure A.2 MALDI-MS spectra of highly deacetylated chitosan oligosaccharides (COS)

A.2Additional NMR spectra

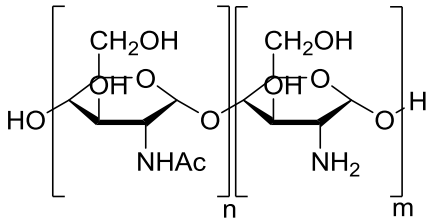

Compound 1

^{1}H NMR (500 MHz, 1 wt% HCOOH/D_2O)

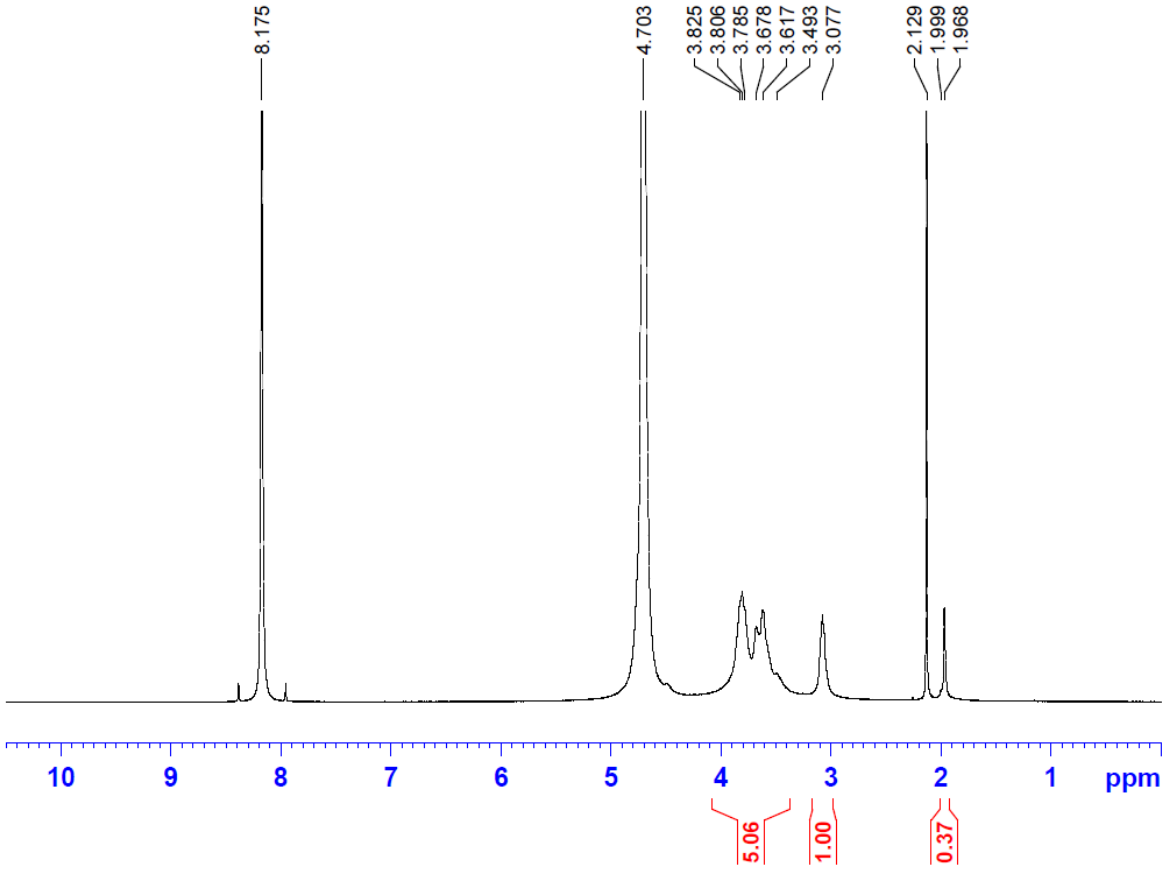

Figure A.3 ^{1}H NMR spectra of compound **1**

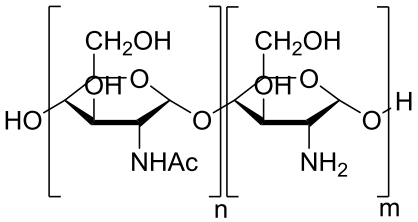

Compound 1

^{13}C NMR (125 MHz, 1 wt% HCOOH/D_2O)

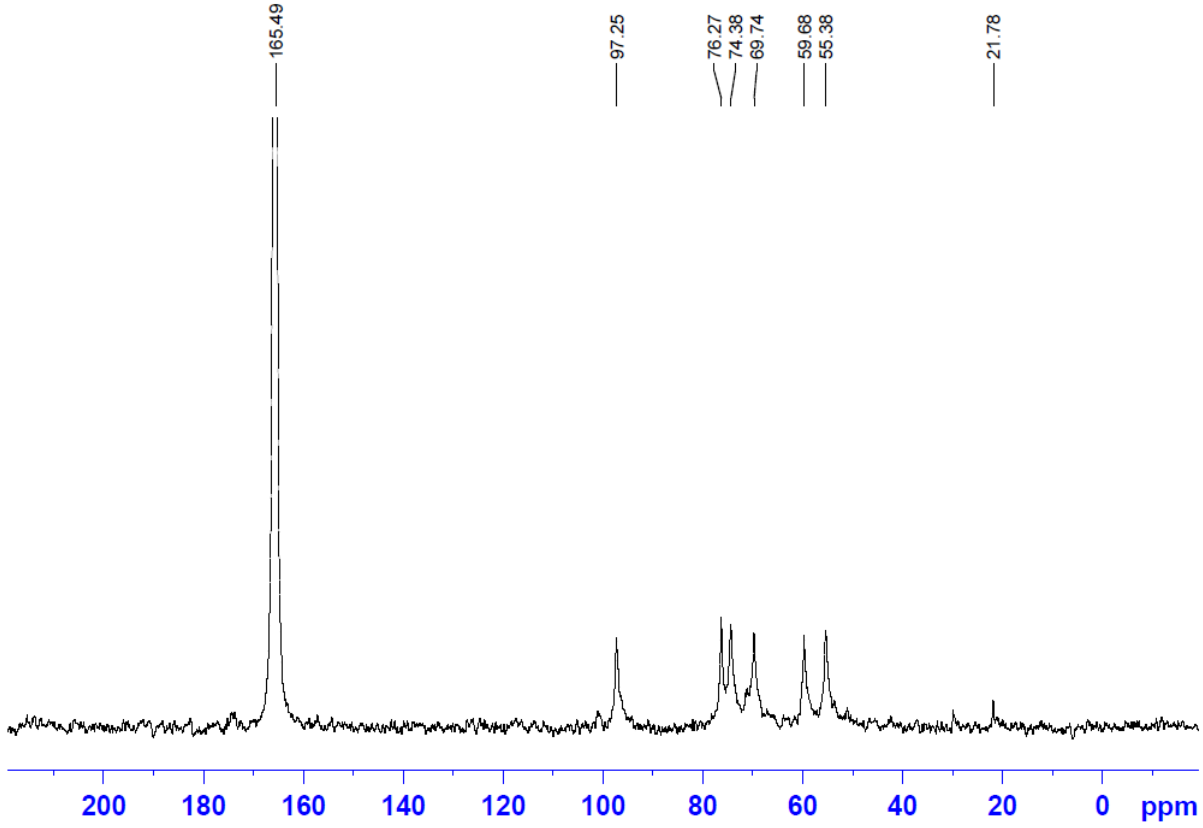

Figure A.4 ^{13}C NMR spectra of compound **1**

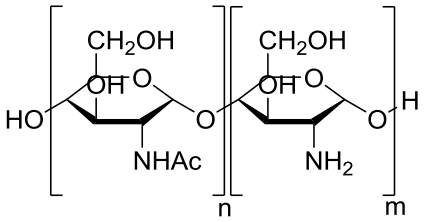

Compound 1

COSY NMR (500 MHz, 1 wt% $HCOOH/D_2O$)

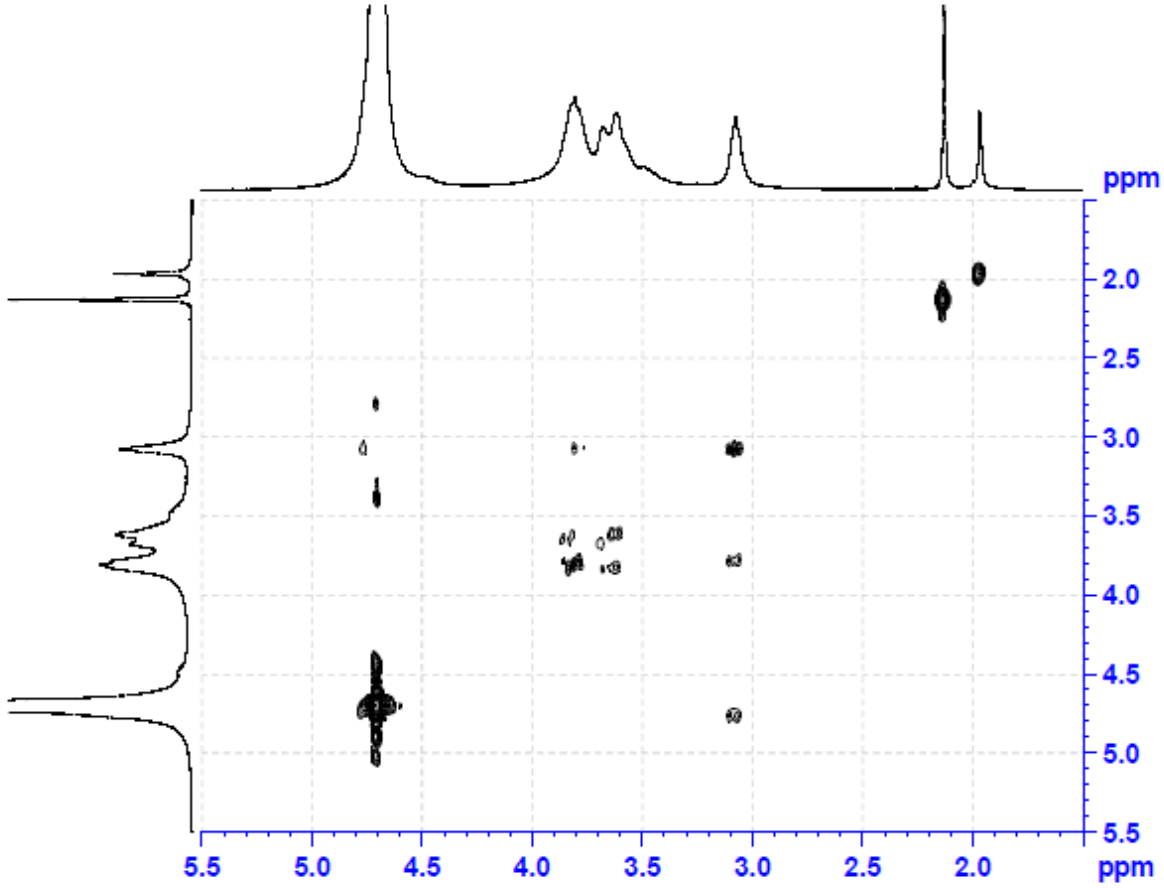

Figure A.5 COSY NMR spectra of compound **1**

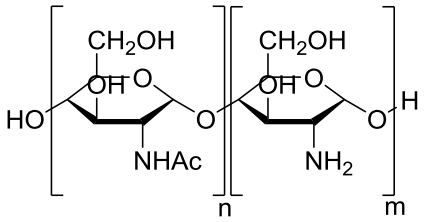

Compound 1

HSQC NMR (500 MHz, 1 wt% HCOOH/D_2O)

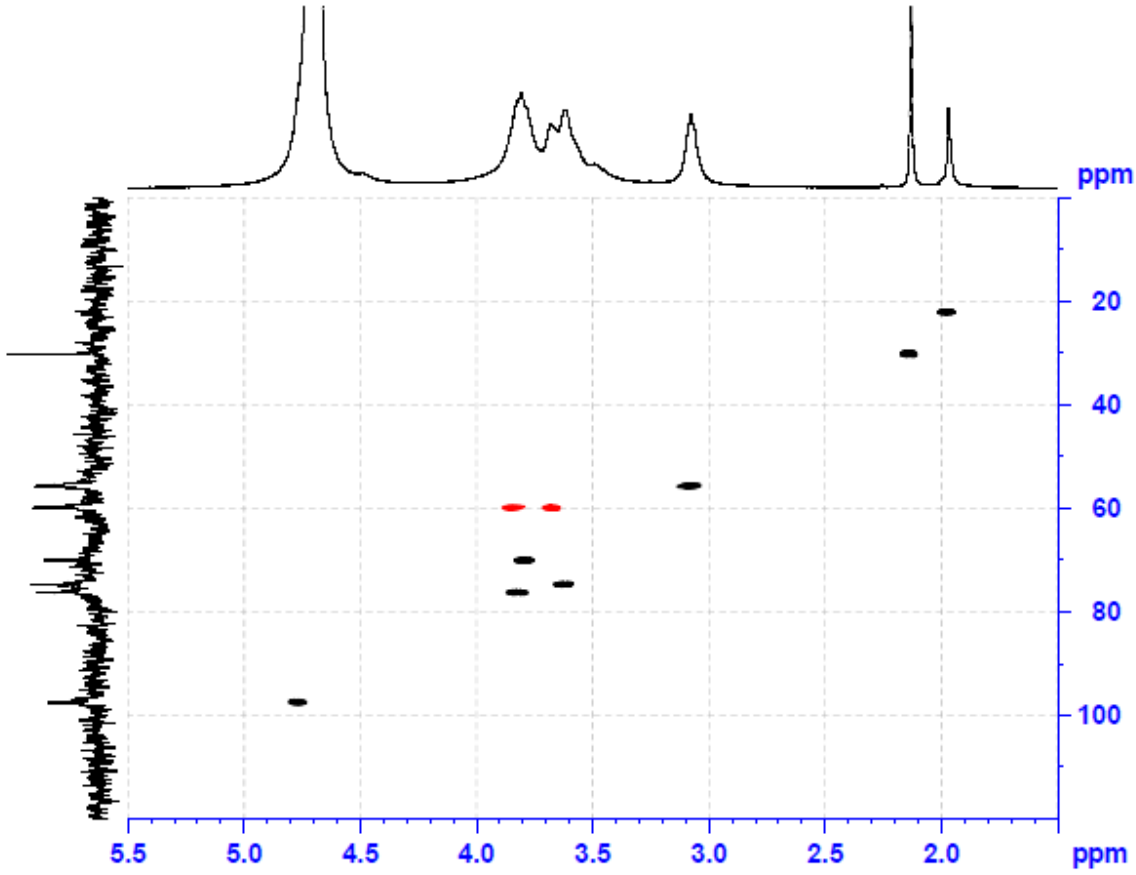

Figure A.6 HSQC NMR spectra of compound **1**

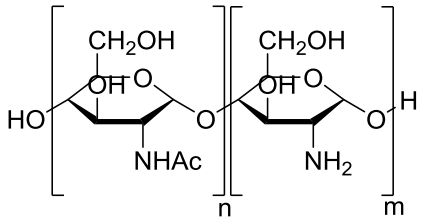

Compound 1

HMBC NMR (500 MHz, 1 wt% HCOOH/D_2O)

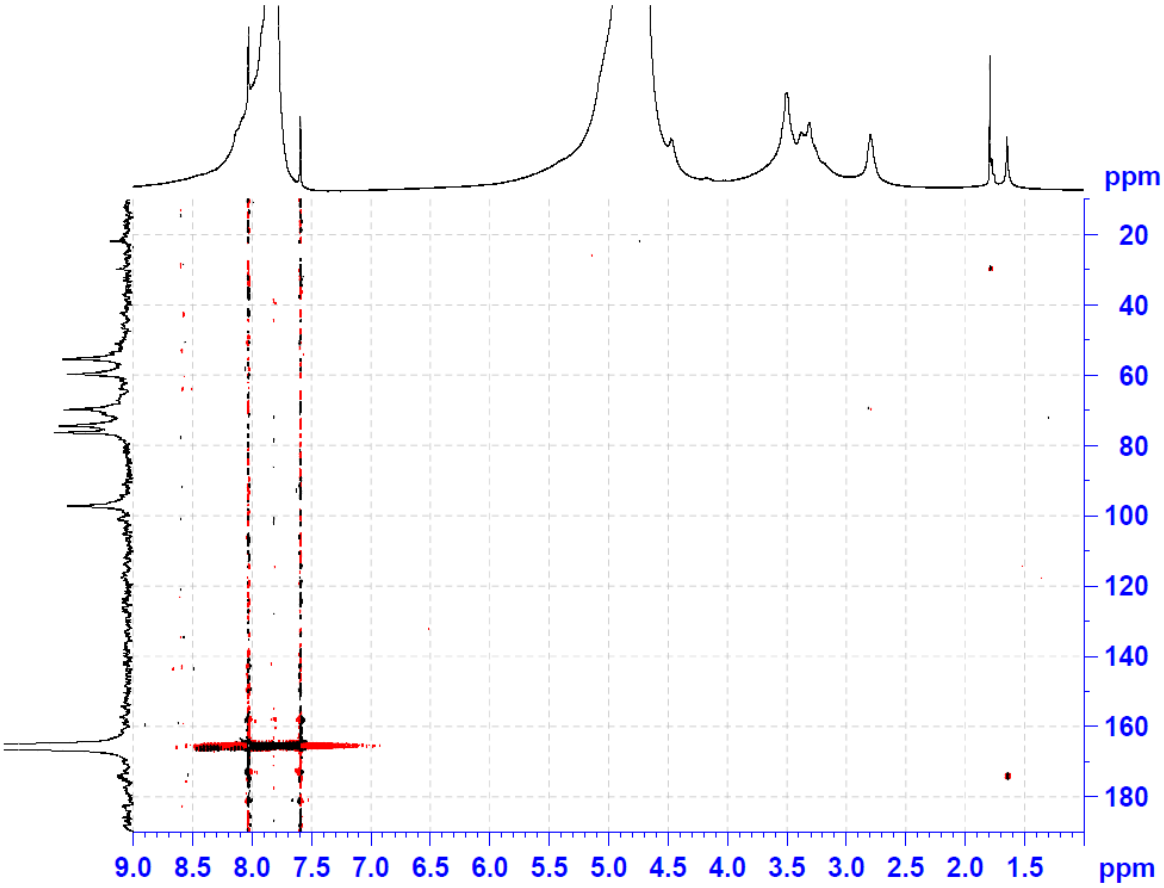

Figure A.7 HMBC NMR spectra of compound **1**

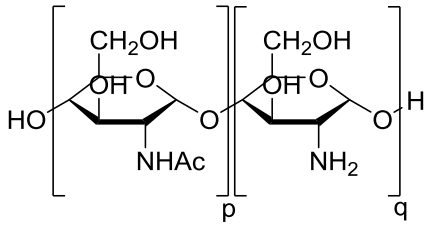

Compound 3

^{1}H NMR (500 MHz, 1 wt% HCOOH/D_2O)

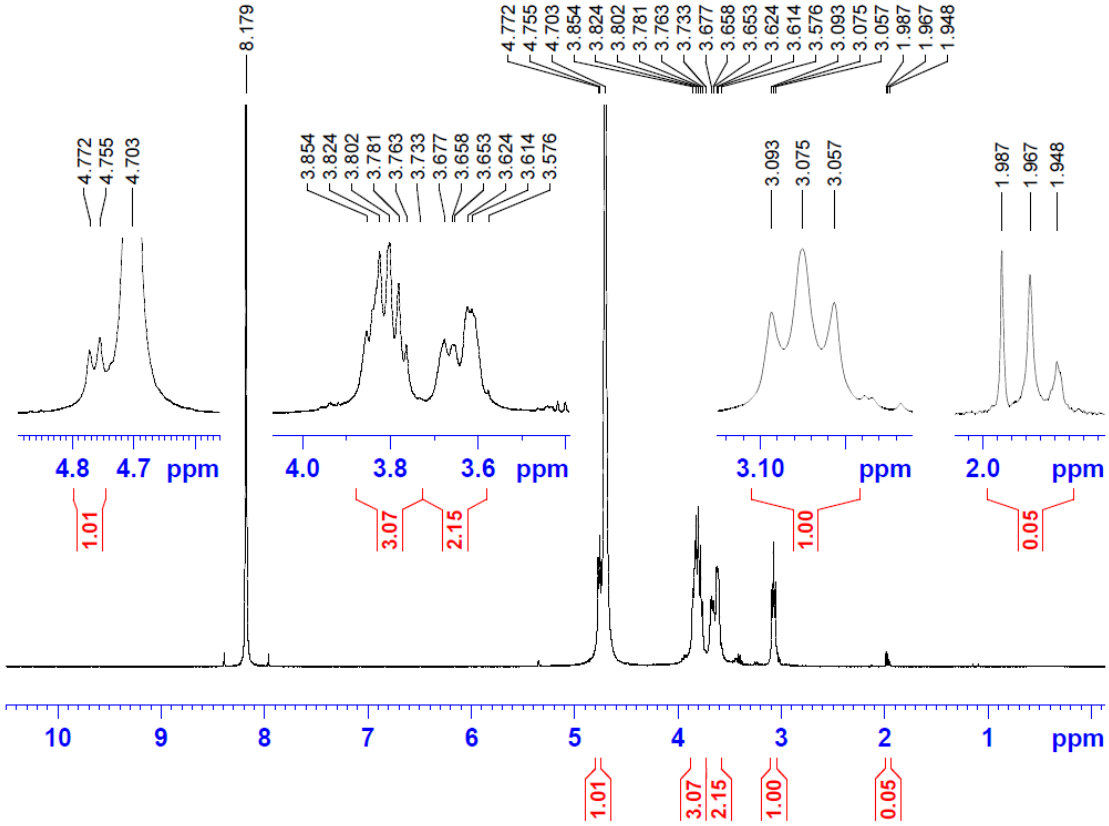

Figure A.8 ^{1}H NMR spectra of compound **3**

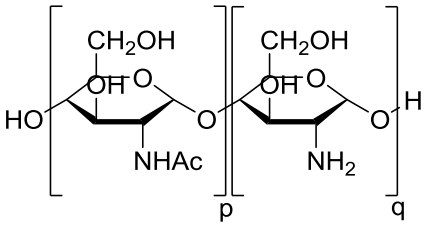

Compound 3

COSY NMR (500 MHz, 1 wt% $HCOOH/D_2O$)

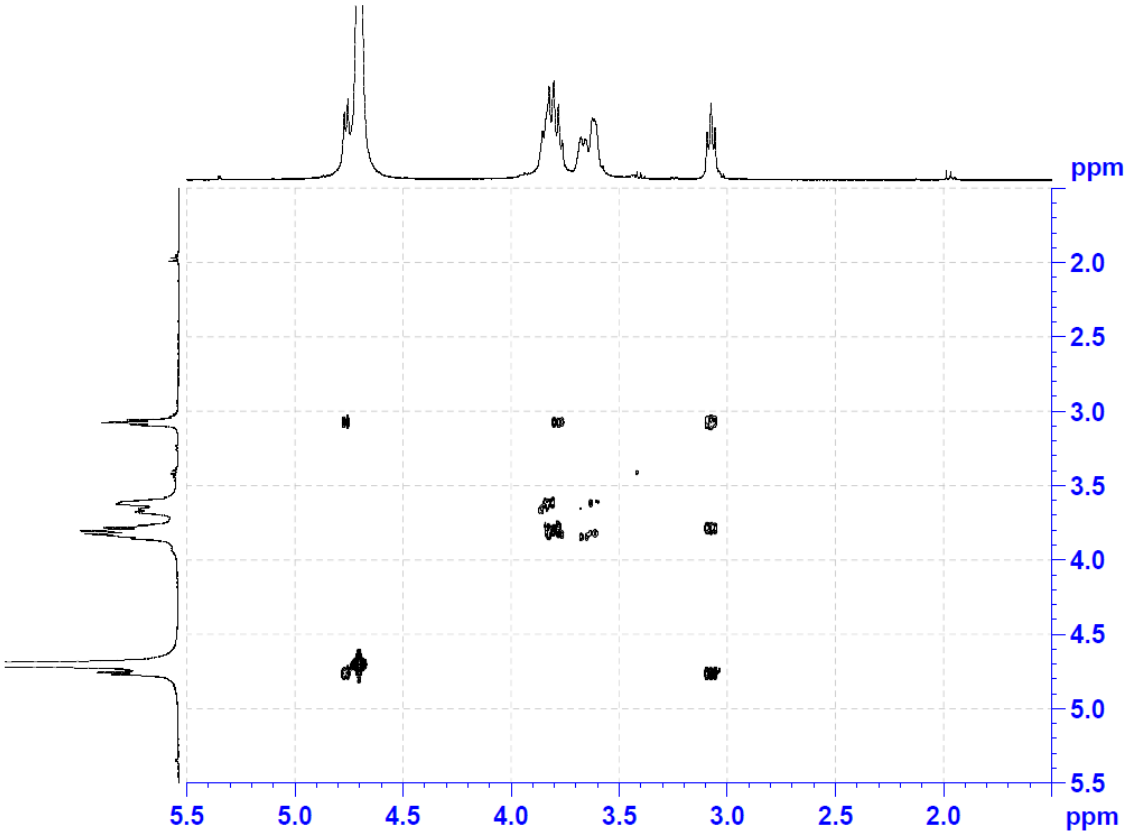

Figure A.9 COSY NMR spectra of compound **3**

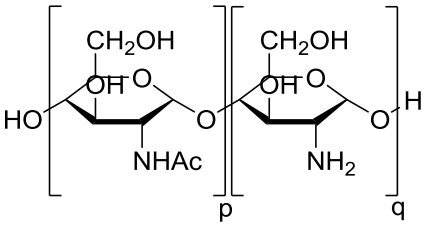

Compound 3

HSQC NMR (500 MHz, 1 wt% HCOOH/D_2O)

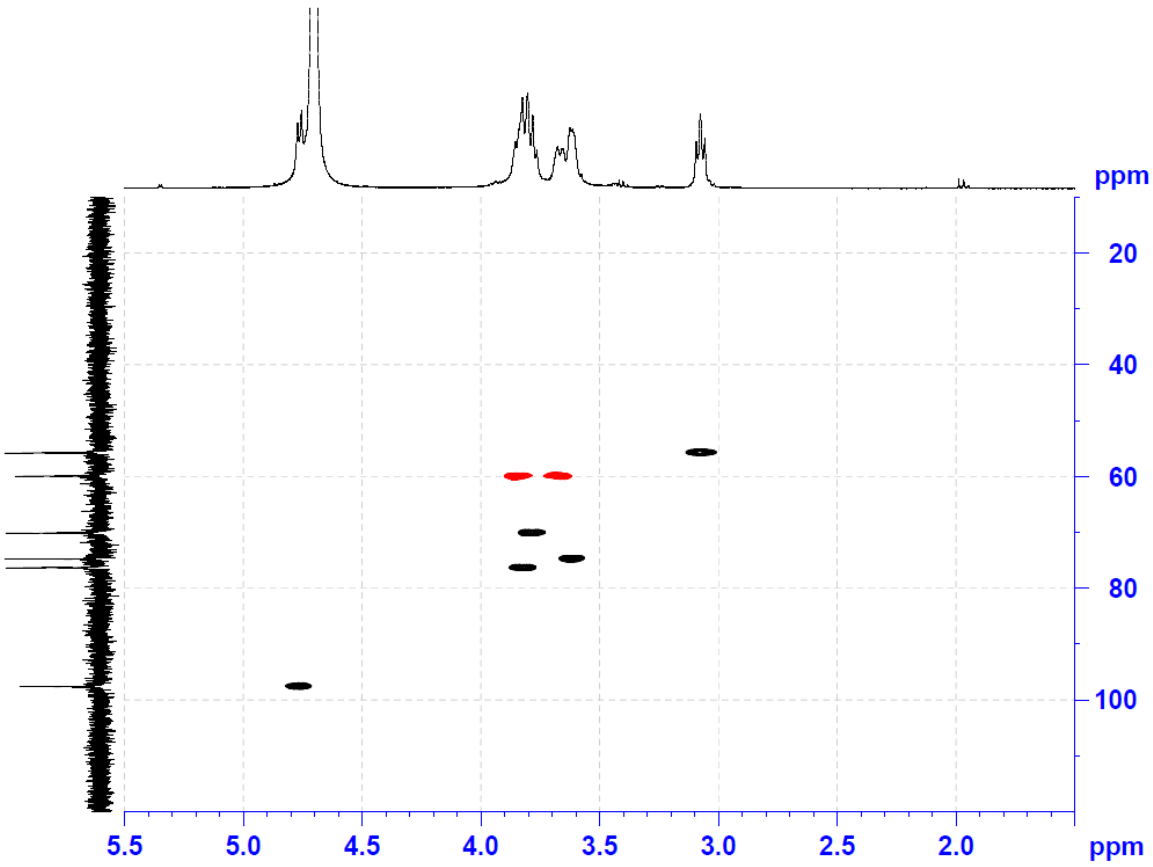

Figure A.10 HSQC NMR spectra of compound **3**

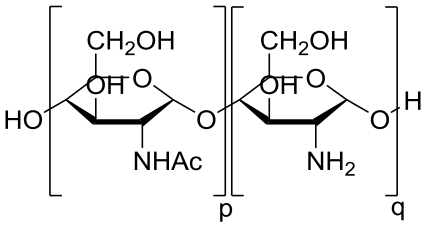

Compound 3

HMBC NMR (500 MHz, 1 wt% HCOOH/D_2O)

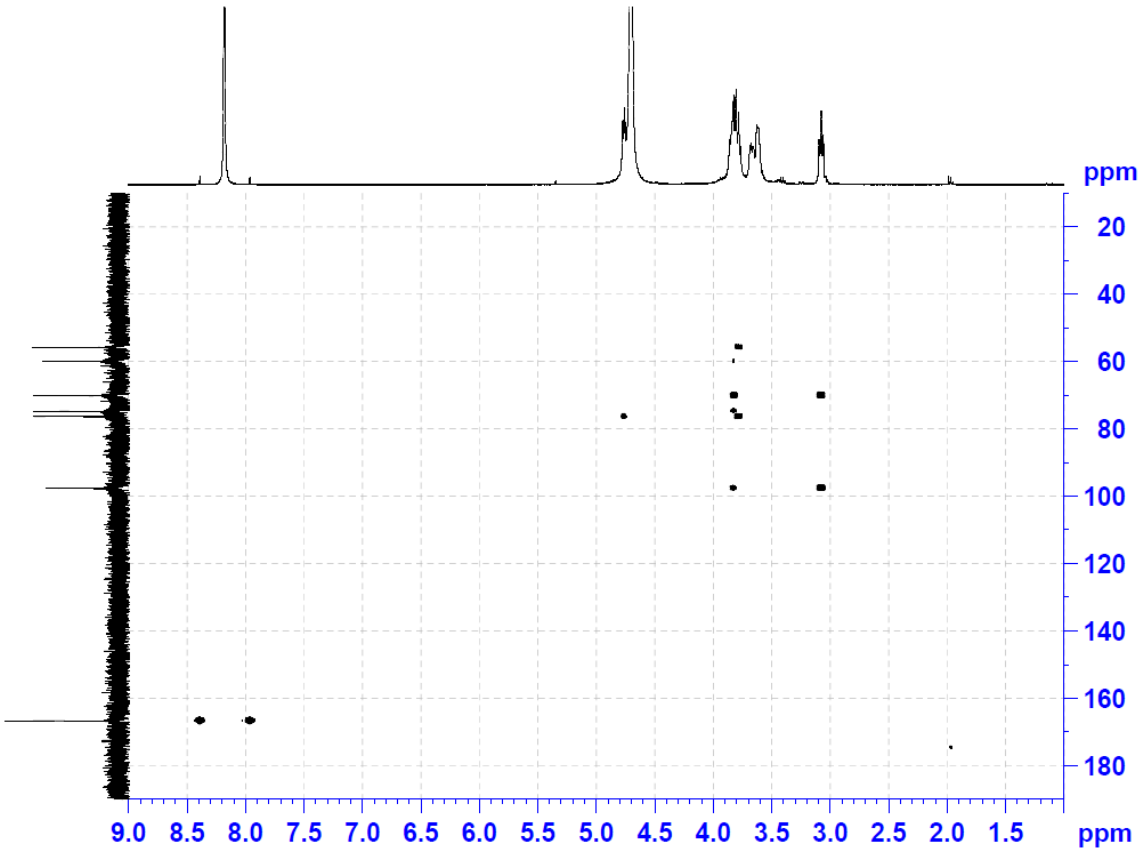

Figure A.11 HMBC NMR spectra of compound **3**

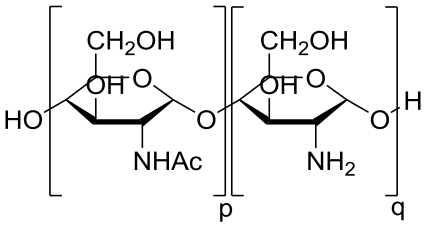

Compound 3

HMBC NMR (500 MHz, 1 wt% HCOOH/D_2O)

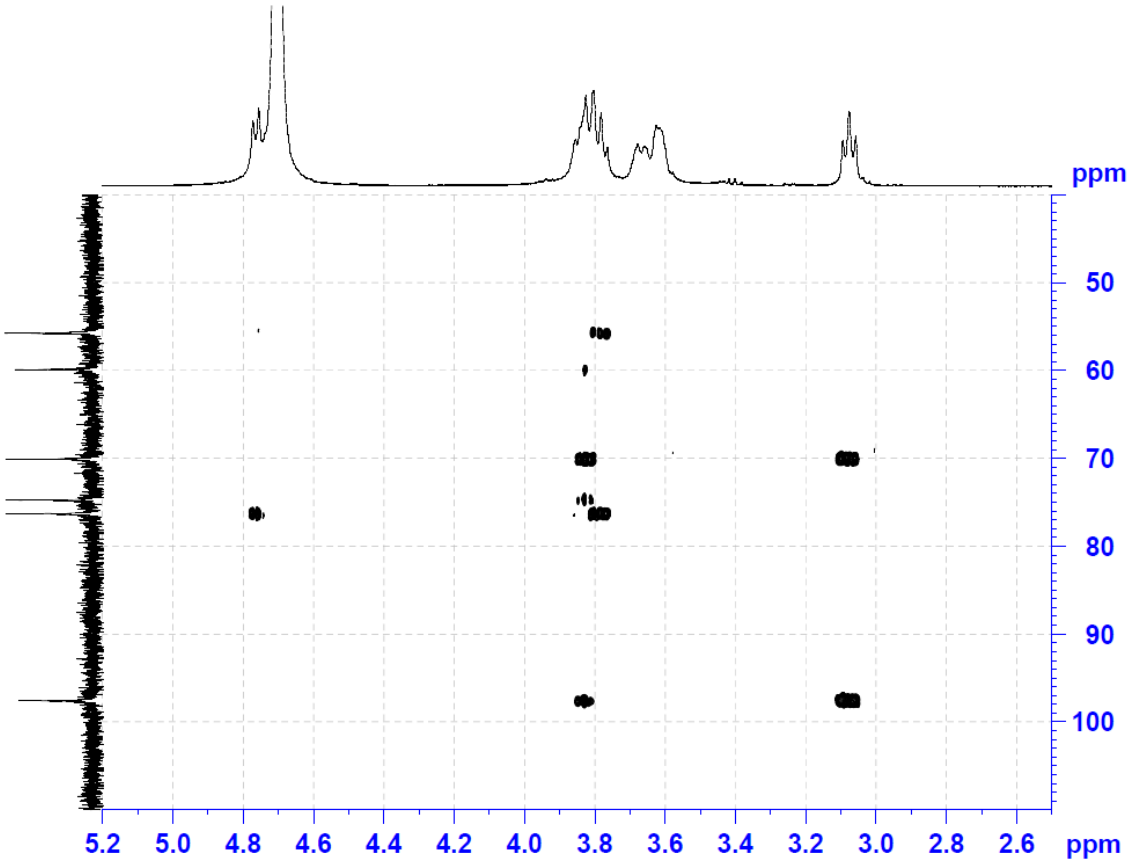

Figure A.12 HMBC NMR spectra of compound **3**

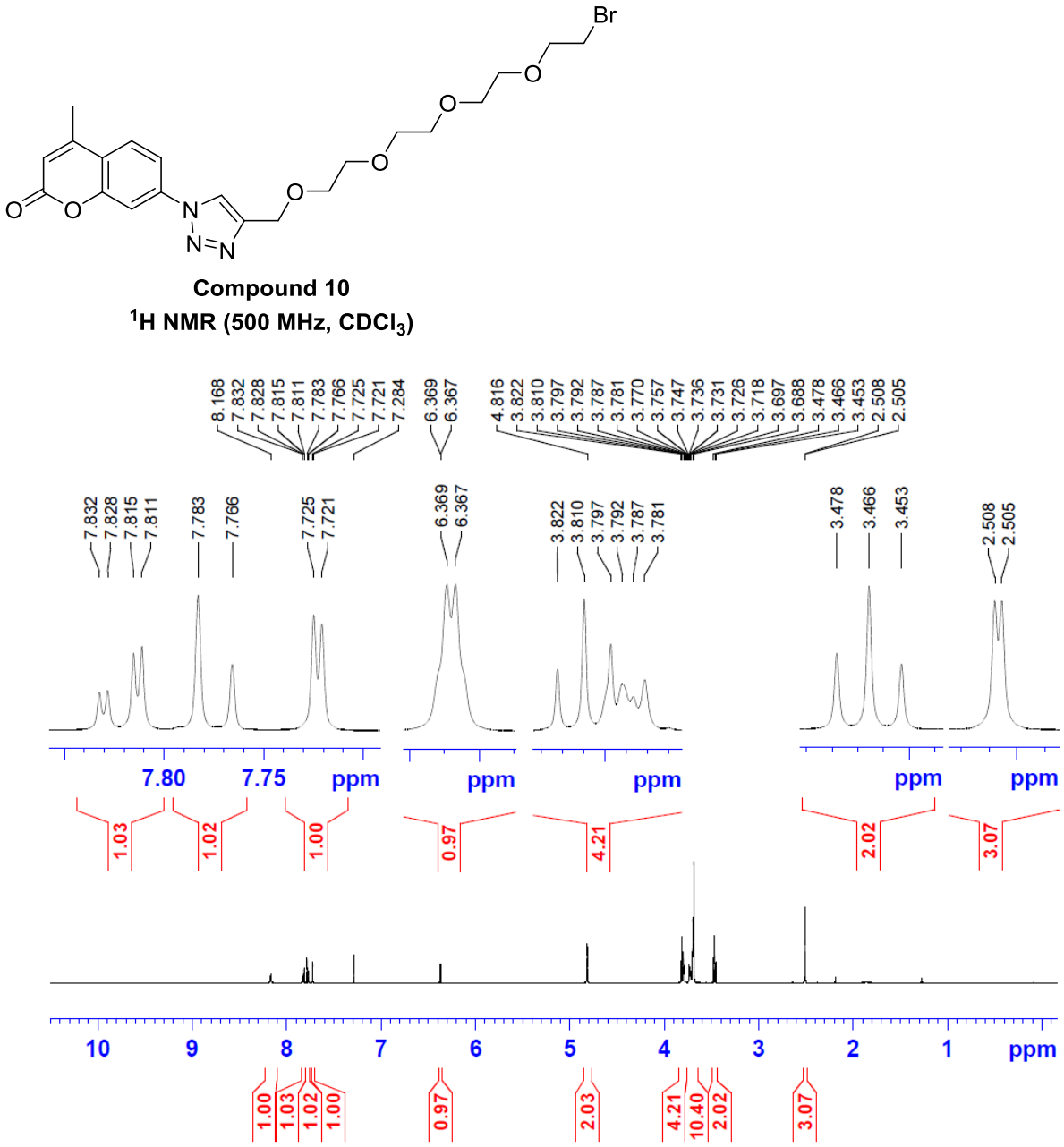

Figure A.13 ^{1}H NMR spectra of compound **10**

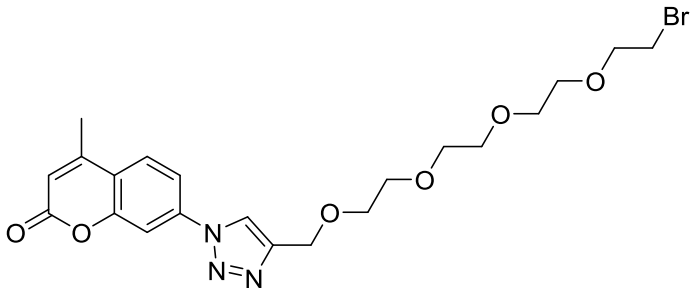

Compound 10
COSY NMR (500 MHz, $CDCl_3$)

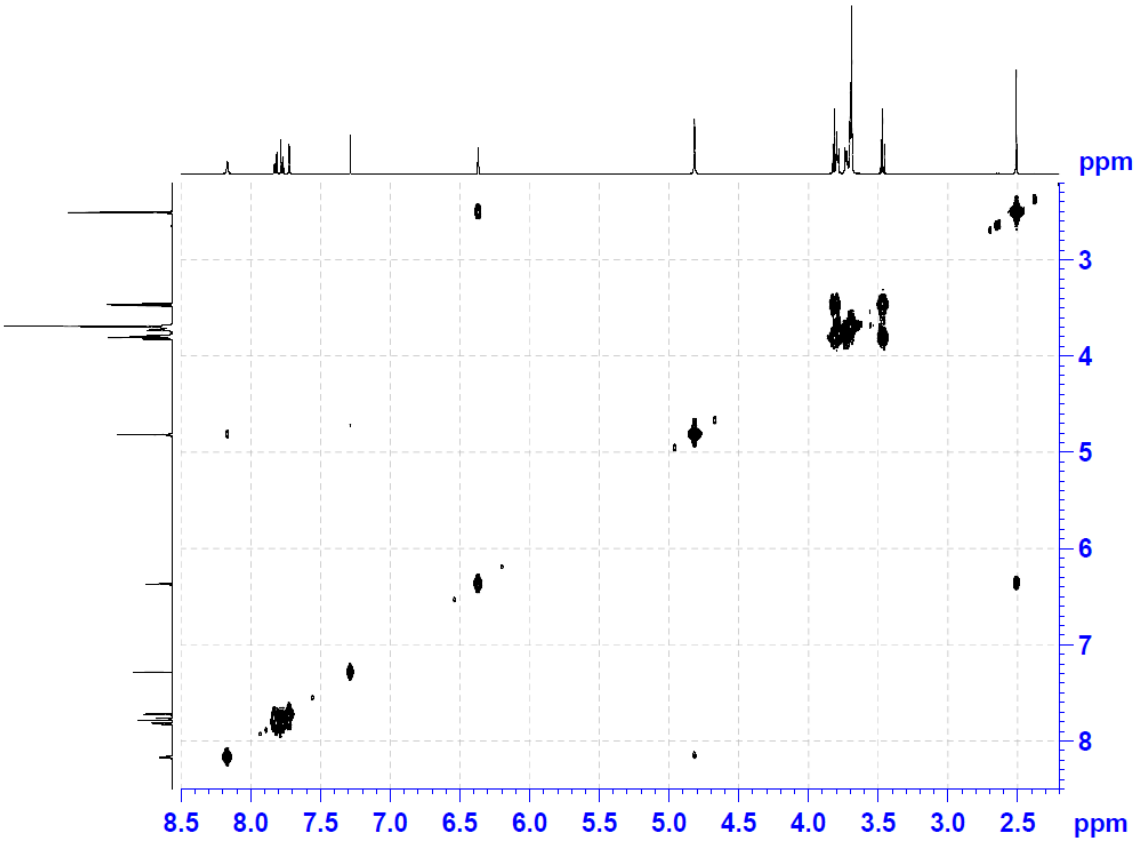

Figure A.14 COSY NMR spectra of compound **10**

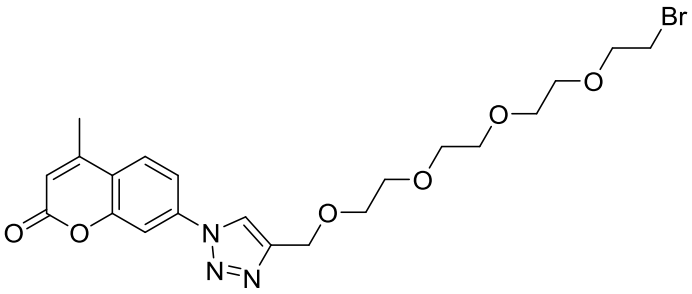

Compound 10
COSY NMR (500 MHz, $CDCl_3$)

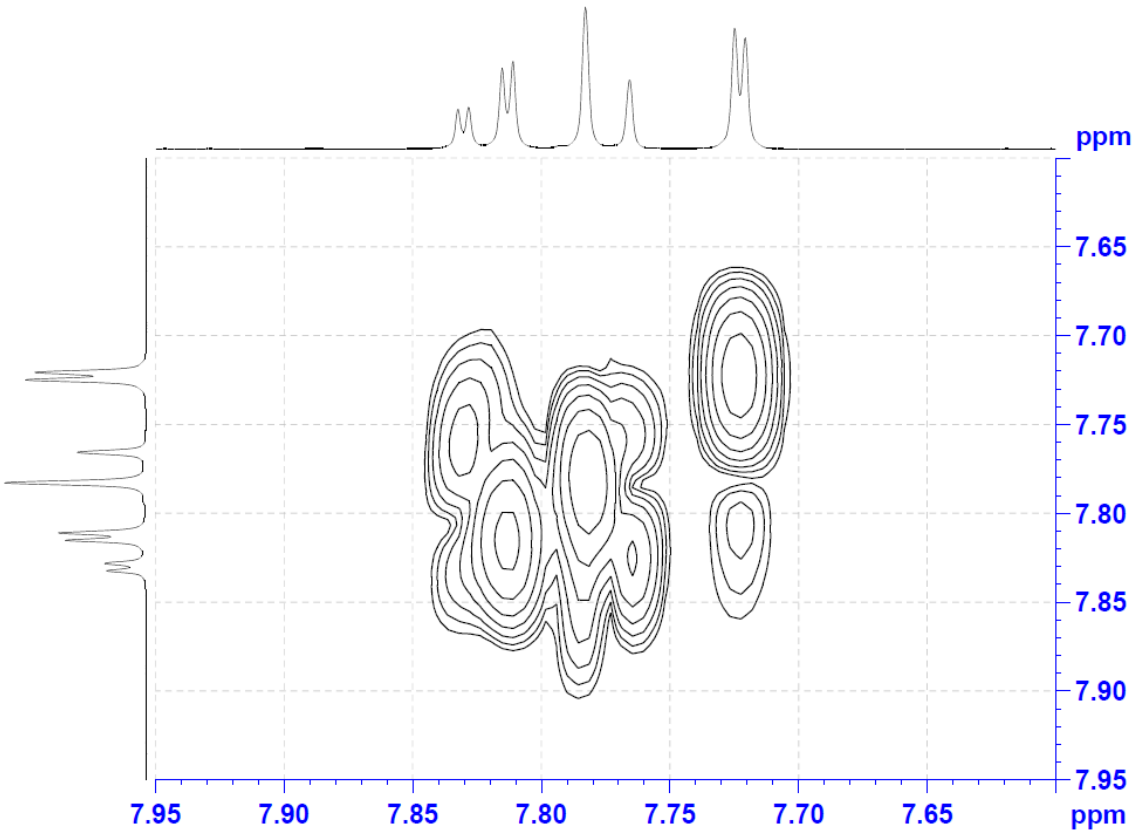

Figure A.15 COSY NMR spectra of compound **10**

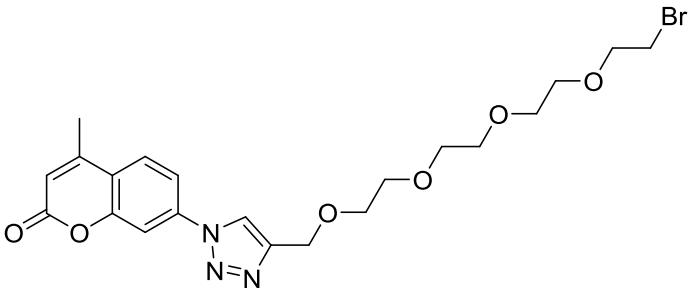

Compound 10
COSY NMR (500 MHz, $CDCl_3$)

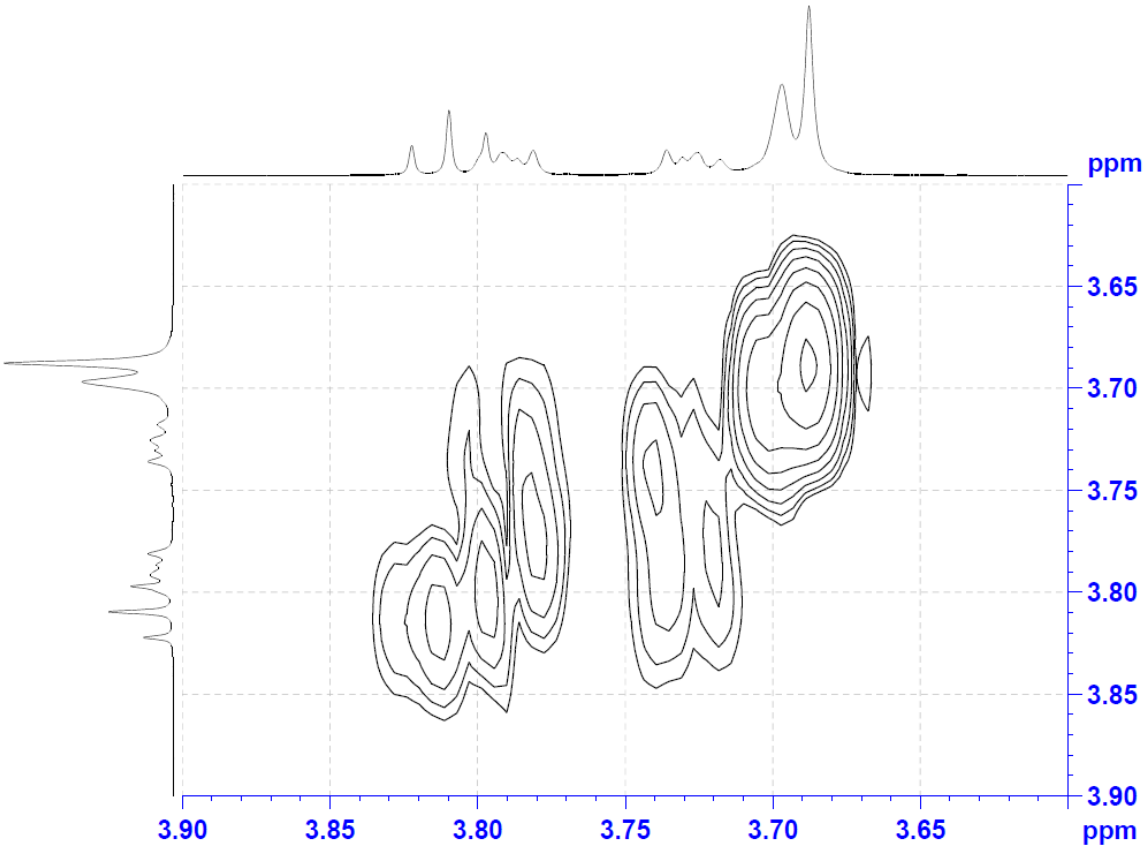

Figure A.16 COSY NMR spectra of compound **10**

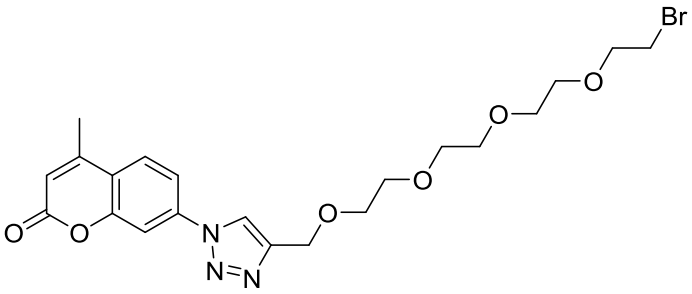

Compound 10
COSY NMR (500 MHz, $CDCl_3$)

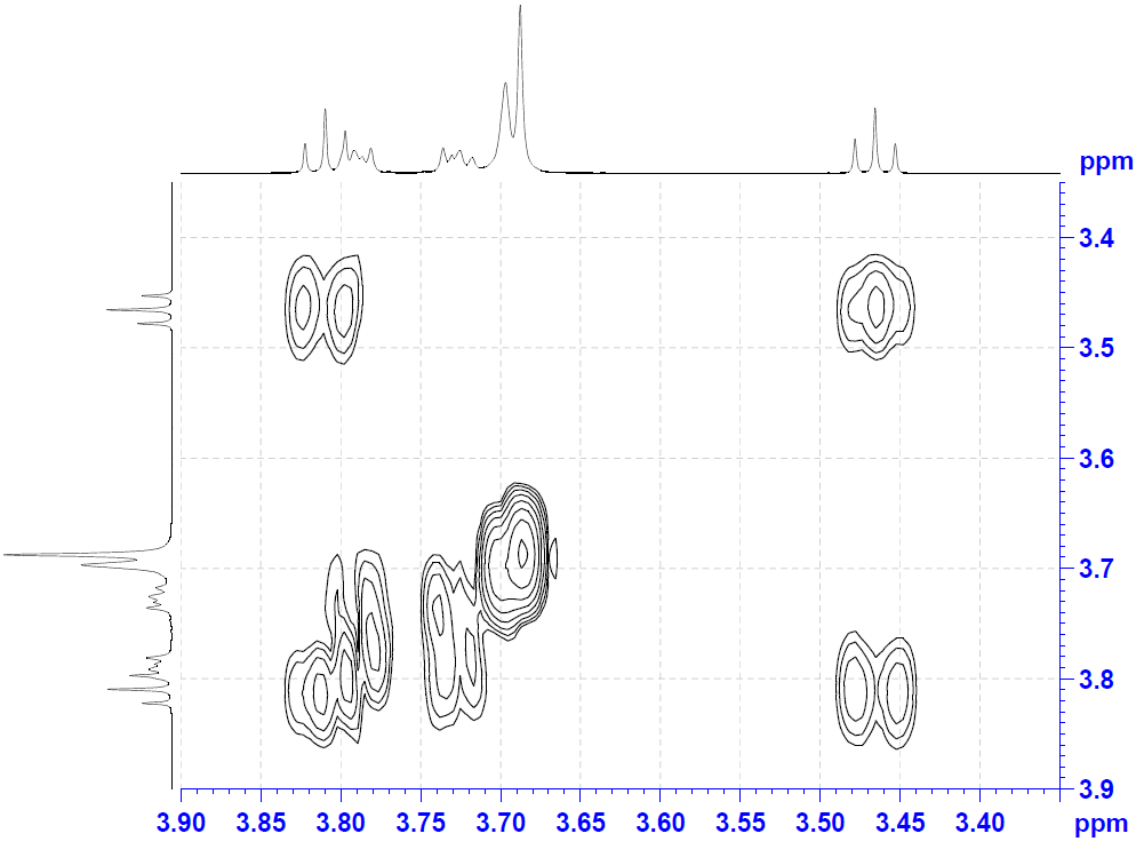

Figure A.17 COSY NMR spectra of compound **10**

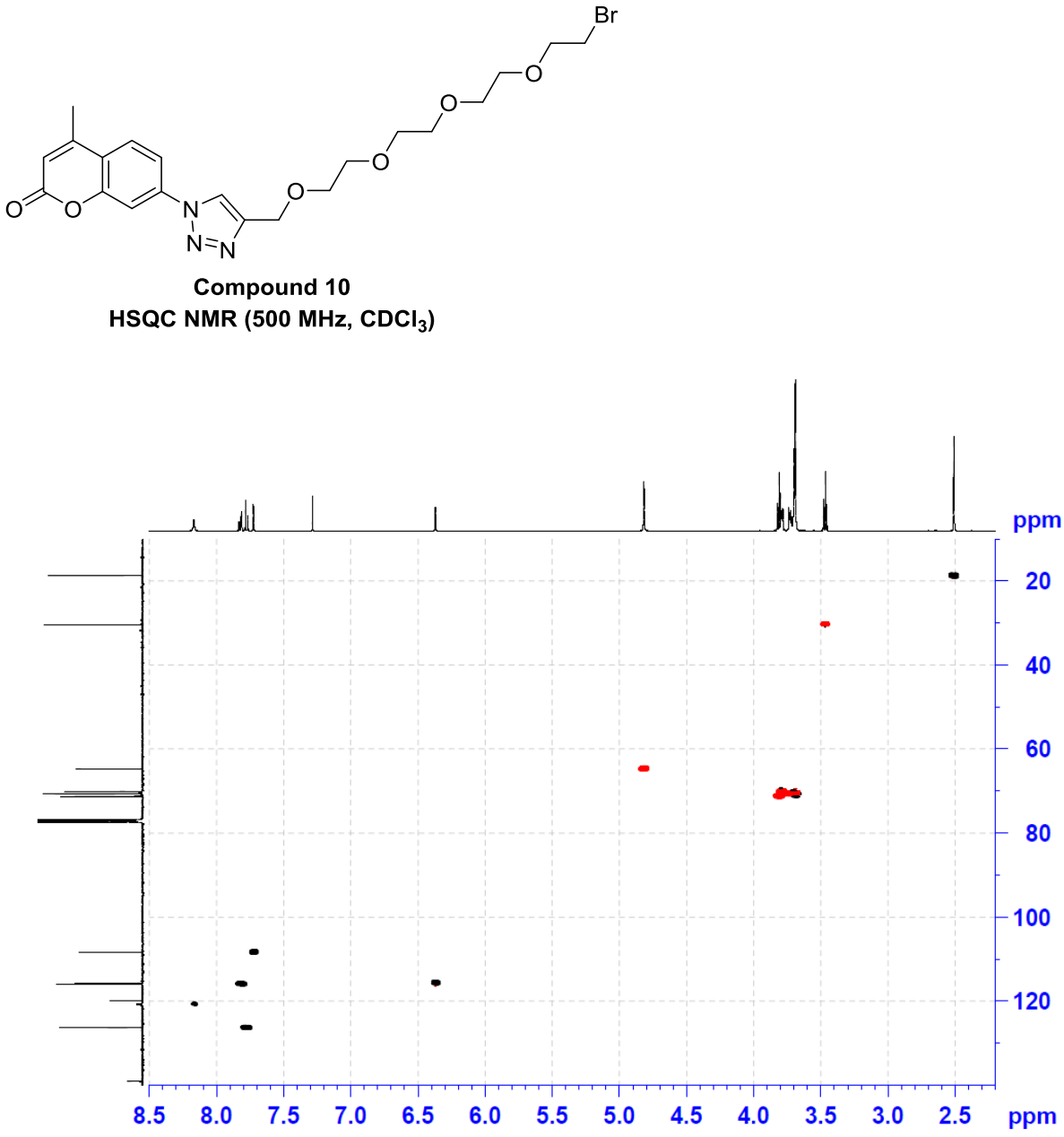

Figure A.18 HSQC NMR spectra of compound **10**

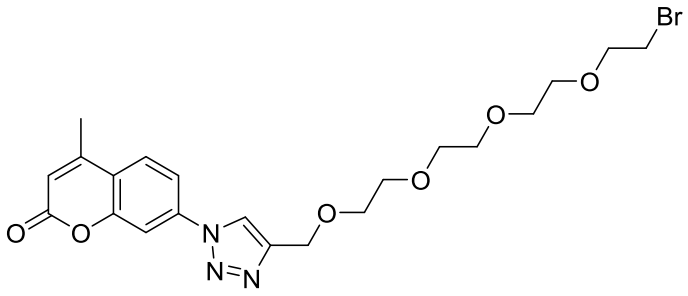

Compound 10
HMBC NMR (500 MHz, $CDCl_3$)

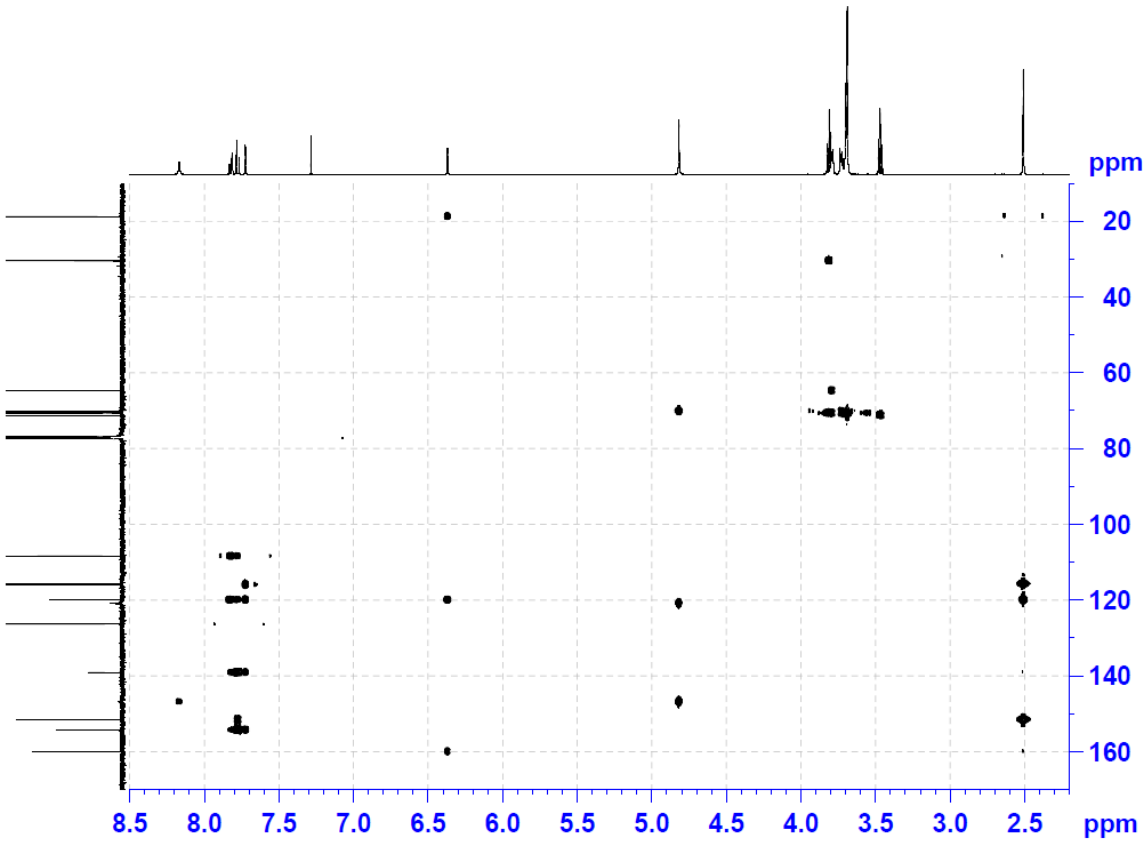

Figure A.19 HMBC NMR spectra of compound **10**

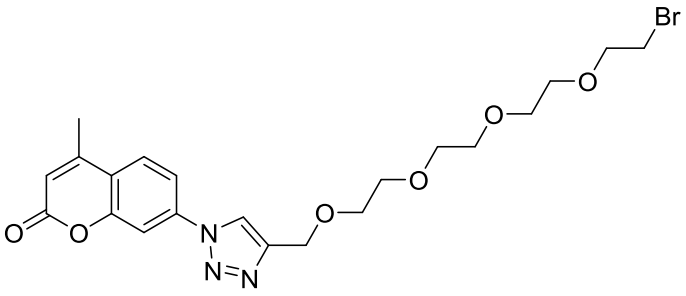

Compound 10
HMBC NMR (500 MHz, $CDCl_3$)

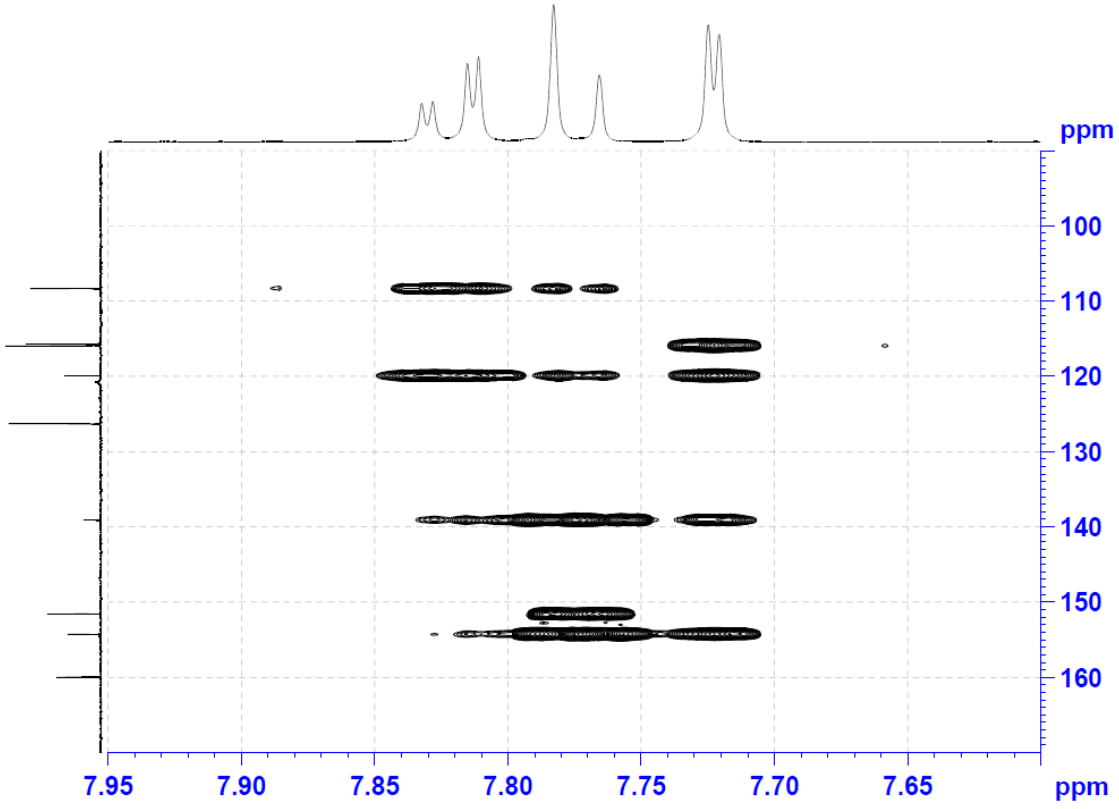

Figure A.20 HMBC NMR spectra of compound **10**

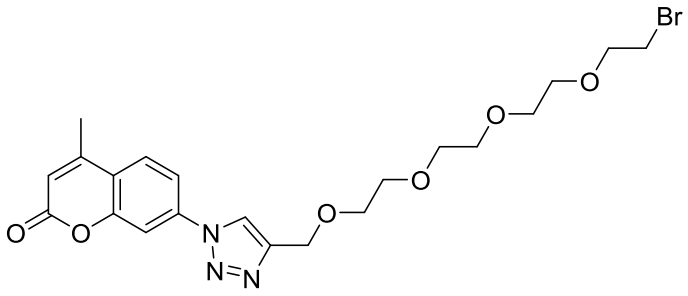

Compound 10
HMBC NMR (500 MHz, $CDCl_3$)

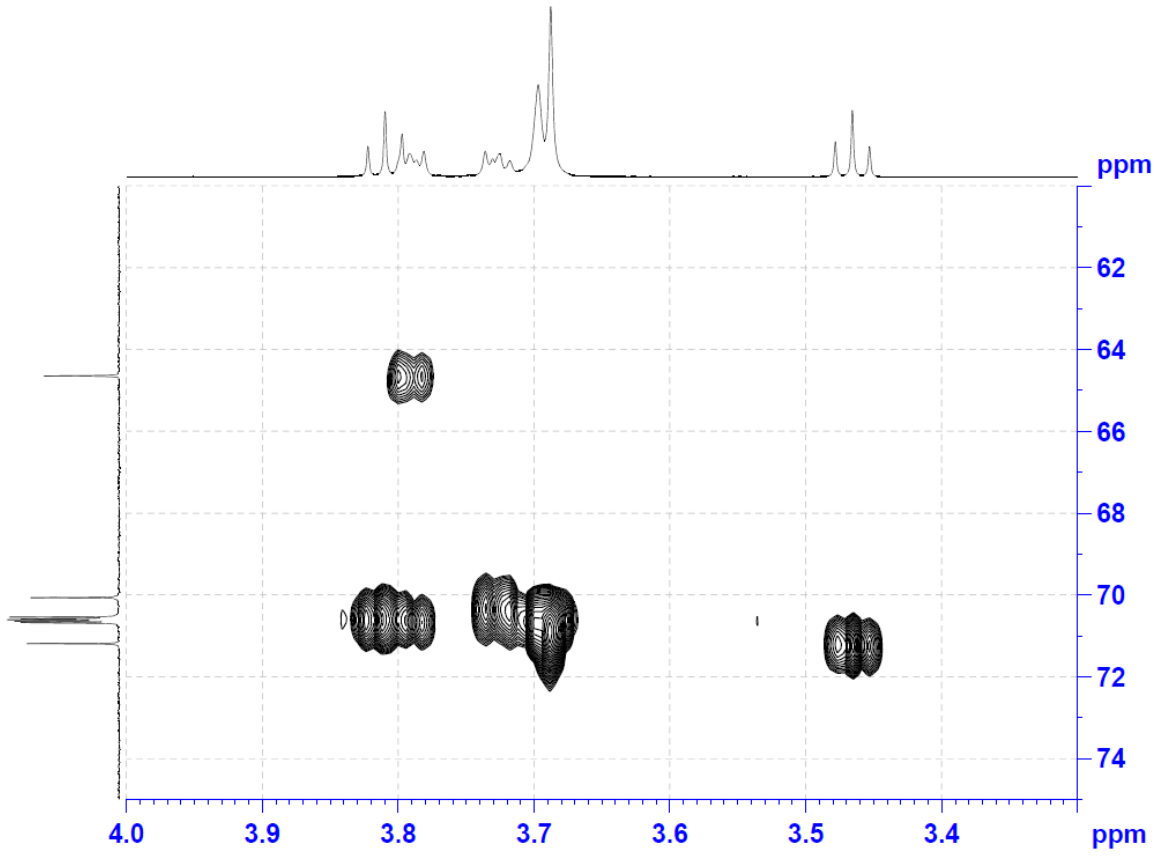

Figure A.21 HMBC NMR spectra of compound **10**

A.3 Additional figures

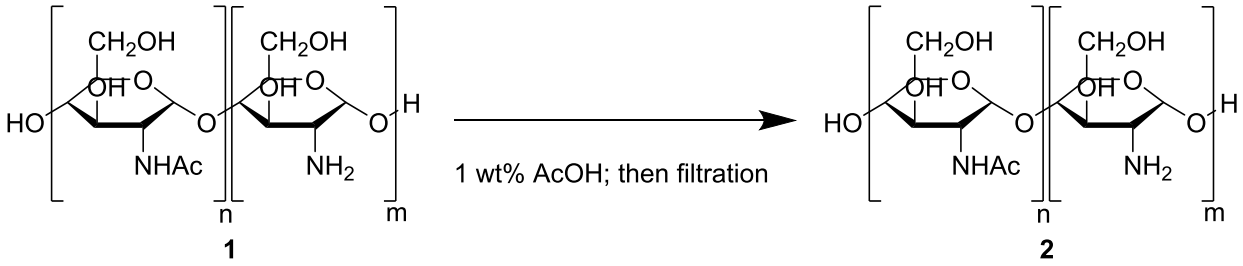

Figure A.22 Purification of polymeric chitosan (starting material)